T.R.
VAN YUZUNCU YIL UNIVERSITY
INSTITUTE OF NATURALANDAPPLIEDSCIENCES
DEPARTMENT OF MECHANICAL ENGINEERING

FLOW ANALYZING AND DETERMINING FORCE OF TWO DIFFERENT BUCKET IN THE PELTON TURBINE

M.Sc THESIS

PREPARED BY: Azhin Abdullah SABER
SUPERVISOR: Assoc.Prof.Dr.Sedat YAYLA

VAN-2017

T.R.
VAN YUZUNCU YIL UNIVERSITY
INSTITUTE OF NATURALANDAPPLIED SCIENCES
DEPARTMENT OF MECHANICAL ENGINEERING

FLOW ANALYZING AND DETERMINING FORCE OF TWO DIFFERENT BUCKET IN THE PELTON TURBINE

M.Sc THESIS

PREPARED BY: Azhin Abdullah SABER

VAN-2017

ACCEPTANCE and APPROVAL PAGE

This thesis entitled "**Flow Analyzing And Determining Force of two Different Bucket in the Pelton Turbine**" presented by Azhin Abdullah SABER under supervision of Assoc. Prof. Dr. Sedat YAYLA in the department of Mechanical Engineering has been accepted as a M.Sc. thesis according to Legislations of Graduate Higher Education on 05/09/2017 with unanimity of vote's members of jury.

Chair: Assoc. Prof. Dr. Sedat YAYLA Signature:

Member: Assist. Prof. Dr. Ali Bahadır OLCAY Signature:

Member: Assist. Prof. Dr. Mahsum AYDIN Signature:

This thesis has been approved by the committee of The Institute of Natural and Applied Science on 08/09/2017 with decision number 2017/41-I.

Signature
Prof. Dr. Suat SENSOY
Director of Institute

Yrd.Doç.Dr.Ayhan BAŞTÜRK
Fen Bilimleri Enstitüsü
Müdür Yardımcısı

THESIS STATEMENT

All information presented in the thesis obtained in the frame of ethical behavior and academic rules. In addition, all kinds of information that does not belong to me have been cited appropriately in the thesis prepared by the thesis writing rules.

Signature

Azhin Abdullah SABER

ABSTRACT

FLOW ANALYZING AND DETERMINING FORCE OF TWO DIFFERENT BUCKET IN THE PELTON TURBINE

SABER, Azhin Abdullah
M.Sc. Thesis, Mechanical Engineering Department
Supervisor:Assoc.Prof.Dr.Sedat YAYLA
August 2017, 118pages

The Pelton turbine is utilized in low water stream and high head in building micro-hydro-electric power plant. For obtaining a Pelton hydraulic turbine with highest efficiency throughout different working circumstances, the turbine parameters have to be encompassed in the designing process. For the simulations of liquid flow, the ANSYS FLUENT was applied.

This work is set out to investigate the effect of bucket splitter angle, inlet velocity values and different diameter for two models of the bucket for determining the force and visualizing the flow pattern on the pelton turbine bucket. The study utilized two diverse bucket models at various inlet velocities (20, 25, 30,35and 40m/s), four diverse splitter angle (55, 75, 90and 115) and two diameters (30and 40) mm for finding out the impacts of every single parameter on the effective force on the bucket. The acquired outcomes revealed that there is a linear relationship between force and inlet velocity on the bucket. Furthermore, the results also uncovered that the relationship between splitter angle and force on the bucket is linear until 90 degree. Consequently, turbine efficiency reached higher value at 90 degree for model 1. These outcomes provide vision into the expected advantage of steady flow calculations over the pelton turbines design optimization process.

Keywords: Bucket Design, CFD, Free Surface Flow, Two-Phase Flow, VOF.

ÖZET

PELTON TÜRBİNDE İKİ FARKLI KOVADAKİ AKIŞ ANALİZİ VE KUVVET BELİRLENMESİ

SABER, Azhin Abdullah
Yüksek Lisans Tezi, Makine Mühendisliği Anabilim Dalı
Tez Danışmanı: Doç. Dr. Sedat YAYLA
Ağustos 2017, 118 sayfa

Pelton türbini düşük su debisi ve yüksek rakımlarda mikro-hidro-elektrik enerji santrali inşasında kullanılmaktadır. Değişik çalışma koşullarında en yüksek verimlilikle çalışabilen bir Pelton hidrolik türbini elde etmek için türbin parametrelerinin daha tasarım aşamasında ele alınması gerekmektedir. Yapılan araştırma kapsamında incelenen sıvı akışı simülasyonlarında ANSYS FLUENT yazılımı kullanılmıştır.

Bu çalışma kova ayraç açısının, besleme hızının ve iki farklı model için kova çaplarının etkilerini ve toplam gücü belirleyip pelton türbinindeki akış yapısını tespit etmek amacıyla yapılmıştır. Çalışmada farklı besleme hızlarına sahip (20, 25, 30, 35 ve 40 m/sn.) iki farklı kova modeli, dört değişik ayraç açısı (55, 75, 90 ve 115) ve iki akış çapı (30 ve 40 mm), her bir parametrenin kova üzerindeki etkin güce olan etkileri açısından incelenmiştir. Elde edilen veriler, kova üzerindeki güç ile besleme hızı arasında lineer bir bağlantı ortaya çıkarmıştır. Sonuçlar aynı zamanda 90 derece açıya kadar ayraç açısı ile kova üzerine uygulanan güç arasındaki bağıntının da lineer olduğunu ortaya koymuştur. Sonuç olarak model 1 için türbin verimliliği 90 derecede azami seviyeye ulaşmıştır. Bu sonuçlar pelton türbin tasarımında optimizasyon süreci için daimi akış hesapları kullanmanın beklenen faydaları üzerine bir öngörü kazandırmaktadır.

Anahtar kelimeler: CFD, Iki-Fazlı Akış, Kova Tasarımı, Serbest Yüzey Akışı, VOF.

ACKNOWLEDGEMENT

First and foremost, I would like to thank the ALLAH for his guidance and rewards toward me and my family. Then, I would like to express my deepest respect and most sincere gratitude to my supervisor, Assoc.Prof. Dr. Sedat YAYLA and very special thanks toAssist.Prof. Dr. Ali Bahadir OLCAY, for these guidance and encouragement during all stages of this mutual work. I will always be grateful for their valuable advice and insight supervision and encouragement to me during this research. Finally, I would like to express my deepest regards and respects to my roommate, a graduate student Mr. Ahmed Ezaddin for his encouragement and support throughout my thesis study.

2017
Azhin Abdullah SABER

CONTENTS

pages

LIST OF TABLES

Tables **Pages**

LIST OF FIGURES

Figures **Pages**

Figures **Pages**

Figures **Pages**

Figures **Pages**

Figures **Pages**

Figures **Pages**

Figures **Pages**

SYMBOLS AND ABBREVIATIONS

Some symbols and abbreviations used in this study are presented below, along with descriptions**.**

Symbols	Description
$\mathbf{R_e}$	The Reynolds number
$\mathbf{g}$	The gravitational acceleration (m/sec^2)
$\mathbf{Vj}$	The velocity of jet (m/sec)
$\boldsymbol{\mu}$	Viscosity of the water (kg/(m s))
$\boldsymbol{\rho}$	The density of water (kg/m$^{3)}$
$\mathbf{l}$	Characteristic length (m)
$\mathbf{D}$	The nozzle diameter(mm)
$\boldsymbol{\alpha}$	splitter angle (deg)
$\boldsymbol{\upsilon_1}$	The velocity of pipe (m/sec)
$\boldsymbol{\nu_2}$	The velocity of jet (m/sec)
$\mathbf{VOF}$	The volume of fluid
$\mathbf{H_n}$	The net head of the nozzle(m)
$\boldsymbol{\nabla}$	The Nabla or delta
$\mathbf{F_{max}}$	The max force on the bucket (N)
$\mathbf{H}$	The head of the nozzle (m)
$\boldsymbol{\gamma}$	Nabla or delta
$\mathbf{Q}$	The volume flow rate(m/sec)
$\mathbf{C_v}$	The net head of the nozzle(m)
$\boldsymbol{\nabla}$	The velocity in the x-direction
$\mathbf{CFD}$	Computational Fluid Dynamic
$\mathbf{P}$	The pressure (pa)

1. INTRODUCTION

Hydropower is an energy resource that produces electricity from machines powered by moving water thus considered as renewable. However, the processes and activities involved in the production of hydroelectricity such as dam construction, the change in water level and water flow, and building new infrastructures have a negative effect on the environment when show in the Figure 1.

Hydroelectricity is produced by a renewable energy source known as hydroelectric plant. It's a system of machines that are power-driven by running water specifically done by reserving piling water to cause energy when goes through the nozzle that will then be transformed to kinetic energy that will power the hydro turbines which in turn will produce mechanical power. The mechanical power will be transformed to electrical energy as it goes through the generators where these hydro turbines are connected to.

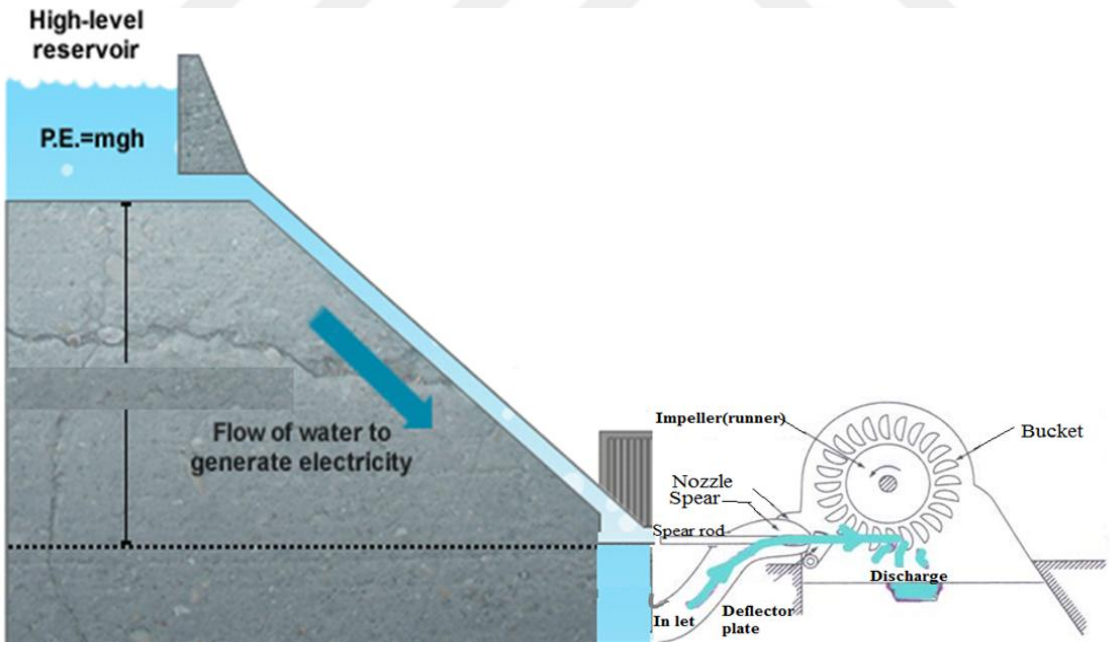

Figure 1.1. Showed that the hydro power details.

Generally, as the moving water produces kinetic energy, it turns the turbines in motion producing mechanical energy, which powers the generator to create electrical energy, and this has 65% to 80% efficiency rate. Steel-made turbines are better but will

still depend relatively on the volume of water or its operation impulse or reaction. Impulse and reaction turbines differ as to which energy it converts into, kinetic energy from flowing water for Impulse turbines (Ex. Pelton, Turgo, Cross flow, etc.) and potential energy from pressurized water for Reaction turbines (Ex. Francis, Propeller, Kaplan, etc.). See Table 1.1 for reference.

Table1.1. Show the various types of turbines

Turbine type	Head range, (m)
Kaplan and Propeller	2<H<40
Francis	10<H<350
Pelton	50<H<1300
Banki-Michell	3<H<250
Turgo	50<H<250

Hydraulic turbines can act as an impulse and reaction turbine as it can convert both kinetic and potential energy into mechanical energy. Hydroelectric power plants commonly use both types of turbines however the two have differences as to its performance based on engineering insights discussed below.

1. Unlike impulse turbines, reaction turbines do not have water energy to kinetic energy converter.
2. Impulse turbine facilitates running water through the nozzle to the storage but reaction turbines let the water flow on moving vanes.
3. Flowing water and equal to atmospheric pressures are steady in impulse turbines however in reaction turbines, as the flowing water slide along the vanes water pressure decreases.
4. Impulse turbines' water storage is imposed by kinetic energy whereas pressure energy on reaction turbine's vanes as water slides over it.
5. To fully function, impulse and reaction turbines depend on different points, changes in kinetic energy, and changes in velocity and pressure head, respectively.
6. Water flow regulation without any instance of water loss is not possible in reaction turbines unlike the impulse turbines.

7. The wheels in impulse turbines do not have to be run in full, just enough air between its vanes whereas in reaction turbine, wheels fully ran and sufficient water is necessary.
8. Full water access into the wheels' circumference is vital for reaction turbines unlike the impulse turbines.

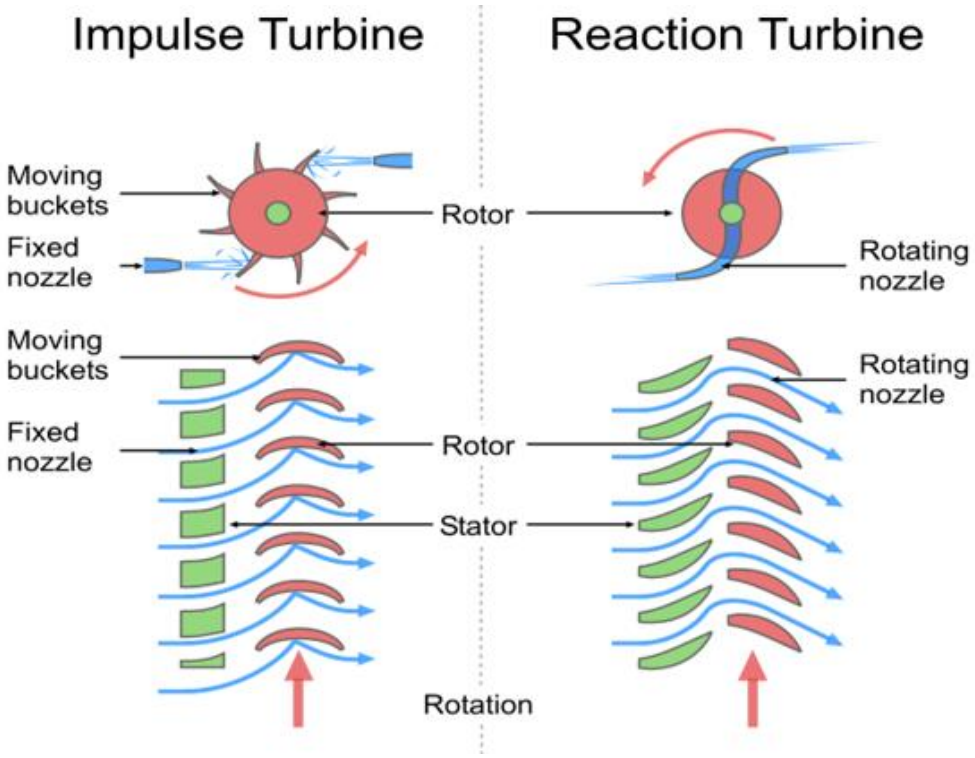

Figure 1.2. Comparison between pelton turbine and reaction turbine.

The Pelton wheel is among the most commonly used turbine for high head power plant. The Pelton wheel extracts energy due to change of impulse (momentum) of moving water, as opposed to its weight like traditional overshot water wheel. Although many variations of impulse turbines existed prior to Pelton design, they were less efficient than Pelton's design, the water leaving these wheels typically still had high speed, and carried away much of the energy.

Therefore, all researcher, designers and engineer attempt for acquiring high efficiency by modifying the bucket and nozzle. This investigation utilized two different bucket models of the pelton turbine for determining the force and visualization fluid flow on the bucket by altering some working conditions and geometrical parameters. An

example of working conditions is the inlet velocity which affects the force and visualization fluid flow. Moreover, the instance of the geometrical parameter is the splitter angle between nozzle and bucket which impacts the value of the force on the bucket of peloton turbine. The jet of circular cross section is distributed from nozzle and transfers in air before striking the bucket in Pelton turbines. Via a sharp edge splitter, the bucket is separated into two symmetrical semi ellipsoidal cups. The jet strikes the bucket on the splitter. The jet is separated into two identical sheets of water having free surface which transfers on the curved path of bucket by the splitter. The force and also pressure and velocity distribution over bucket are affected by the profile of curved path of bucket. For example, only Kvicinsky,(2002) compared the calculated pressure distribution to experimental data and another researcher utilized a stationary pelton turbine bucket when water impinged it experimentally Grozev et al (1988). The current study utilized computational fluid dynamic and some CFD models like VOF model and K-epsilon model. Several researchersexanimate of the steady bucket like Janetzky et al., (1998).The coming out water of the nozzle is circular in cross-section. The water jet transfers liberally in air and imposes on a bucket of the runner therefore resulting in rotation. For better understanding of the flow, Visualization was helpful. The outcomes displayed at the end of this study, are utilized for providing vision into the advantage we can anticipate of stable–state calculations of the flow during the universal process of pelton design optimization.

1.1. Pelton Turbine

Pelton wheel turbines which are widely used in hydro plants are impulse turbines. For a hydro plant to work, these simply designed turbines facilitate high head and low water flow. Pelton turbines works in a manner where water energy to kinetic energy conversion happens when pass through the nozzles contracted present and the runner takes a spin as the water jet moves. As the spinning scenario goes through, it produces mechanical energy flowing to the input lines of the generator.

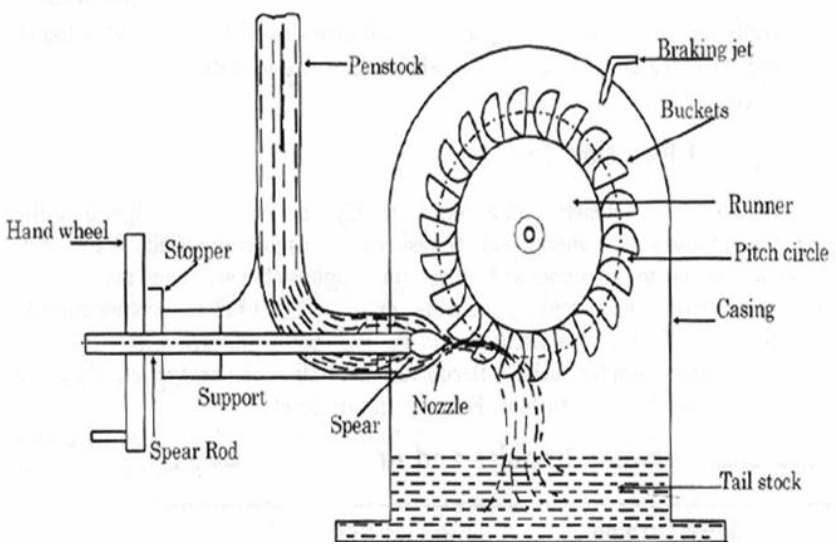

Figure 1.3. Shows that the main components of a Pelton turbine.

1.2. The Important Components of a Pelton Turbine.

1.2.1. Jet of the pelton turbine

The nozzle is a circular device used as a water flow rate regulator and navigator. Its spear inside controls the volume of water that comes through the nozzle as the spear is pushed inside otherwise, large volume of water comes in if it is shoved outwards. The spear can be manually controlled or automated. Bypass nozzles are also incorporated to keep away from bursting pipes when water supply is abruptly halted since these nozzles forbid the water to hit the buckets in place. Defectors come along with some pelton wheel turbines to interrupt water jet and prevent hitting the buckets with large volume of flowing water.

1.2.2. Breaking jet

The purpose of the braking jet attached at the back of the buckets is to literally put a stop rest to something or reduce speed of a moving body such as in the control of the runner's speed. This small nozzle known as braking jet will give the runner a short time rest stop from rotating by making the runner rotate reversely through directing the

water in the opposite direction, especially in a case when the flowing water suddenly stops from hitting the bucket.

1.2.3. Penstock

In hydroelectric systems, a gate mechanism and a surge tank is what comprise a penstock. It is in null mode when turbines are not in use and it must be preserved by manual cleaning using hot water, antifouling coatings, and by keeping it dry to keep this device from early damage. Penstock as a general term is referred to as a way to accessing sluice gates back and forth in irrigation dams. The term is also used in dam construction and is mainly located at the tailing dam's middle section. It is constructed with the use of penstock rings and is used to control the level of the water by taking the water back through the penstock pipeline into the plant.

1.2.4. Runner and buckets

The pelton wheel comprises of a disc attached to the horizontal shaft and its runner and the buckets bowl shape are evenly set. Buckets are made of cast iron and either bronze or stainless steel or alloy for low water and high water head, respectively. For chemically contaminated water cases, special alloy-made buckets are produced. Runner discs are usually bolt fastened to buckets so as for easy replacement when buckets are worn out or damaged.

1.2.5. Casing

To protect the runner and bucket segment from mishaps and other unwanted circumstances such as water splatter that may lead to the tail race, the casing is necessary which is made of fabricated parts. And that's the primary function of the Pelton wheel's casing, no hydraulic functions.

1.3. Number of Bucket in the Pelton Turbine.

The number of buckets in a pelton wheel is a very essential attribute in the design of a pelton turbine. This attribute determines and influences the efficiency of the turbine since when there is not enough number of buckets in the turbine; water jet may be lost and causes the buckets to be detached from all the other. Shown below is the illustration of the case and where at some point in the operation the number of buckets is reduced see rightmost image. To keep the water from spilling out, the number of buckets must be enough see leftmost image.

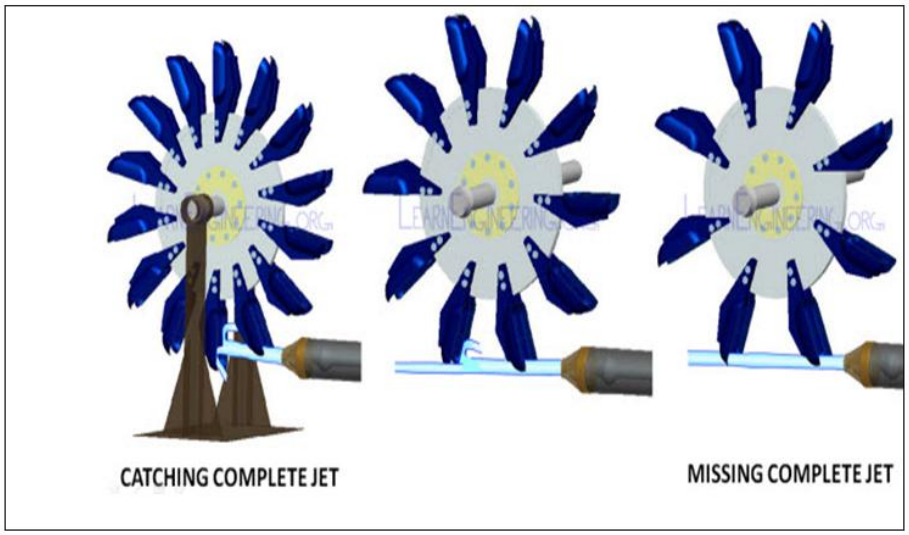

Figure 1.4. Shows the effect number of bucket in pelton turbine.

1.4. Energy Conversion

As an impulse turbine, the pelton turbine converts velocity-based water energy and is encased with atmospheric pressure considering that the turbine's inlet and outlet pressure is the same. Energy conversion is illustrated in Figure 1.5 and highlights the following points.

1. As the water gets inside the nozzle, it has high potential energy in 1*.
2. As it comes through the nozzle, pressure- kinetic energy conversion commences changing states from high pressure-low velocity condition into atmospheric pressure-high velocity state.

3. In a pelton turbine, kinetic energy of 1 is transformed to rotational energy as it gets into the bucket.
4. In step 2, it shows that the energy at the turbine's outlet has velocity of $\frac{C^2 m_2}{2}$ (almost same with the jet's) and potential energy of gh (almost same with tail water energy). Step 1 emphasizes that it's in the runner where kinetic to mechanical energy conversion takes place. An energy analysis is conducted to find the pelton turbine's converted energy is provided that it's a function of the peripheral and absolute velocity (inlet and outlet):

$$Em = cu1u1 - cu2u2$$

where Em = transferred mechanical energy (water to turbine)

The energy converted to mechanical energy less the energy lost in the turbine is what's left.

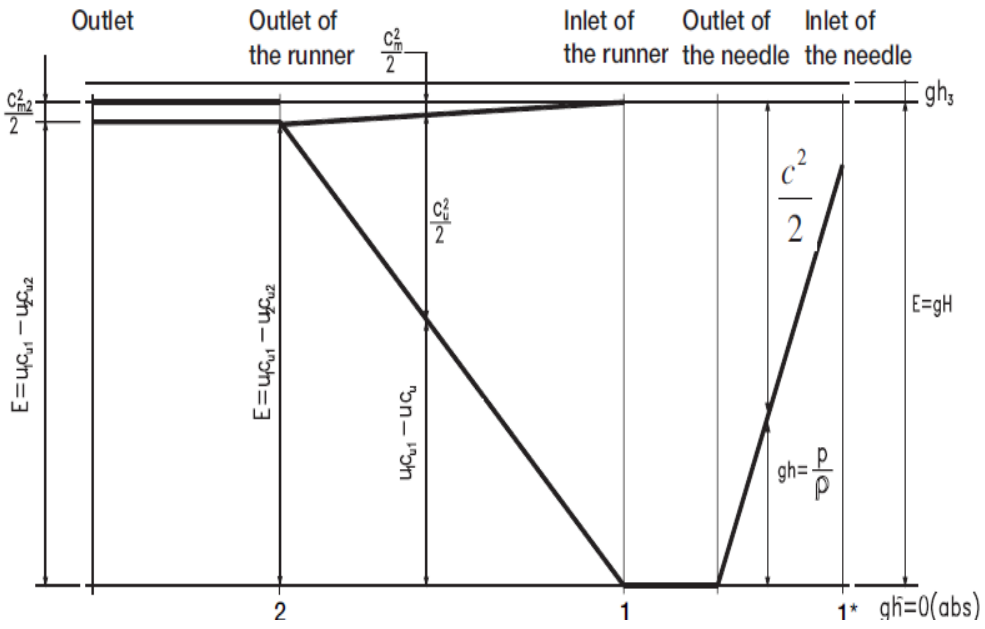

Figure 1.5. Shows that the Energy conversion in a Pelton turbine.

1.5. Advantages of Impulse Turbine

The following are cited to be the advantages of the impulse turbines.

1. The utilization of impulse turbines is ideal in the generation of hydroelectricity.
2. Efficient in extracting energy in any rapidly flowing fluid.

3. Easily manufactured and maintained.
4. It can be made in metal which is better, ceramic material, or plastic.
5. A pelton wheel with several jets may be used to generate more power.

1.6. Disadvantages of Impulse Turbine

1. With a high flow rate in a low pressure watercourse, impulse turbines are not preferable.
2. Pelton turbines are the only impulse turbines that is best used if flow rates are low and for small bodies of fluid.
3. They are only best used on streams with high quantity of pressure with low flow rate.
4. When there is low stream discharge, large amount of head loss happens.
5. Dissipation of energy extraction in small streams is possible.

1.7. Computational Fluid Dynamics (CFD) Program

Fluid flow problems are analyzed and solved by applying computational methods and algorithms known, as Computation Fluid Dynamics CFD.CFD is a branch of fluid dynamics that aims to facilitate in the reduction of time and cost in the creation of a real-world behaviour modelling. Still, similar to other experiment outputs, the model produced in the CFD analysis must be examined as to its validity. For small bodies of water and low water flow volume, pelton turbines are best utilized although the turbine’s flow is complex and several turbines have been manufactured, cases of which are not easily understood still exist. In such cases, a CFD analysis may be used to understand the relationship of high-speed water against the pelton buckets (in motion).

1.8.The Aim of the Study

The aim of this project is to visualize flow on the bucket and determine maximum force on the bucket by:

1. Apply various inlet velocities.
2. Apply two different model of the bucket.
3. Apply two jet diameters.
4. Apply four different splitter angles.

2. LITERATURE REVIEW

The study of Leila et al(2013), focused on the computational research on the organization of rotating buckets in a turbine. With this, an analysis of the non-stationary flow was established using the numerical method with sliding mesh incorporated in the FLUENT code and a comparison between the results relative to static pressure and water displacement and bucket thickness against the experimental study of Kvicinsky et al, (2002) was also conducted.

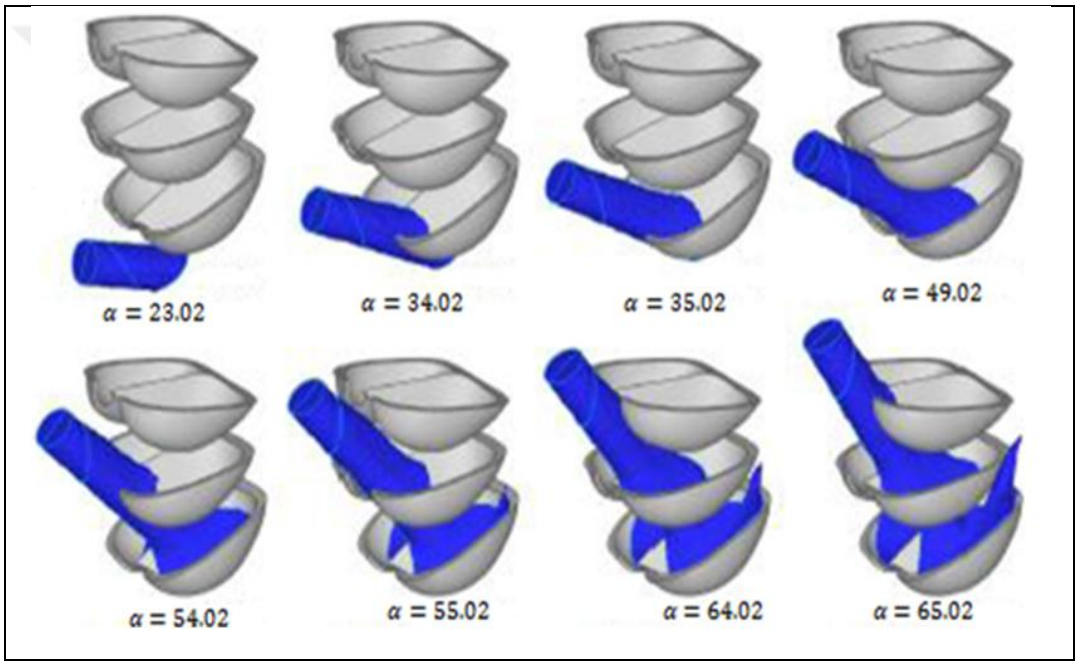

Figure 2.1. Shows that the Evolution of flow pattern along the runner rotation angle (Leila et al., 2013).

Jostet al. (2010), demonstrated the computational flow analysis of a Pelton turbine with two water jets with which various operational cases and schemes were incorporated in the model (during analysis) to come up with the desired results. The computer program known as ANSYS CFX-12.1 and the turbulent model k-ω SST were employed in the numerical analysis. The results of the analysis were assessed and matched up to the results of an analysis previously made with the same model. The two-phase homogenous model was used in the modeling of water flow's surface: the steady state analysis and unsteady state analysis phases. The steady state analysis was executed

in the water flow's distributor having two injectors in it. The resulting outcome highlights the loss of water flow energy in the distributor, the jets' shape and velocity. The second phase or the unsteady state analysis was performed in the runner with inclusion of the jets after which with the data on pressure distribution, the calculation of the torque on the shaft took place.

Nakanishi et al. (2002), discussed the Pelton bucket's water flow numerical simulation using the Particle method. The moving-particle semi-implicit method of flows striking the fixedly rotating plate is the primary basis of the computational examination conducted. In this, the results matched up with the theoretical outcome on the congruency of the force (exerted by the jet on the plate) and flow rates of the separated branches.

Vishal et al. (2014), presented several endeavors in trying to validate the influence of the jet's shapes (four) into the Pelton turbine runner's water flow and torque attributes. The attempt was acted upon by conducting a numerical simulation.

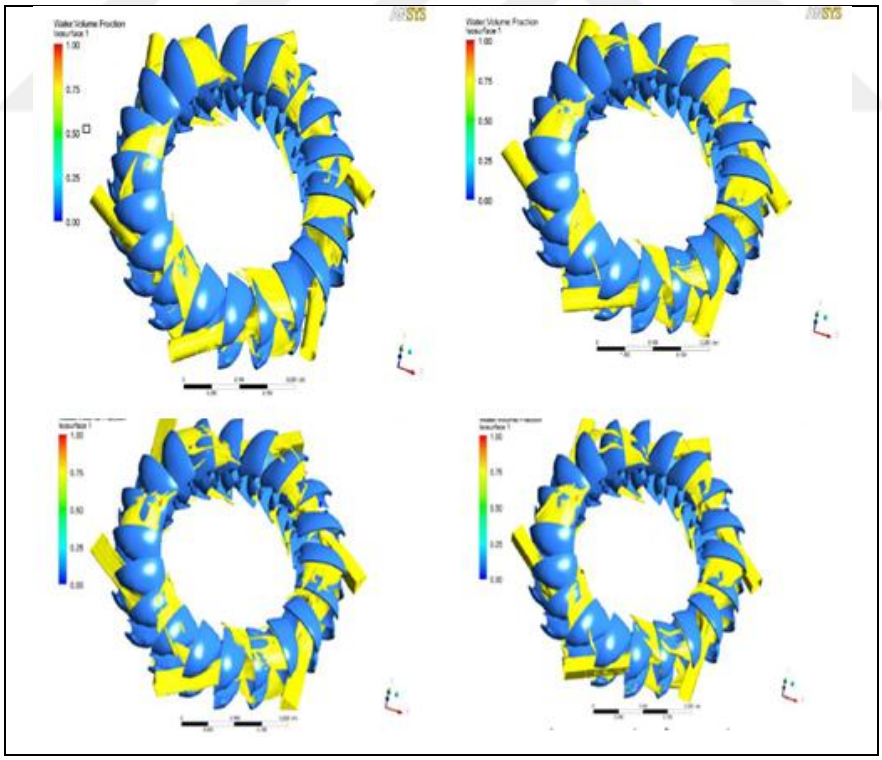

Figure 2.2. Shows that the four different shape of jet (Vishal et al., 2014).

Klemetsen (2010), carried out a research experiment regarding the Pelton Bucket flow (free surface).The computational study and experiment of the surface flow's free

flow in a stationary Pelton turbine bucket was simulated with the use of the CFD-solvers, CFX and FLUENT computer programs. The resulting data proved to be consistent as the numerical examination results were weighed against the experimental data results. Hence, it was implied based on the inconsistencies on the calculated and measured wall pressure, that in the real-world scenario, the jets do not have attributes as being 2-dimensional and axis-symmetrical.

Ujam et al. (2012) underlined the effects of the bucket splitter angle on the distribution of pressure in the surface of the bucket which in turn affects the pelton turbine's power output by performing evaluations on the case. To examine the case, a simulation (utilizing an emulator or simulator) on the force present on the surface of the bucket was essential for the reason that there is a 10° – 15° existing value on water jet impingement and a bucket splitter angle of $1° - 25°$ as predicted value.

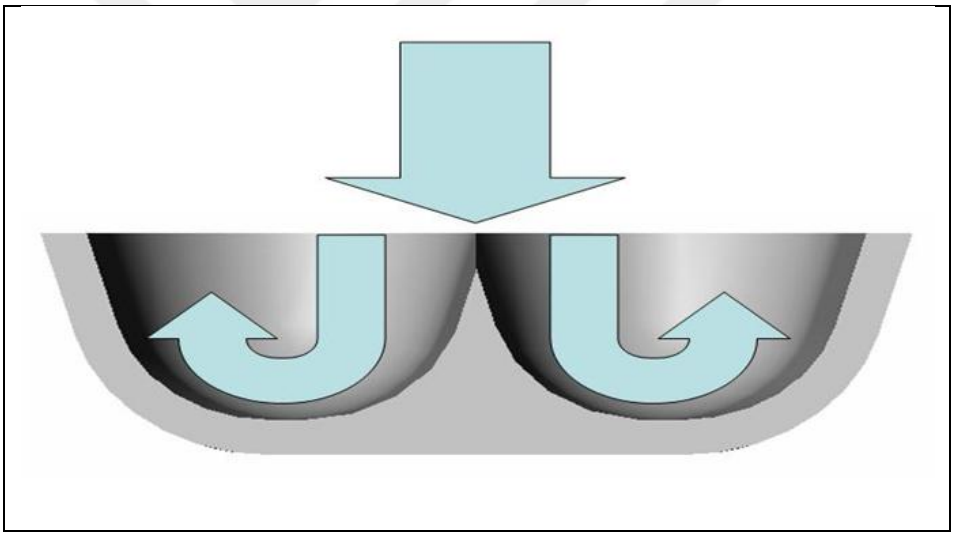

Figure 2.3. Shows Entry position of the fluid jet and the path it follows within the bucket (Ujam et al., 2012).

Ujam et al. (2014), emphasized on the consequences that the bucket tip angle add up in the power that the bucket splitter receives, so the case has been assessed. Mat lab software was used in the development of the simulation program that facilitates the examination on the relationships between attributes such as bucket tip angle, energy coefficient, exit angle of the bucket, and hydraulic efficiency.

Adriana et al. (2004), concentrated on the flow coming through the Pelton turbine nozzle and the use of the Navier-Stokes equation with inclusion of the velocity

distribution (within the jet) assessment in cases where needle tip is positioned on several ways.

Bilal (2013), emphasized on the examination and calculation of attributes relative to turbines. The following attributes were assessed so as to determine the turbine's functionalities: turbine's power and torque; the runner's diameter, length, and speed; the number and dimensions of the bucket; the nozzle's dimension and turbine's speed.

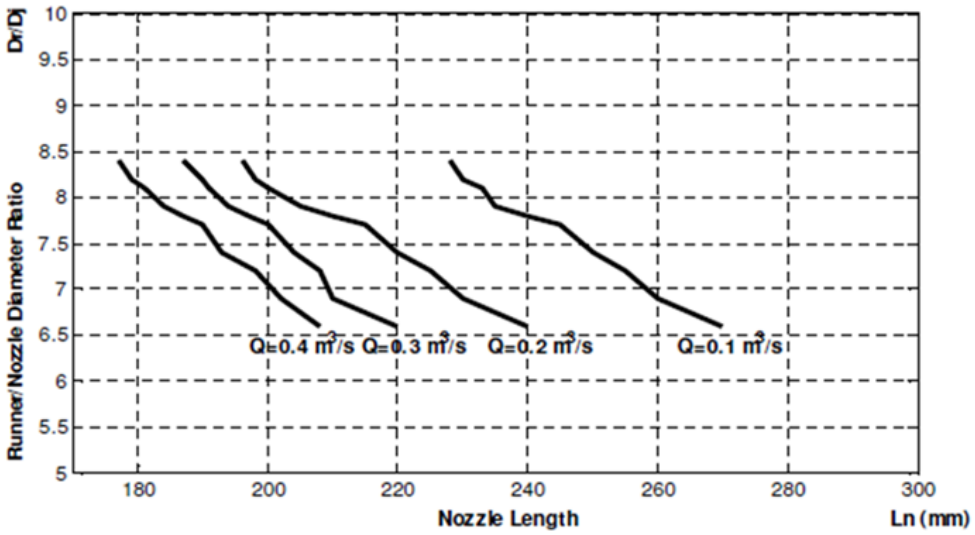

Figure 2.4. Shows that the Variation of runner to nozzle diameter ratio with nozzle length at different values of water flow rate (Bilal, 2013).

In the paper of Anagnostopouloset al. (2012), the lagrangian simulation method was concentrated on. The lagrangian simulation method is an algorithm originated from the lagrangian methods used in the analysis of flow and runner design in Pelton turbines. The free-surface flow (unsteady) within the interactions between the jet and the bucket was simulated with the use of the lagrangian simulation method. To observe the hydraulic losses and water spatters, cases were incorporated into the particle motion equation and the shape of the bucket was examined and performed computational design to it to develop an optimized design. Based on the results, a relatively high hydraulic efficiency was shown.

Mbiu et al. (2003), highlighted the bucket optimization for the purpose of the Pelton turbine buckets to perform better and functions well for the Pico hydroelectric

systems. The CAD (Computer-Aided Design) and ANSYS software were used in the modeling and structural analysis of the pelton turbine buckets. There were two turbine buckets illustrated and simulated in CAD with the same specifications (152mm pitch circle diameter) and parameters such as force and stress between the turbines were examined.

Barstad (2012), presented the Pelton turbine analysis using computation fluid dynamics with a computational model of the torque in a dynamic Pelton bucket as resulting output which had been evaluated for validity. The software CFX was used in the development of the model of which is based on DynaVec manufactured turbine models. An approximate of 1.5% of over-forecasting was identified as the experimental and simulated data results were compared and analyzed.

Varun et al. (2014), underscored the pelton turbine blades' stress analysis. The pelton turbine analysis began with an experiment and examination using the software Ansys 12.0 where it showed that the runner blade of the pelton turbine was imposed by its jets and with the aid of the software, the change in stress with respect to the blades' geometry was computed. The pro-E software was utilized to produce a model of the blade reflecting the calculated stress enclosing the runner blade.

Sourabh et al. (2012), characterized the Turgo impulse turbine blades' design and development simulated in the software Solid works. Utilizing the Ansys V14 in the finite element simulation, the analysis on attributes concerning the Turgo impulse turbines was sound. Attributes including stress and deformation taking place within the turbine were considered in the analysis and performing finite element simulation with which it is considered effectual on strain and stress distribution analysis. The resulting data shows the blade suction area root of the turbine is where generally the maximum stress arises.

Abhishek et al. (2012), examined and simulated the pressure distribution in a Pelton turbine nozzle. Taking into account the various shapes of the spear and with the use of the software ANSYS, the numerical simulation was performed with the application of the concepts in computational fluids dynamics. Several models and design can be optimized by employing high-end technology and advanced computational techniques in the conduct of analysis and simulation.

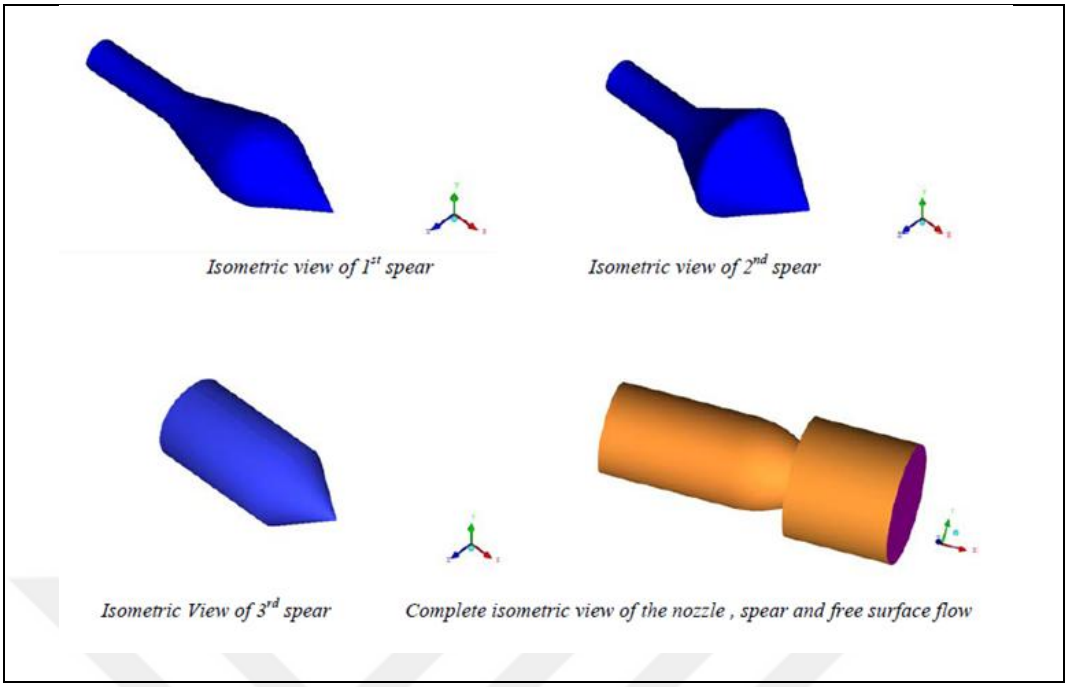

Figure 2.5. Shows that the complete isometric view of the nozzle, spear and free surface flow (Abhishek et al., 2012).

Suraj (2011), discussed the efficeincy of turbines. It is also presented on his study the concept that served as the basis on simulation. In the conduct of the experiment, the blades in a turbine were modified and was attached with peripherals so as to limit or to reduce the water spatter and making it to perform better and more efficient.

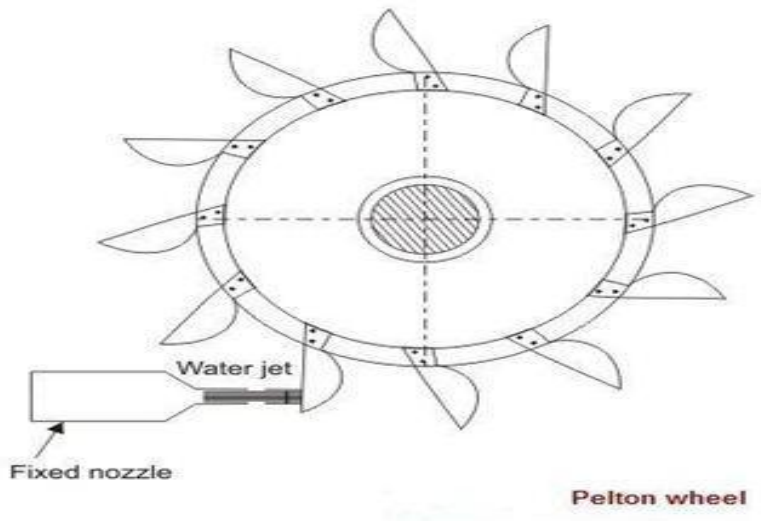

Figure 2.6. Shows that the Outline of pelton wheel (Suraj, 2011).

The paper of Amod et al. (2014), discussed the analysis of pelton turbine applied in the khimti hydropower in nepal.The computational fluid dynamics analysis was conducted for the purpose of identifying the bucket's pressure distribution and the turbine's torque to be used in the fatigue analysis as the next satge of analysis.To reduce the cost and time in the conduct of the computational experiment, a scale of 1:3.5 in the model size pelton runner was utilized and the operating conditions for it is based on the IEC 60193 and IEC 1116 standards.It is also presented in the paper the techniques applied in the CFD analysis using ANSYS CFX software.

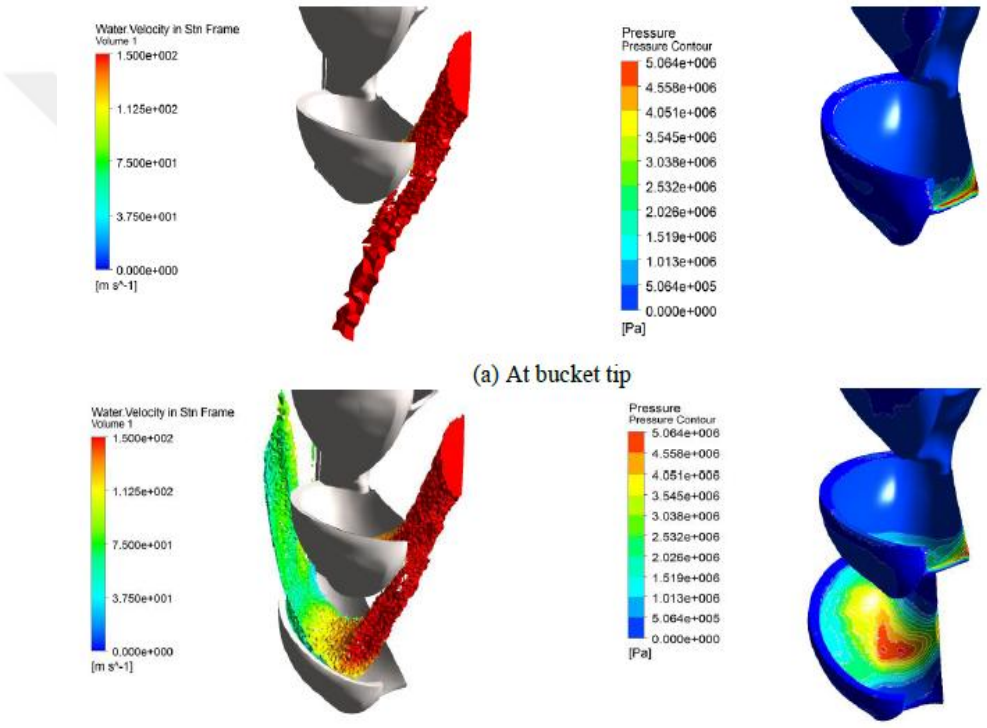

Figure 2.7. Shows that the water volume fraction above 0.75 left and pressure contour in pelton bucket right (Amod et al, 2014).

Gotfred (2003), analyzed of the Pelton jet flow (two-phase)employing a single-phase model and the break-up phenomenon that occurs in the the Pelton jet surface was highlighted.The analysis was based from the numerical experiment conducted and the analytical discussions on the phenomenon that occurred in the pelton jet surface was based on the research results.The resulting analysis has led into the development of the single-phase CFD model also referred to as the virtual interphase method (VIP) by

Bernsten.Any free surface jet with high density ratio calculations can be conducted with the use this model.

Sanam et al. (2014),expressed the analysis of the Pelton runner used in the Khimti Hydropower.The CFDanalysis of the pelton runner was done using the software ANSYS-CFX in the simulation and the scale of the pelton runner was adjusted but within the standards set by IEC 60193.It was observed in the simulation results that there is a high pressure present in the splitter and in thebucket deep face after which the torque was also computed to determine the runner's efficiency and effectiveness.

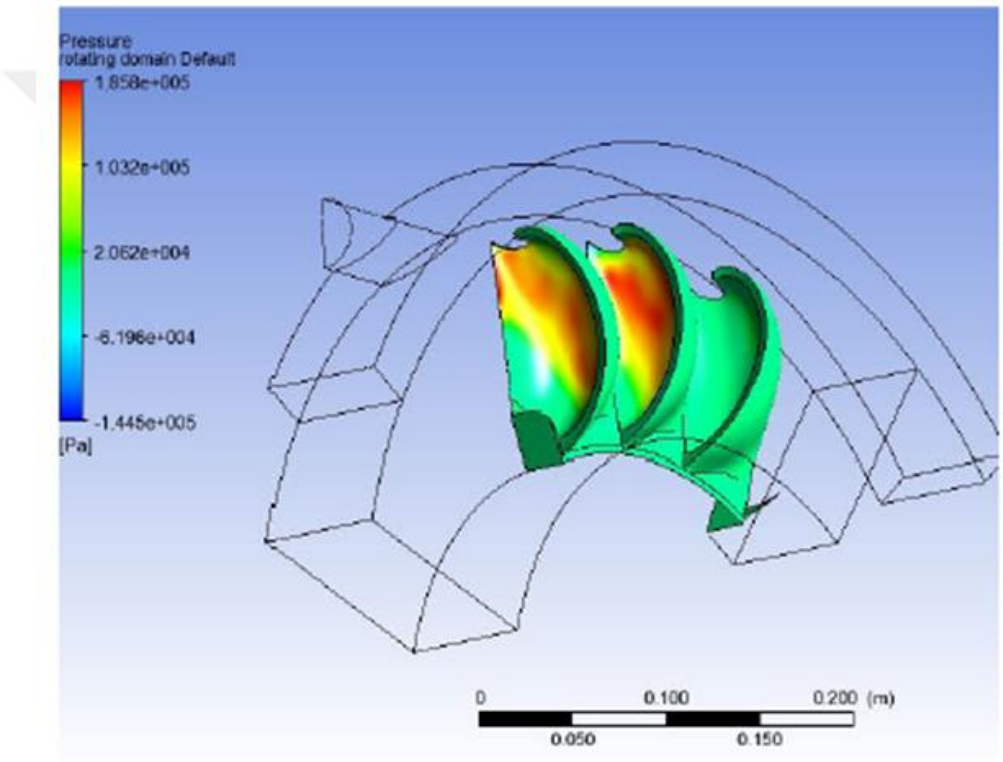

Figure 2.8. Shows that the pressure distribution (Sanam et al., 2014).

Raj (2009), investigated the pelton wheel design modifications.The common design of the pelton wheel was altered and assessed for the purpose of making it usable for low-head and heavy-discharge cases.Primarily, during operation, the runner wheel devours the kinetic and potetial energy produced by the flowing water which led to creating design alterations for the Pelton wheel considering also the water jet's gravitational influence.This modified Pelton wheel turbine can power up heavy generators with lowhead and heavy-discharge cases.

Vishal Gupta et al. (2012), carreid outa comparison between the circular and rectangular jet of a Pelton bucket relative to the flow attribute.The analysis was done using the numerical multi phase flow simulation and the results were closely tied up when the numerical and theoretical results were assessed against the common bucket profile.

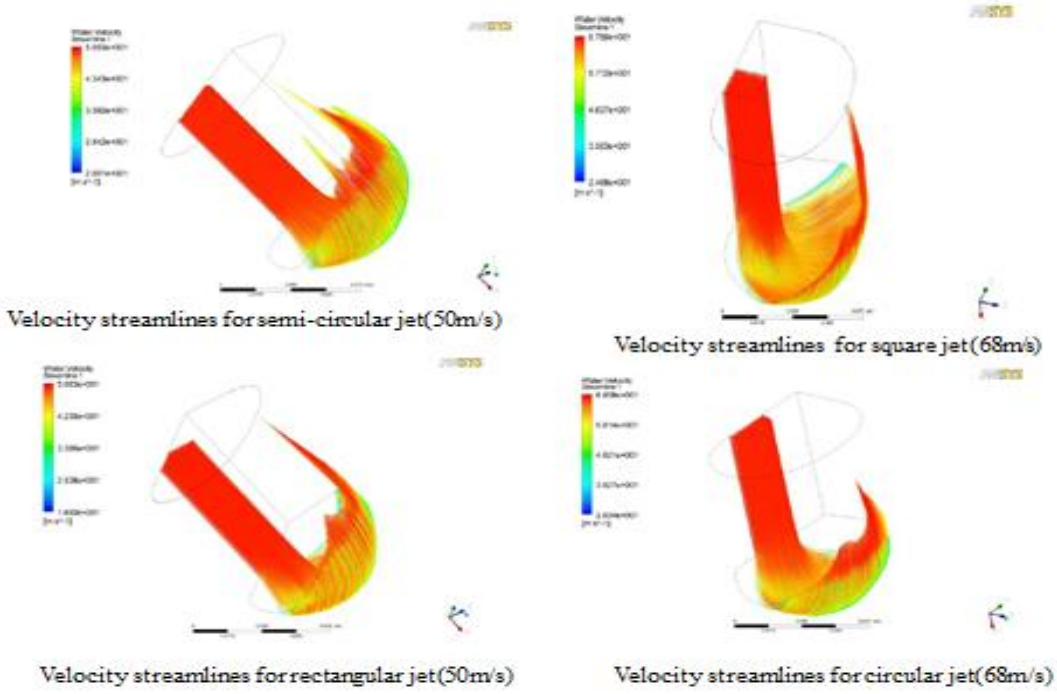

Figure 2.9. Shows that the velocity streamlines for different shape of jet (Vishal Gupta et al.,2012).

Alexander et al. (2006), evaluated the outcomes in the free surface flow analysis in a Pelton turbine model bucket. The analysis and simulation was conducted using the unsteady numerical simulation outlined from the two-phase homogenous model and data provided on measurementswall pressure and flow illustrations. With the given results on the flow patterns and pressure signal shapes examination, five different areas in the bucket were determined in which the numerical simulation results were matched up to each of these areas. Moreover, the results permitted the analysis of the liquid flow patterns. The momentum transition from the water particles to the bucket illustrating the areas of the surface bucket where torque is highly caused to occur was also scrutinized.

The back portion of the bucket was also examined which turned out to have proven that the Coanda interaction between the water jet and the bucket cut-out area exists.

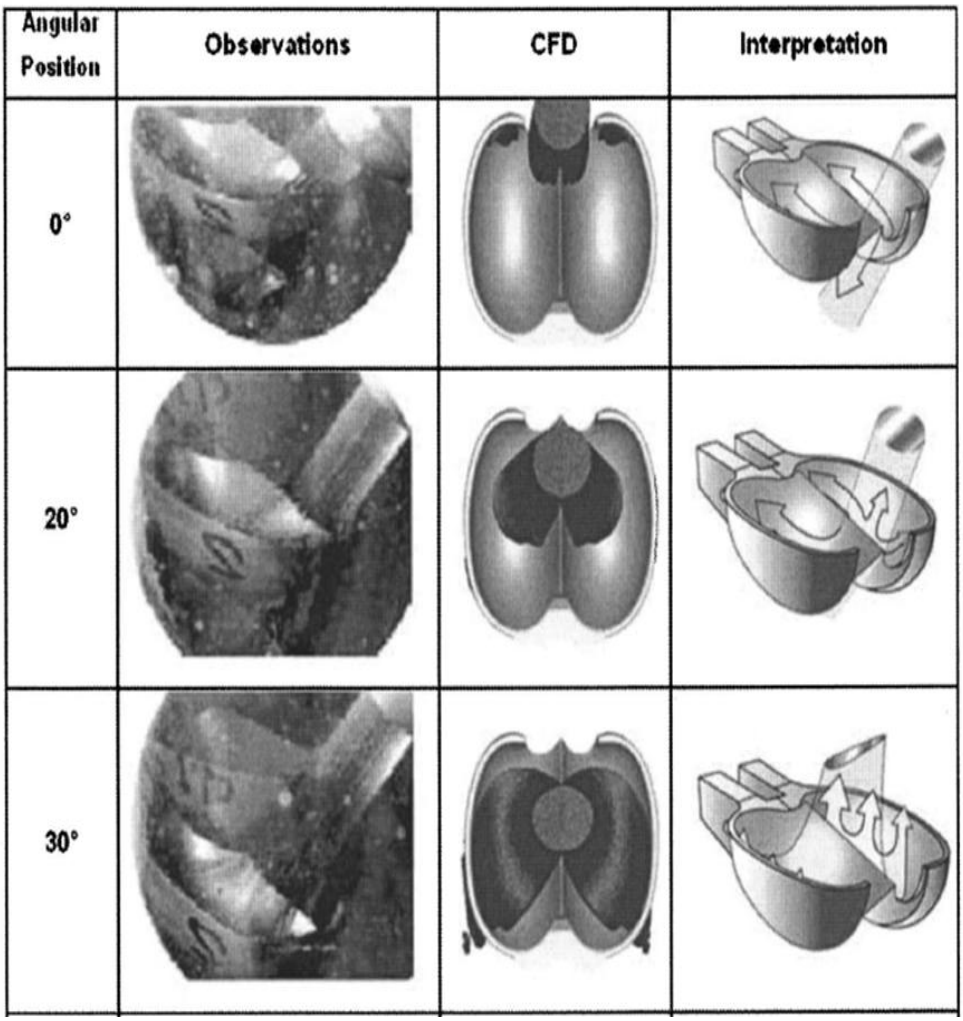

Figure 2.10. Shows that the evolution of flow pattern along the runner rotation angle. (Alexander et al., 2006).

Gaurangkumar et al. (2010), discussed and presented the conventional and hooped runners hydraulic comparison results mechanical's point of view. The hoop runner actual lab scale was designed and simulated to provide evidence of its value and contribution to its practical uses.

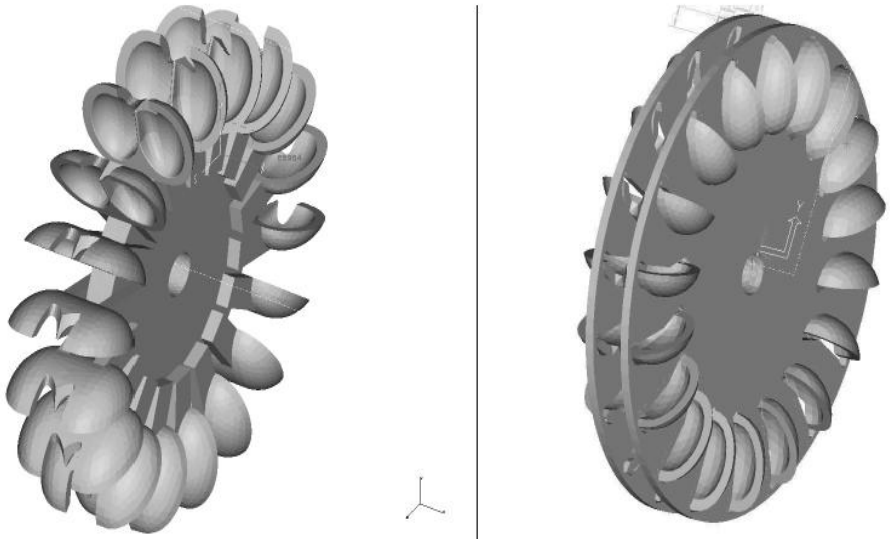

Figure 2.11. Shows that the 3D view of (traditional pelton runner& hooped pelton runner) (Gaurangkumar et al., 2010).

Alnakhlani et al. (2014), aimed to determine the maximum level of efficiency of a pelton turbine. The examination that was conducted in the energy conversion laboratory in sebelas maret University began with testing each type of pelton turbine with specific modifications each such as alterations in bucket volume, target bucket angle, seat ring of the nozzle's needle and its tip. With the specified modifications, the highest efficiency rate of 21.65% was established based from the comparison analysis provided that the needle seat ring is in 90° and needle tip at 45°, a bucket size increased to +15%, and angle of attack set to 92°.

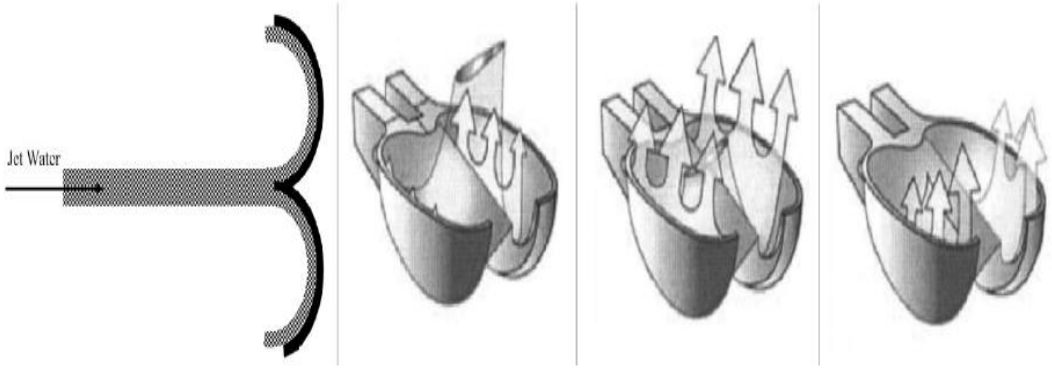

Figure 2.12. Shows that the Jet water (Alnakhlani et al., 2014).

Binaya et al.(2009), analysized four different shapes of buckets (DB01, DB02, DB03 and DB04) experimentaly with regards to its pressure distribution. During the conduct of the experiment, the flow and head rates were fixed and unchanged to arrive with valid results.There were three distinct angles in the bucket-jet incidence used in the measurement of the pressure distribution within the bucket's surface (inner part).Data angles used (closestdistance from the jet) are as follows: Normal to the jet: 0°, Inclinedoutwards: +15°, and Inclinedinwards: -15°.

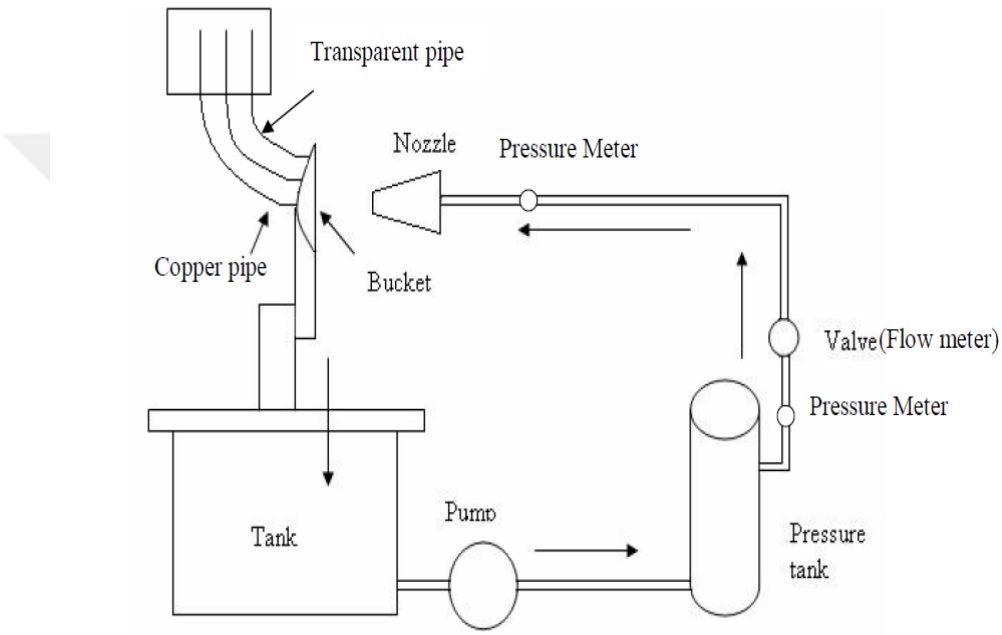

Figure 2.13. Shows that the bucket test rig (Binaya et al.,2009)

Zoppeet al. (2006), demonstrated of a flow analysis of a Pelton turbine in a fixed bucket. A thorough experiment and computational analysis was carried out to understand the case at hand so different values of the head, jet incidence, and flow rate were used to examine the full functional capabilities of the turbine. Measurements of the flow pressure and the torque were the results of the experimental analysis that was executed with the use of the software FLUENT employing the flow volume of fluid method (two-phase) after which results acquired were consistent with the experimental data.

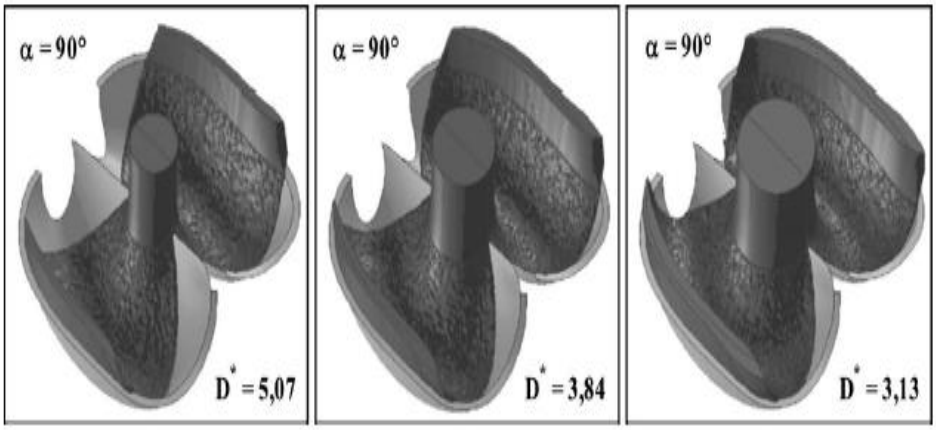

Figure 2.14. Shows that the free surface of the jet (Zoppe et al., 2006).

Chukwuneke et al. (2014), studied the impact of the angular positionof the head and bucket splitter on the power that a pelton turbine may produce. Primarily, it was concerned with the increased power generation using enhanced hydro-electric powergeneration mechanisms.The results of the experiment showed that when the pelton turbine has high head and low flow with high pressure produces more energy on the bucket splitter that enables the wheel to rotate in contrast with the low head and high flow operational status. Generally, the results illustrate that at 23° splitter angle, power generation is at its highest level, and descends at 21°, 15°, 10° and 3° providedwith different turbine speed of 1700, 1400, 1200 and1000rpm. In addition, it is shown that as the turbine speed increases, the force produced by the bucket also increases.

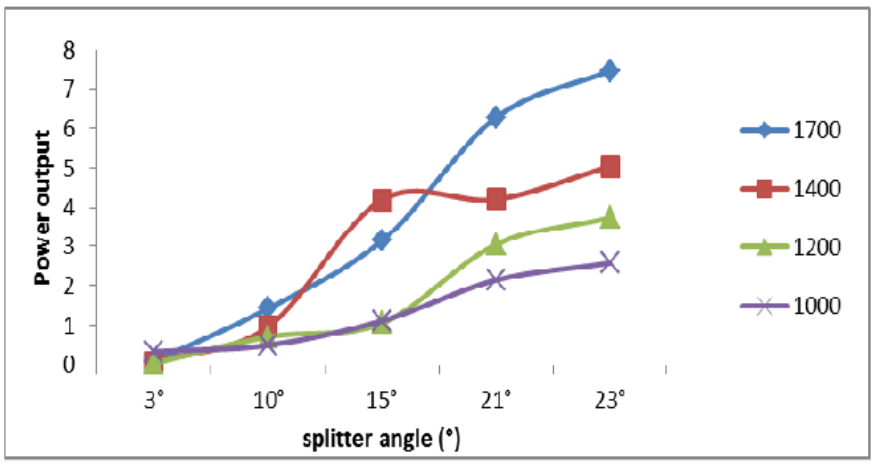

Figure 2.15. Shows the power output and splitter angle at different turbine speeds (Chukwuneke et al.,2014).

Nikhil et al. (2014), illustrated the Pelton bucket's underlying theories and experimental facts.The software CATIA V5 was used to model the pelton wheel bucket and its properties were investigated in a very specific manner so as to be used in the analysis utilizing the software ANSYS Workbench 14.0.The force and the pressure applied on the different areas of the bucket was taken into account to examine the bucket geometry including the stationary cases and the changes of the buckets' shape structural.The comparison between the theoretical results and computed interpretations was also conducted.

Ujam et al. (2014), presented the investigation results of the influence the head and the bucket splitter have on the pelton turbine's power generation. This was done for the purpose of increasing the power generation of any hydroelectric systems. The software MatLab was utilized in the development of the simulation program that aims to expose the amount of force the bucket generates when flowing water hits in given an actual splitter angle of 10-15 and predicted value ranging from 1-25. Other than the six actual splitter angles given, it was also tested with six other splitter angles, such as for high head and low flow with high pressure: 25, 6 and 19 for low head and high flow with low pressure: 23, 21, and 3, under two different operating conditions to validate its efficiency. The simulation results provide higher turbine power compared to the experimental results as the outcome for different head conditions and bucket splitter angles given.

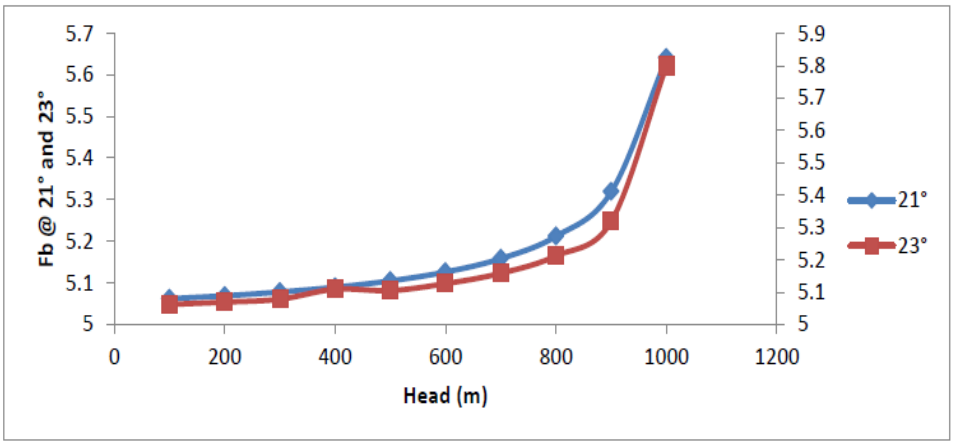

Figure 2.16. Shows the force generated on bucket at 21° & 23° splitter angle (Ujam et al., 2014).

3. MATERIAL AND METHOD

3.1. Computational Fluid Dynamics (CFD)

Computational fluid dynamics (CFD) is the process of investigating and designing of flow over wind and marine turbines, heat transfer, non-industrial and industrial CFD utilization are described in the followings;

- Analyzing river, ocean, streams flow and designing tidal and current turbines.
- examining the airplane and wind turbines aerodynamics.
- Medical investigations such as blood flows inside nervous system.
- Electronic and electrodynamics utilization such as cooling apparatuses for example micro circuits.
- Internal circulation of air, heating and wind load system of high and multistory buildings.
- Hydrological purposes like precipitation, meteorology, penetration and overflow.
- Environmental engineering like studying and analysis of pollutant mater.
- Chemical engineering, such as inchemical material mixing for separating them.
- Mechanical purposes, gas turbines and engines burning system.
- Hydrodynamics in Ship.

Starting from 1950s, the Computational fluid dynamics is utilized in aerodynamic design, production process of aircraft and jet engines and research and development. After that, methodology of Computational fluid dynamics has been utilizedfor designingengines internal burning system, furnaces and combustion chambers of gas turbines. In addition, it is utilizedfor predicting the lift and drag aircrafts forces and aerodynamics of mobile cars. Gradually, it is applied in designing industrial processes and products like a vital element.Providing a competence comparable with other CAE (computer-aided engineering) apparatuses like stress analysis codes are the idea of developments in the CFD field.

The followings are numerous incomparable advantageous of Computational fluid dynamics over experiment-based accesses to fluid systems design, for example:

- cheap and does not require long period.
- able for studying a great system that is complicated and difficult with experiment.
- Throughout the study, there is no hazard or risk.

Codes of CFD can supply very huge sizes of outcomes at efficientlytinycostsfor performing parametric studies (Versteeg and Malalasekra, 2007).

3.2. How does a CFD code works?

The entire commercial CFD packages include improved user boundaries to input problem parameters and for examining the outcomes CFD codes so as to prepare easy access to their solving power. These codes contain three key components: post-processor, solver and pre-processor.

3.3. Pre-processor

It is the input of a flow issue for a Computational fluid dynamics system by the way of an operator-friendly boundary and the following of alteration of this input into appropriate form for user. The costumer ought to do the subsequent things at the pre-processing phase;

- In this section, the geometry has to be defined like anarea of involvement.
- Mesh ought to be produced that is the partition of the domain into an amount of tinier and non-overlapping components.
- The chemical and physical phenomena ought to be chosen that is required to model.
- The whole fluid characteristic sought to be defined.
- The boundary condition definition ought to be made and divided the domain by name.

The Computational fluid dynamics solution accuracy is relying on the amount of nodes and components in the network. Thus, increasing the number of cells supplies enhanced alteration and precision. At inside each cell, the solution to a flow issue (turbulence, temperature, pressure, velocity, etc.) is defined. Because both of precisions

of solution and its expenses is associated with needed computer hardware, the fineness of grid is significant. The zones of the mesh which are sensitive to the difference sought to be finely meshed, bigger meshes are appropriate in other zones. With a character meshing capability, products are in development for developing Computational fluid dynamics codes. Lastly, this program automatically isolated the zone that big difference is happened and enhances it to less differed zone.

For defining the domain of the geometry and for mesh it, higher than 50% time of a CFD project is necessitated. So as to escalate productivity of CFD personnel, the whole major codes currently include their private CAD-style interface and/or facilities for importing data from proprietary surface modelers and mesh producer like PATRAN and I-DEAS. Present user admission to libraries of material characteristics for general liquids and a facility for invoking particular chemical and physical process models (for instance radioactive heat transfer, turbulence models, combustion models) beside the chief liquid stream equations are supplied by pre-processors.

3.4. Solver

The three different approaches of numerical solution techniques are Finite difference, finite element and spectral approach. For most of the CFD codes, the finite volume method is used. The following steps are included in numerical algorithms:

- The algebraic equations are solved by an iterative approach.
- Function replacement the of unidentified stream variables to the mathematical management in order to discrete.
- Alter or estimated the unidentified stream variables to a simple function.

The finite volume method from all other CFD techniques is classified by the control volume integration. Resulting statements demonstrate the precise preservation of related characteristics for every finite volume cell. The close relationship between underlying physical and the numerical algorithm conservation forms and makes its concepts much simpler to be understood by users compared to the finite element and spectral methods is the key responsibility of the finite volume method. The main phenomena of transport, convection transport because of liquid stream and

dissemination transport be differences of variables from position to position in addition to the source terms related with formation or dissemination of variables and the proportion of alteration in regards to time are treated by CFD codes as it contain appropriate separation methods. An iterative solution method is necessitated because the underlying physical phenomena are complex and non-linear. For ensuring as atisfactory association between pressure and velocity, process of solution is conducted by the TDMA (tri-diagonal matrix algorithm) line-by-line solver of the algebraic equations and SIMPLE algorithm because it has the most popular calculation process (Versteeg and Malalasekra, 2007).

3.5. Post Processor

In entire branches particularly in mechanics and hydraulics, the engineering workstations are well developed. Thus, a lot of development is occurred in post-processor field such as pre-processor numerous of which have exceptional graphics capabilities. Nowadays, the leading CFD package is equipped with visualization data apparatuses. The post-processor comprises:

- Show and display vectors
- Show the geometry and mesh generation of the entire domain.
- demonstrates the surfaces 2D and 3D.
- View surfaces, sections and domain flow.
- Demonstrate scaling, translation and rotating domain.
- Dispersed the zones of domain via color.

More freshly, these services might also contain animation for dynamic outcomes with graphics. (Versteeg and Malalasekra, 2007). This Figure demonstrates the stream chart the methodology of CFD work.

3.6. Turbulence

Flow properties where the viscous forces are tiny in comparison to the inertial forces are called Turbulence. In turbulent stream, the viscous force has no capabilityfor damping out tiny perturbations in border and primary condition. On the other hand, these perturbations are augmented resulting in rapid variation in velocity and pressure in time and space. The criterion to determining the force dominating (inertial or viscous) is the Reynolds number.

$$R_e = \frac{\rho V L}{\mu}$$

There is no clearly limit, for open channel, where Re the turbulence advanced in flow however frequently it takes more than 2000(Sam, 2010).

3.7. Turbulence Models in CFD

They are the models or processes of computational, which are utilized for simplifying the governing equations solution in an engineering utilization particularly for mechanical processes. It is required for representing scales of the stream that are not solved.

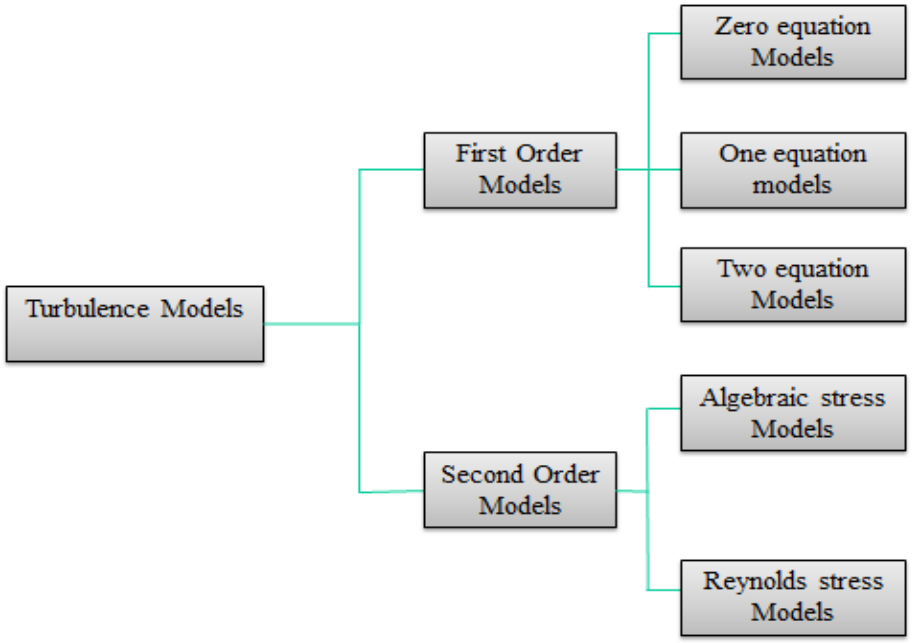

Figure 3.1. Classification turbulence models (Miller, 2010).

3.8. Reynolds Average Navier-Stokes Equations (RANS)

Turbulent streamcomprises fields of velocity that are fluctuating chaotically over a huge range of spatial and temporal scales. Capturing these fluctuations necessitates a highly resolved stream field and computationally intensive work whereas direct numerical simulation is possible. The Reynolds Averaging approach is a very popular alternative in CFD for modeling turbulent flow fields. In Reynolds Averaging the variables in the Navier-Stokes equations are decomposed into their mean and fluctuating components, known as Reynolds Decomposition (Pope, 2008). In accordance to Newton's second law of motion for liquid stream, the continuity equation can be written as (Taylor, 2012).

3.8.1. The standard k-epsilon model

The terms and*k* denote to the kinetic turbulence energy, which are the fluctuations difference in velocity. The viscosity multiplied by the fluctuating vortices is equal to turbulence eddy dissipation. A precise transport equation for the vortices

fluctuation definite as proportion of dissipation of fluctuations of velocity (SarvanMamaidi, 2009).

3.8.2. The RNG k-ε model

It is employed for incompressible flows. It is similar to the standard *k-e* model, but includes some improvements as follows (Miller, 2010);

- It has an additional term in the equation to improve the accuracy.
- The RNG models have enhanced accuracy for swirling flows.
- Instead of the user-specified, constant-value turbulent Prandtl numbers implemented with the standard *k-ε*model.

3.8.3. TheRealizable k-εmodel

For incompressible streams, The RNG k-εmodelis utilized. This is same as the standard *k-e* model, nevertheless, itcomprisesof several enhancements as follows (Miller, 2010);

- for swirling flows, The RNG models have improved accurateness.
- for improving the accuracy, it has an additional term in the *ε*equation.
- constant-value turbulent Prandtl numbers applied with the standard *k-ε*model, instead of the user-identified.

3.8.4. The realizable k-ε model

In the realizable *k-ε*developmentsare:

- Instead of constant, variable $C\mu$is utilized.
- for ε the equation is enhanced.
- Shares the same turbulent kinetic energy equation as the standard *k-ε* model.

- Enhanced performance for streams including aground and planer jets. The model expects the round jet dispersal appropriately.

3.8.4. Standard k-omega model

The terms *k* and *omega* represent two transport equations turbulent frequency and turbulent kinetic energy, correspondingly. The values are computed based on the concept of eddy-viscosity (SarvanMamaidi, 2009).

3.9. Large Eddy Simulation (LES)

From the other liquid stream, computation methods Large-eddy simulations (LES) are differed. The biggest eddies are clearly solved and the minor eddies are modeled in this simulation method. Even though the real large-eddy simulations of the atmosphere and ocean are astonishingly occasional, modeling the ocean and atmosphere stimulated the first large-eddy simulations. For incompressible flow, The LES equations designate the evolution of the large-scale eddy in the flow-field (Goldstein, 2004).

3.10. Mathematical Model and Equations Utilizing.

3.10.1. Reynolds number

It has to be identified for determining the regime of turbulent or laminar stream. The average velocity, characteristic length of geometry and fluid properties are influencing the alteration from laminar to turbulent flow. In general, Re can be expressed as for two phases flow.

$$\mathrm{Re} = \frac{\text{Inertial forces}}{\text{viscous forces}} = \frac{\mathrm{VD}}{\mathrm{v}} = \rho \mathrm{vl}/\mu \quad (3.1)$$

μ Viscosity of fluid.

ρ Density of fluid.

L length

V velocity of fluid

The flow regime classification according to the Reynolds number for a below

Laminar flow Re ≤2300

Transitional flow 2300 ≤Re ≤4000

Turbulent flow Re ≥4000

3.10.2. Flow low through nozzle

Gradually, a nozzle is a converging short tube, which is fixed at the outlet and of the penstock for the conversion of total energy of the flowing water into kinetic energy. Nozzles are utilized in which elevated velocities of flow are needed to be advanced. In impulse turbines, it is necessitated for hydraulic energy into kinetic energy.

$$Q = a_1 v_1 = a_2 v_2 \quad (3.2)$$

The nozzle is horizontal, the nozzle axis is assumed as datum for elevation, and hence head at nozzle is given by,

$$\mathrm{H} = \frac{\mathrm{v}^2}{2\mathrm{g}} + \frac{\mathrm{p}}{\gamma} \quad (3.3)$$

$$\mathrm{H_j} = C v^2 \mathrm{H}_n \quad (3.4)$$

$$V_\mathrm{j} = C_v \sqrt{2g\mathrm{H}_n} \quad (3.5)$$

The governing equations of viscous flow are based on conservation of mass, momentum and energy which are lagrangian in nature. The governing equations are expressed using equations.

3.10.3. Continuity equation

The increase rate of the liquid mass restricted inside the zone have to be equal to the variance between the proportion where the liquid mass go into the zone and the rate where the mass departs the zone. Nonetheless, the escalation rate of fluid mass within the region is equal to zero when the flow is steady. At that point, the proportion where the mass of the fluid penetrates the zone is equal to the proportion where the mass of liquid departs the zone.

$$\nabla.(\rho v^{\rightarrow}) = 0 \tag{3.6}$$

In addition, the general quantity equation can also be expressed differently, as the following (Ansys fluent theory, 2009).

$$(\partial u/\partial x) + (\partial v/\partial y) + (\partial w/\partial z) = 0 \tag{3.7}$$

3.10.4. Momentum equation

Through the field, a sole momentum equation is solved, and the resultant of the field velocity is shared among the phases. As demonstrated below that the momentum equation relies on the volume fractions of all phases during the properties ρ and μ.

$$\nabla \cdot (\rho vv) = -\nabla p + \nabla \cdot [\mu(\nabla v + \nabla Vt)] + \rho g + F \tag{3.8}$$

As big velocity difference exists among the phases, the correctness of the velocities calculated close to the interface might be fascinated unpleasantly, this isa on case restriction of the shared-fields (Ansys fluent theory, 2009; Computational analysis for multi-phase flow in helical water, 2006; Xia, 2004).

3.11. Simulation and Procedure Modeling

3.11.1. Volume of fluid

For fixed Eulerian mesh, the model of surface-tracking techniques is utilized. The Volume of fluid is planned for two or more unmixable fluids at which the location of the interface between the fluids is of interest. In this model, the fluids share a single set of momentum equations, and the volume fraction of every fluid in each computational cell is followed during the field.

3.11.2. Numerical solver

The second very significant step of the CFD process is the numerical solver or solution. The utilization of a CFD code subsequent reiterations and discretization until convergence is achieved solution of the equations governing of the fluid flow issue is attained. In different word, a solution algorithm comprises the subsequent stages:

a. Function replacement of unidentified stream parameters for the mathematical manipulation in order tobe separated.
b. Convert the diversity of unknown stream parameter for any model to a simple function.
c. Lastly, resolve the entire equations via an iterative approach.

Hence, this part also encompasses the liquid characterization definition such as velocity, viscosity, density, etc.... and the selection of stream models, for example, mixture model.

3.11.3. Stages of calculation

In this step, illumination and analyses of the results, which obtained from above solution steps, are conducted. In accordance to the demand the geometry and mesh creation of vectors whole domain, view sections the surfaces 2D and 3D, translation,

scaling, rotating domain, surfaces, separating the regions of domain by color and XY plots and graphs of outcomes are possible to attained.

3.11.4. Simulation techniques

In this method, ANSYS-FLUENT requires geometry, mesh, and solver settings definition for computing the necessary results. The modeling and simulation procedure gradually from pre-processing to post-processing phases are nominated correspondingly. In this investigation, ANSYS- FLUENT version 14.5 on a Computer (HP) is employed. For defining the impact of altering geometry parameters such as flow parameters, diameters and splitter angle, a series of CFD simulations as a parametric study is utilized as a study methodology. The VOF is a highly important step for any simulations as it includes the preliminary concept and creation of the model. By design modular in ANSYS Workbench in this study, the Mixture model is produced. Then, the geometry is meshed utilizing ANSYS meshing platform. The viscosity, density, and boundary conditions such as velocity, pressure and volume fraction water liquid and air the physical characteristics of the fluid.

3.11.5. Generating the model and describing the geometry

The formation of the flow geometry is the first step in any engineering flow simulation. This could be generated via the utilization of ANSYS Design Modular in ANSYS workbench, or any CAD program. Then, it moved to the ANSYS workbench. ANSYS Design Modular in ANSYS workbench was applied in creating geometry in this study. As long as the stream acknowledged in the Y direction, a sketch of the pelton turbine is created on the XYZ base plane. The two models, which utilized in this research, have alike length of the nozzle and bucket, diameter of the nozzle and splitter angle between bucket and nozzle. As obviously indicated in figures (3.1and3.2), Both models have length of the nozzle 110 mm and width of the bucket 160mm. the major evident variances between both models, however, is the shape of the bucket. For both models, different diameter of the nozzle (30mm and 40mm) is applied. The splitter angle between nozzle and bucket were (55, 75, 90 and 115). The top and bottom of the

geometry is termed wall, in the system, and the end of boundary is termed outlet and the left side called inlet.

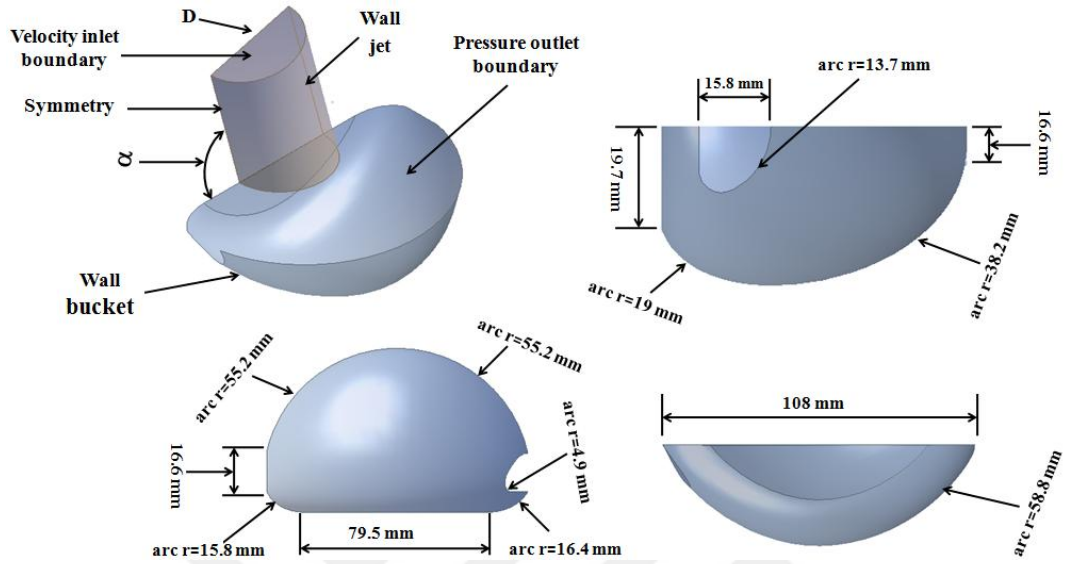

Figure 3.2. Solution domain and boundary conditions of the model 1.

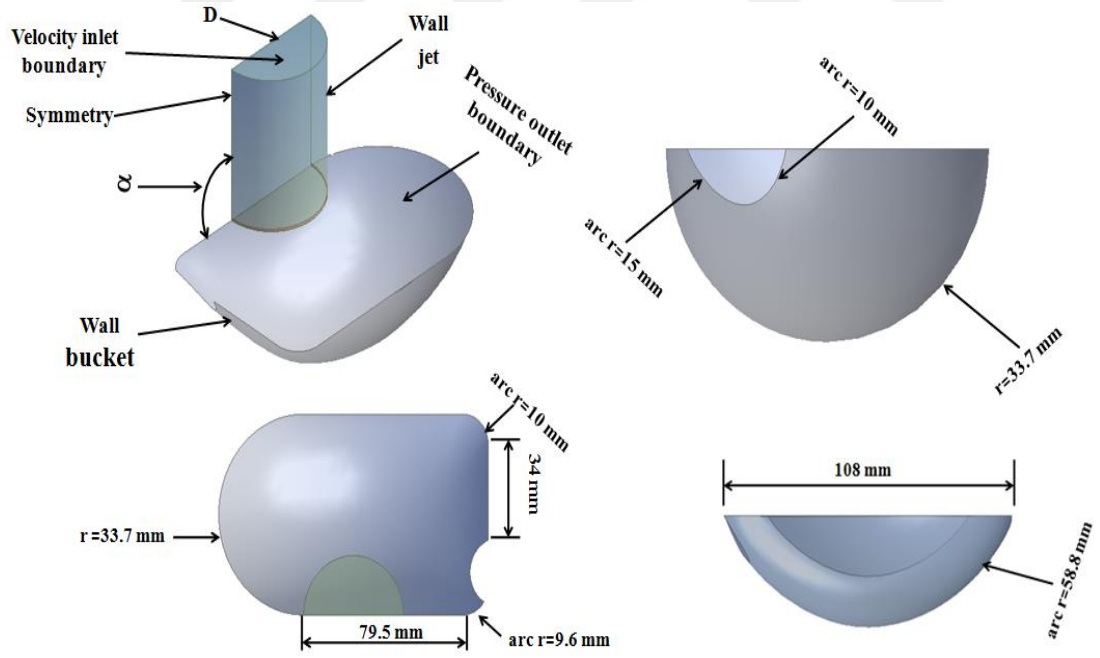

Figure 3.3. Solution domain and boundary conditions of the model 2.

3.11.5.1. Generating mesh

For successful numerical and mathematical simulations, a great property of mesh is very significant. As demonstrated in figure 3.3and3.4, the more detailed and precise stream construction will be arrested, the lesser the volume of the element close the wall of the tube and the slot. Nevertheless, for the three-dimension simulation, a tiny adjustment in the volume of element will results in a significant escalation in the numeral of elements. This results in a vital escalation of computational time. So as to balance the precision of the simulations and (CPU) time, an optimum volume of mesh requirement to be designated**.** By the mesh independence, study the optimum mesh size is nominated. The smallest size of mesh is set to be lower than the first layer thickness close to the wall. For avoiding inappropriate automatic mesh generation in FLUENT program, the minimum mesh sizes are set as 1.5996e-010 m. Lastly, the proportion of the mesh size between two neighboring elements ought to be no larger than 1.5. On this ground, the escalation proportion between two neighboring meshes has been set to 1.2 indicating that five layers are needed for achieving the near-maximum side mesh size. All figures about meshes quality indicated clearly in figure 3.4and 3.5.For both models, Table 3.1 displays meshes element volume with altering length of the throat. ANSYS-FLUENT comprises a novel method, the sweep method, for capturing the free surface stream profile for stream. It should be reported that more mesh provides force on the bucket instead of escalating number elements do not influence the precision. Incidentally, relying on nature of the problem, which illustrated in table 3.2, the difference in the mesh independent test, can be up to 4 % or5%. Refining the mesh size along the direction normal to the flow direction is the purpose of this technique.

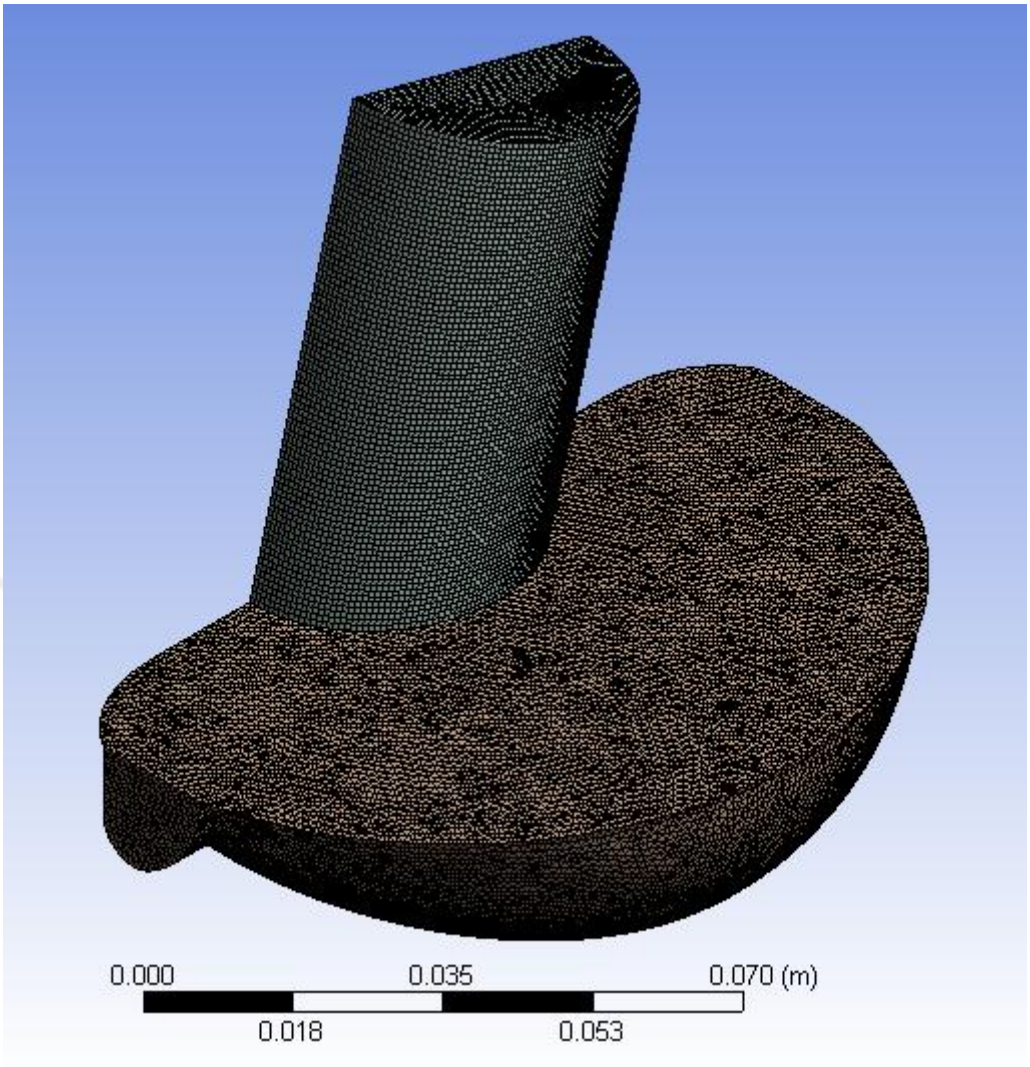

Figure 3.4. Shows full size mesh elements for model 1.

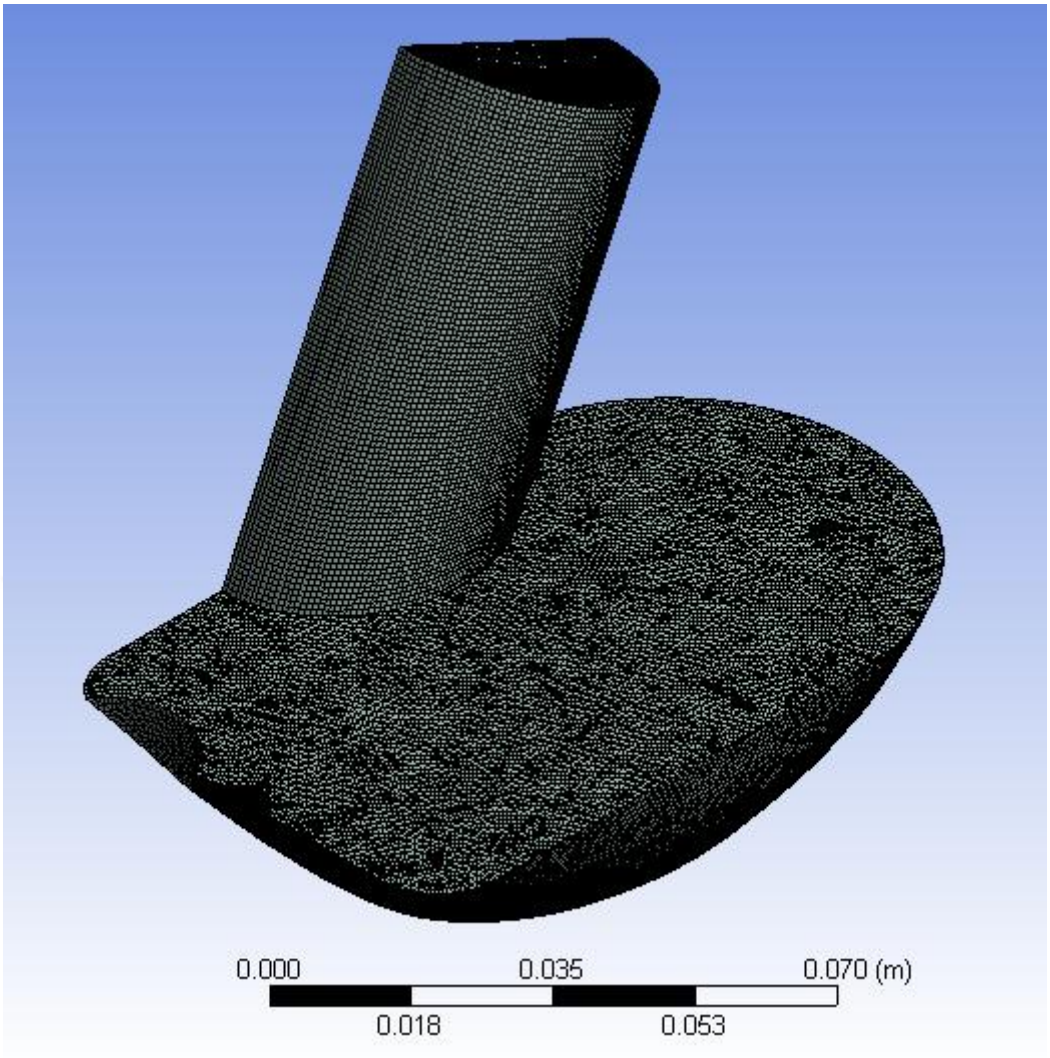

Figure 3.5. Shows full size mesh elements for model 2.

Table 3.1. Denotes investigation of mesh dependence

Number of element	Force on the bucket(N)	Difference (%)
331694	1310	2.6
658152	1324	1.56
966322	1335	0.74
1299188	1345	0

3.11.5.2. The physical technique

In this investigation, implicit formulation and Force solver are elected. In this examination, a multiphase three-dimension plane shape ax symmetric, applied a volume of the liquid model for multi-phase stream. For simulating the characteristics of the two-phase flow, RNG k- epsilon models are utilized.

3.11.5.3. Fluid properties

For the computational domain of the models, thewater liquid was implemented. As illustrated in Table 3.2, the water is elected as main phase hence the water -liquid is elected a primary phase as the water -liquid is bigger compared to the air as a secondary phase is selected.

Table 3.2. The fluid properties of each phase are given

Property	Water liquid	Air
Density	998.2	1.225
Viscosity	0.001003	$1.7894e-05$

3.11.5.4. Boundary conditions

The boundary condition of inlet velocity is imposed at the center of the boundary, the boundary condition outlet pressure is imposed at the exit of the boundary utilizing as for examination of body force required velocity of the stream in inlet and outlet as demonstrated in table 3.3.

Table 3.3. Shows all boundary conditions

Surface	Boundary conditions
Inlet	Velocity inlet
Outlet	pressure outlet
Wall	Wall-bucket
Wall	Wall-nozzle

3.11.5.5. Finding the model and initializations

Here, the properties of turbulent stream are defined and introduced. The inlet is taken as reference for initializing the solution. Relative to inlet, the active reference frame is selected. The velocity inlet input in the Y-direction; hence, the outlet pressure illustrated. In the present calculations, residual is set for continuity, volume fraction, turbulent flows, and pressure out let.

3.11.5.6. Post processing

The necessitated outcomes, in the post-processing phase, are water and air volume of fraction and velocity of streamline of every phase can be separated. The plot kind in various styles of the vector or contour can be gained. In Chapter four, the post-processing outcomes of this study are provided.

4. RESULTS AND DISCUSSION

The study's outcomes are very close to the journal result particularly when the fluid, model and geometries were the same, as displayed in figure (4.1). For finding the correct model for this research, this comparison has conducted. This journal has been chosen for discovering the accurate models for this research because it is close to our investigation. The results of both researches are close to each other. Thus, it can be stated that the model of this research is accurate. Experimental, numerical and computational studies in literature must be used to prove the accuracy of any study. Figure (4.1) give a comparison of experimental and numerical data taken from (zoppe et al., 2006) and (gupta and Prasad, 2012) application by (CFD) work after application see that both of two results near this investigate that too sure that my working is true and easy to determine models of (CFD). This experimental work and application by (CFD) this result after application near of (CFD) results. In this journal paper utilized a two phase flow (free surface), three dimensions for a geometry and turbulent flow. Modeling using to visualization flow on the bucket and determine a force on the bucket. VOF used and velocity inlet and pressure outlet. This figure indicated that the diameter increases to decrease the force on the bucket when the splitter angle 90°, velocity =28 m/s.

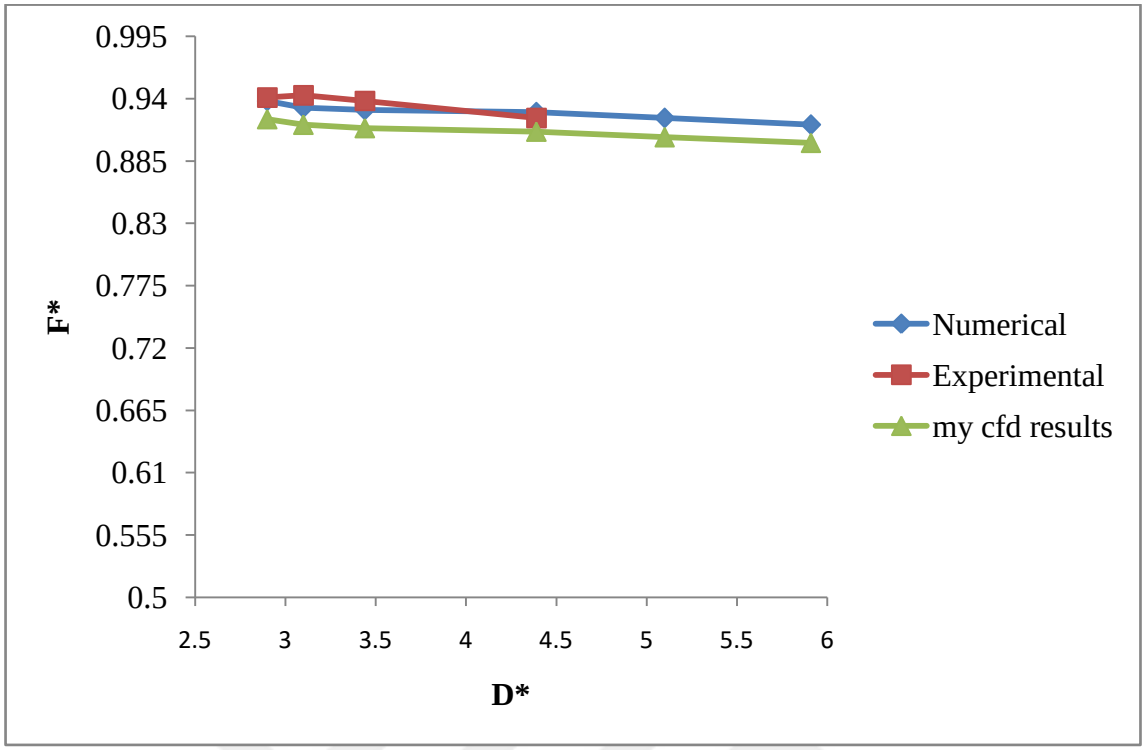

Figure 4.1. Shows the difference between my CFD result and journal paper result (Zoppe et al., 2006).

4.1. The effect of the Version Pressure

The pressure distribution and calculation are displayed in this figure. In the splitter angle (55 degree), the pressure distribution in the bottom edge are varied according to the jet strike of the flow; and the generated pressure on the bucket in this splitter angle is low because the water force is divided into two components, one of these components does not affect the bucket (according to impulse- momentum principle). Furthermore, another reason for the low pressure in the splitter angle of 55 degree is that there is a flow leakage through the bottom edge. In addition, in the splitter angle (75 degree), the effect of pressure is located near the middle of the bucket and the pressure value was greater than 55 and 115 degree, moreover the leakage of the flow is less in comparison to the splitter angle (55 and 115). Regarding the splitter angle 115 degree, the pressure value is lower than in the splitter angle of 115 and 90 degree while it is higher than 55 degree splitter angle. Additionally, the location of the pressure is positioned at the top near the cut off. On the other hand, the pressure distribution in the splitter angle of 90 degree is located at the middle of the bucket and there is no leakage.

In addition, the pressure value is the highest in comparison to the splitter angle of (55, 75 and 115 degree). This is because the proportion of the alteration of the momentum is equal to the applied force and occurred in the force direction. The results agree with (Gupta and Prasad, 2012) and (Zoppe et al, 2006).

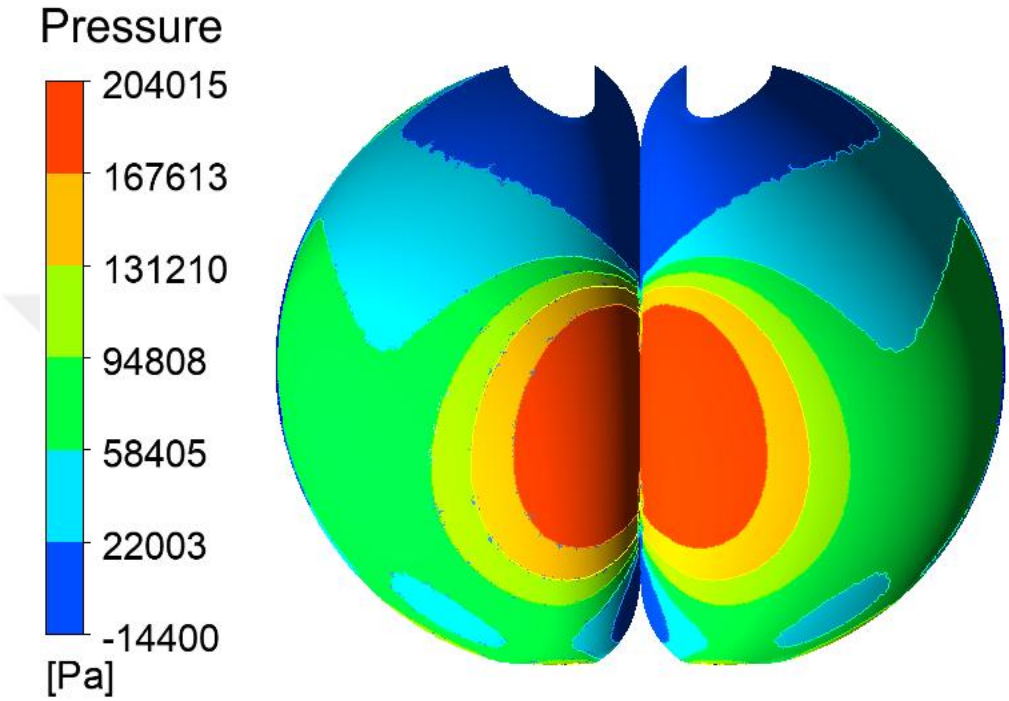

Figure 4.2. Demonstrates variation of pressure when velocity =20 m/s, diameter =40mm and splitter angle=55 degree for model 1.

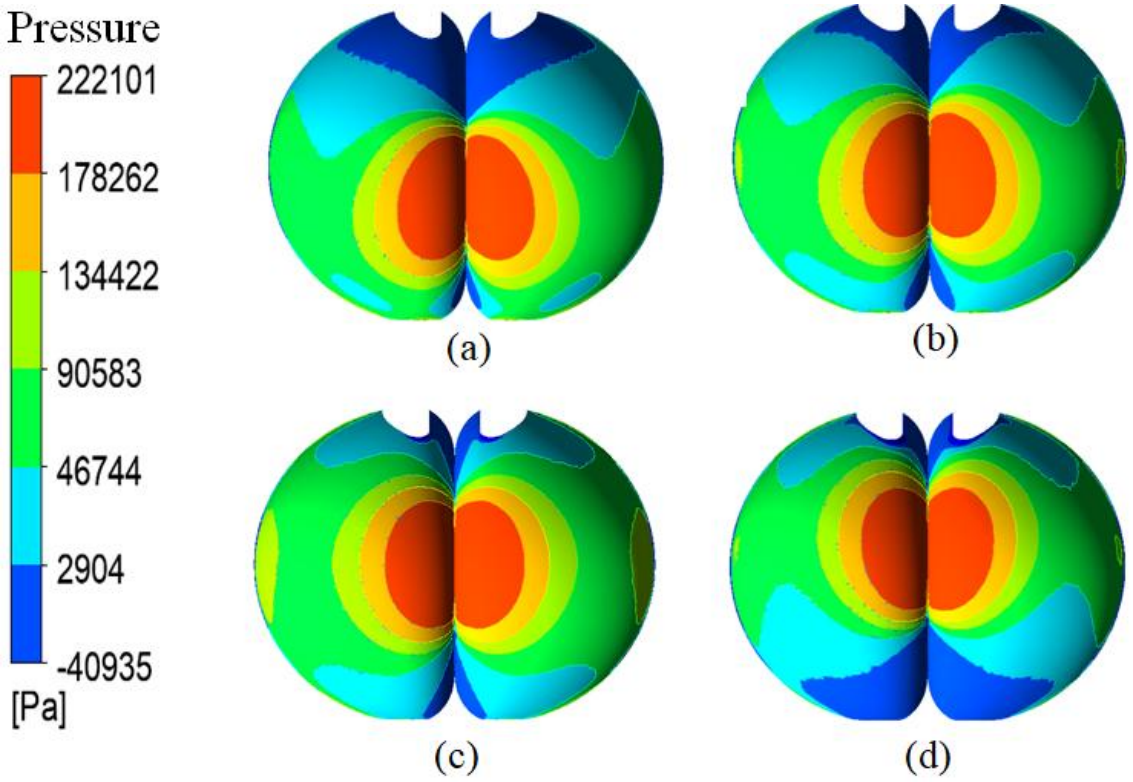

Figure 4.3. Demonstrates variation of pressure when velocity =20 m/s and diameter =40mm for model 1 at figure (a) splitter angle=55 degree, (b) splitter angle=75 degree, (c) splitter angle=90 degree and (d) splitter angle=115 degree.

The calculation and distribution of pressure are shown in this figure. The pressure distribution, In the splitter angle (55 degree), in the bottom edge are differed in accordance to the jet strike of the stream; and the produced pressure on the bucket in this splitter angle is low because the water force is divided into two components, one of these constituent does not impact the bucket (according to impulse- momentum principle). Moreover, a flow leakage through the bottom edge is another reason for the low pressure in the splitter angle of 55 degrees. In addition, the effect of pressure is located near the middle of the bucket in the splitter angle (75 degree) and the pressure value was greater than 55 and 115 degrees, moreover the leakage of the flow is less in comparison to the splitter angle (55 and 115). In regards to the splitter angle 115 degree, the pressure value is less compared to the splitter angle of 115 and 90 degrees where as it is higher than 55 degree splitter angle. In addition, the site of the pressure is positioned at the top near the cut off. Conversely, the distribution of pressure in the splitter angle of 90 degree is situated at the middle of the bucket and there is no leakage.

additionally, the pressure value is the biggest compared to the splitter angle of (55, 75 and 115 degree). This is because the proportion of the alteration of the momentum is equal to the applied force and occurred in the force direction.

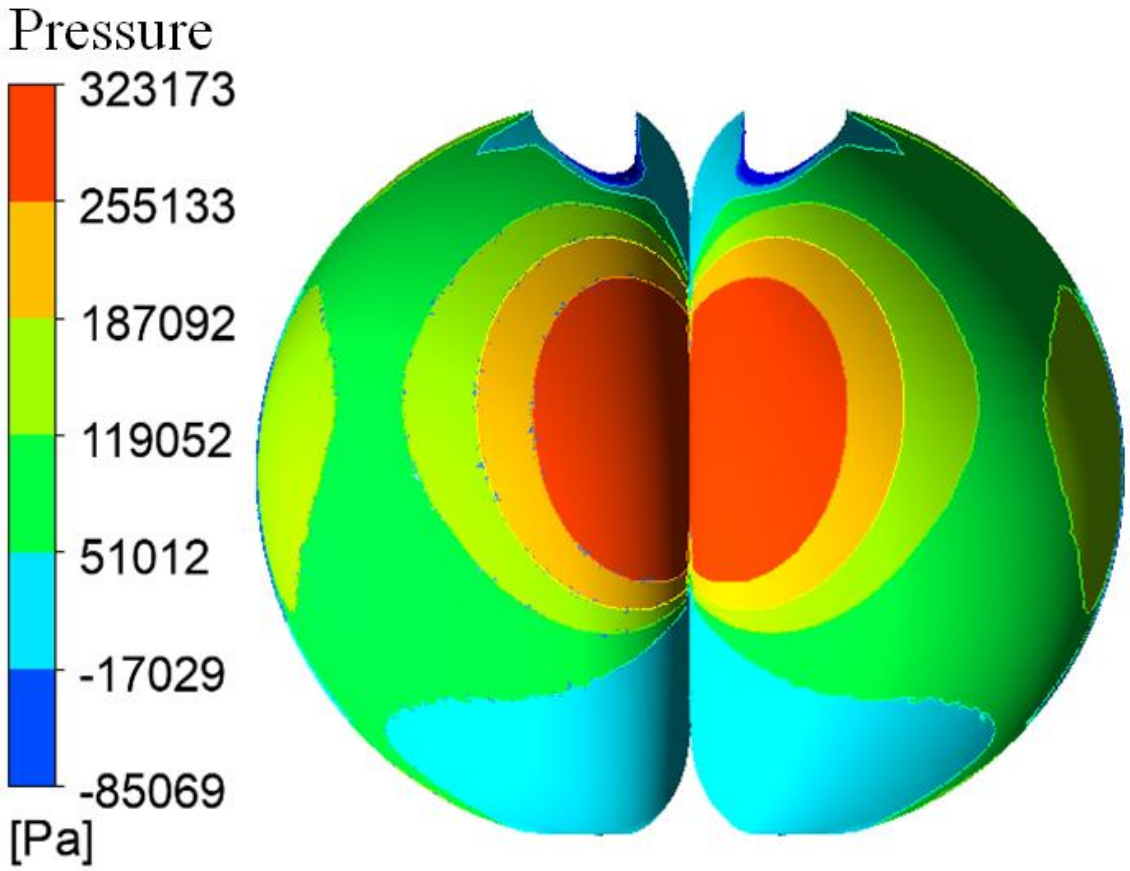

Figure 4.4. Demonstrates variation of pressure when velocity =25 m/s, diameter =40mm and splitter angle=115 degree for model 1.

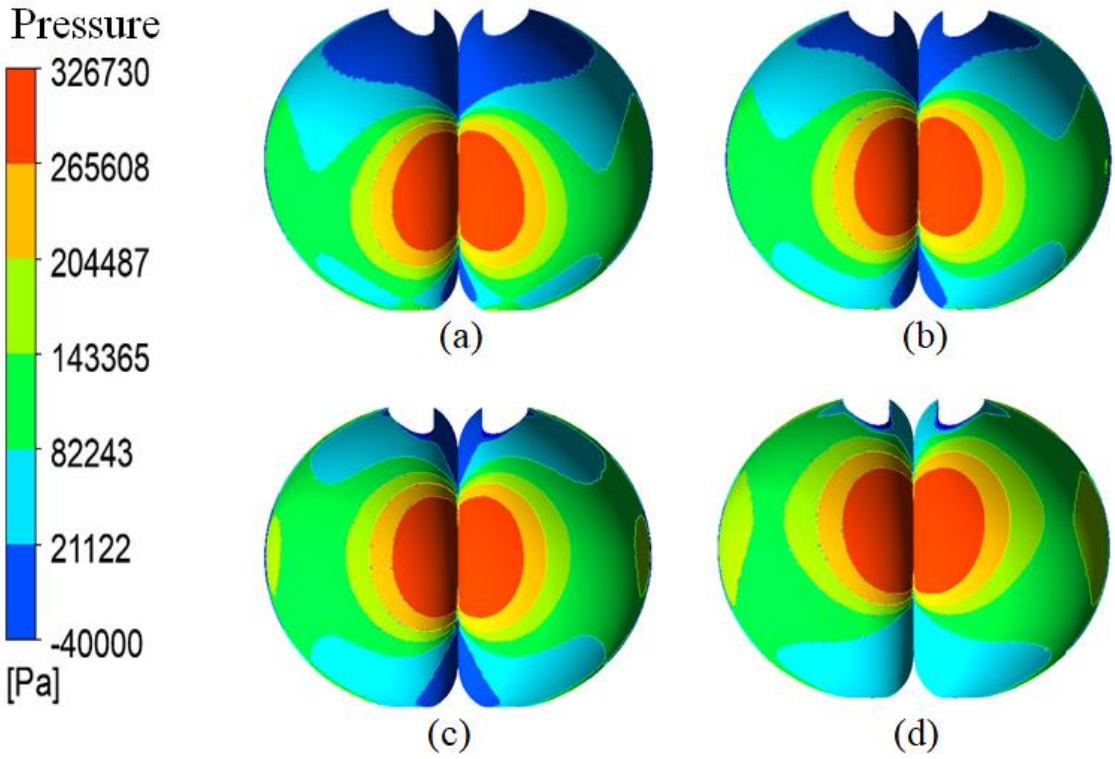

Figure 4.5. Demonstrates variation of pressure when velocity =25 m/s and diameter =40mm for model 1 at figure (a) splitter angle=55 degree, (b) splitter angle=75 degree, (c) splitter angle=90 degree and (d) splitter angle=115 degree.

In this figure, the calculation and distribution of pressure are illustrated. The distribution of pressure in the bottom edge are differed in accordance to the jet strike of the stream, In the splitter angle (55 degree). Because the water force is divided into two components, one of these constituent does not impact the bucket (according to impulse-momentum principle), the pressure generated on the bucket in this splitter angle is low. Moreover, a flow leakage through the bottom edge is another reason for the low pressure in the splitter angle of 55 degree. Furthermore, in the splitter angle (75 degree), the impact of pressure is sited close the middle of the bucket and the pressure value was greater than 55 and 115 degrees, moreover the leakage of the flow is less in comparison to the splitter angle (55 and 115). However, in the splitter angle 115 degree, the pressure value is less compared to the splitter angle of 115 and 90 degree whereas it is higher than 55 degree splitter angle. In addition, the site of the pressure is positioned at the top near the cut off. On the contrary, the distribution of pressure is situated at the middle of

the bucket and there is no leakage in the splitter angle of 90 degree. Additionally, the pressure value is the biggest compared to the splitter angle of (55, 75 and 115 degree). This might be due to the proportion of the alteration of the momentum is equal to the applied force and occurred in the force direction. The outcomes agree with (Gupta and Prasad, 2012) and (Zoppe et al., 2006).

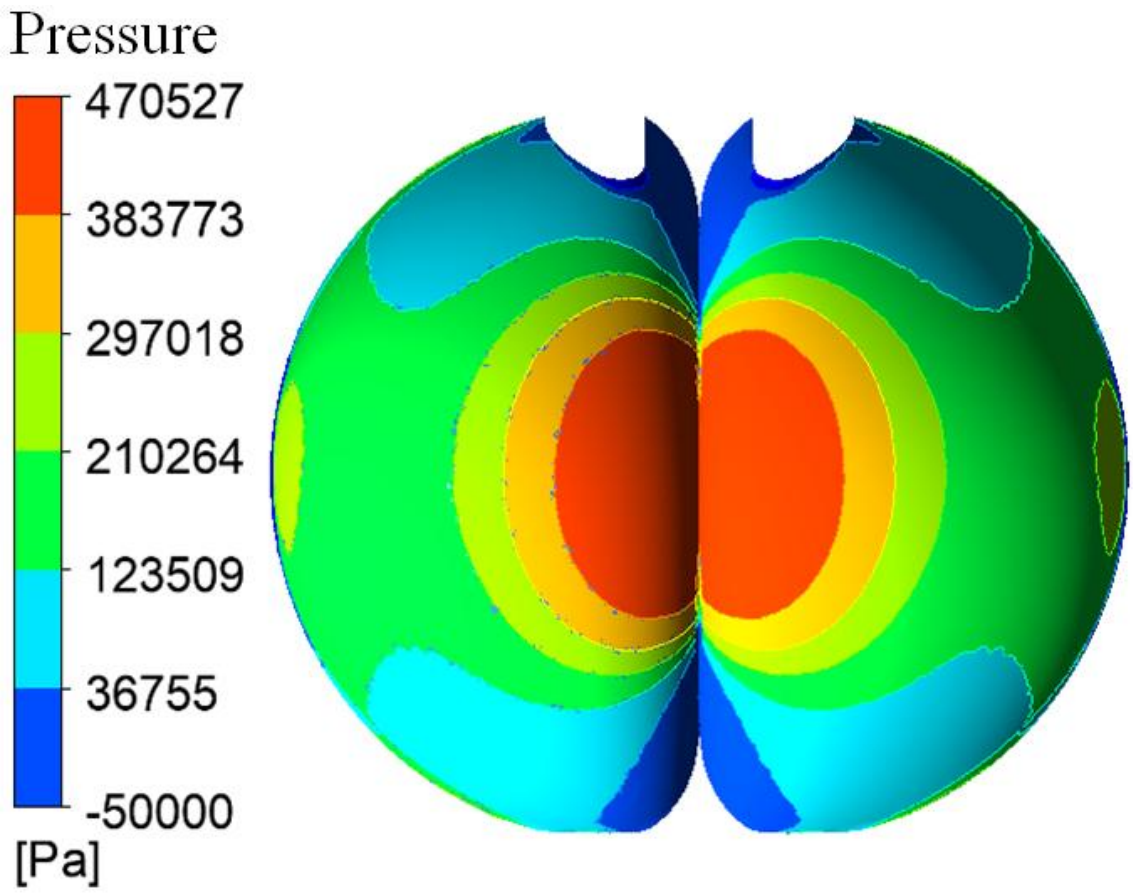

Figure 4.6. Demonstrates variation of pressure when velocity =30 m/s, diameter =40mm and splitter angle=90 degree for model 1.

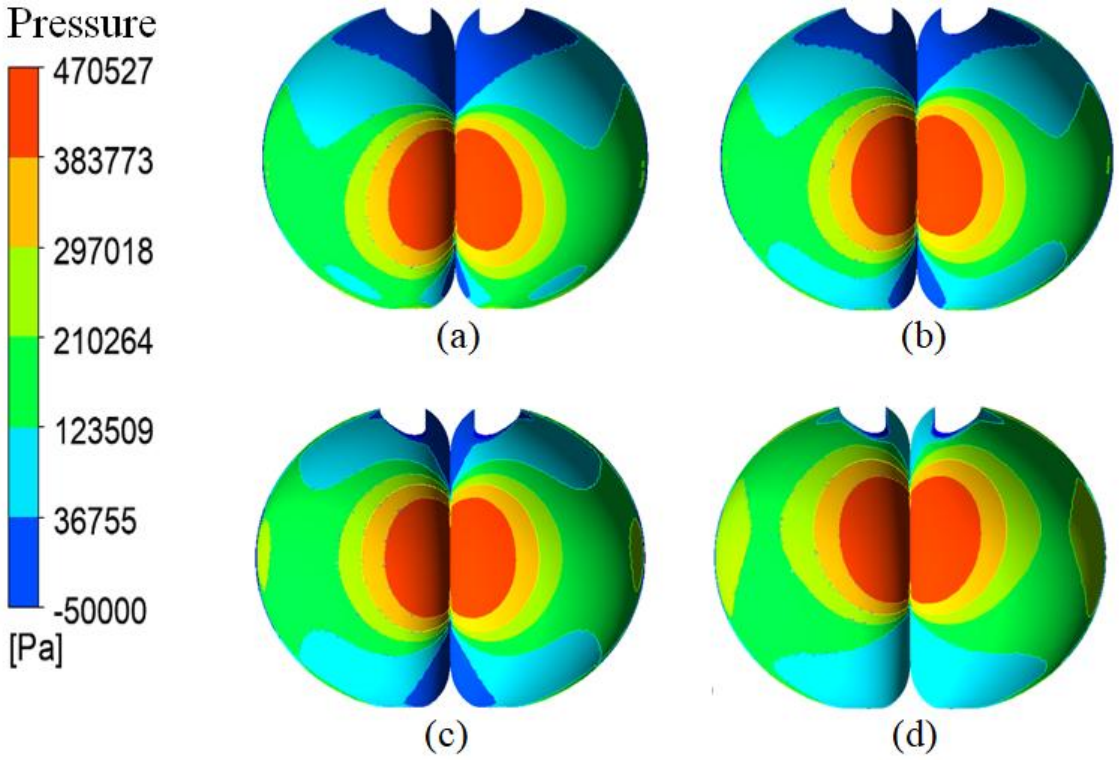

Figure 4.7. Demonstrates variation of pressure when velocity =30 m/s and diameter =40mm for model 1 at figure (a) splitter angle=55 degree, (b) splitter angle=75 degree, (c) splitter angle=90 degree and (d) splitter angle=115 degree.

The calculation and distribution of pressure are demonstrated in figures (4.8and 4.9). In accordance to the jet strike of the stream, the pressure distribution in the bottom edge is differed, in the splitter angle (55 degree). As the water force is alienated into two parts, one of these part does not influence the bucket (according to impulse- momentum principle), the pressure generated on the bucket in this splitter angle is low. Moreover, a stream leakage during the bottom edge is another cause for the low pressure in the splitter angle of 55 degree. Additionally, the impact of pressure is sited close the middle of the bucket and the pressure value was greater in the splitter angle (75 degree), than 55 and 115 degrees, moreover the leakage of the flow is less in comparison to the splitter angle (55 and 115). However, pressure value is higher than 55 degree splitter angle. In addition, the site of the pressure is positioned at the top near the cut off, in the splitter angle 115 degree, the it is lower than the splitter angle of 115 and 90 degrees. In contrast, the pressure distribution is situated at the middle of the bucket and there is no leakage in the splitter angle of 90 degree. Additionally, the pressure value is the biggest

compared to the splitter angle of (55, 75 and 115 degree). This variation might be owing to the alteration rate of the momentum is equal to the applied force and happened in the direction of force.

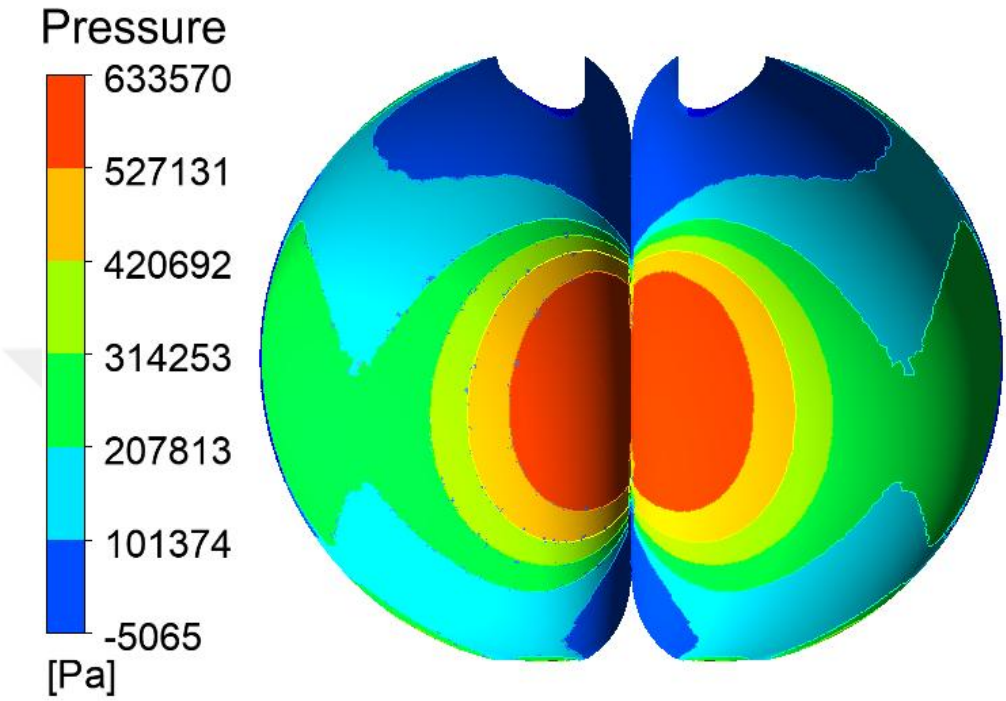

Figure 4.8. Demonstrates variation of pressure when velocity =35 m/s, diameter =40mm and splitter angle=75 degree for model 1.

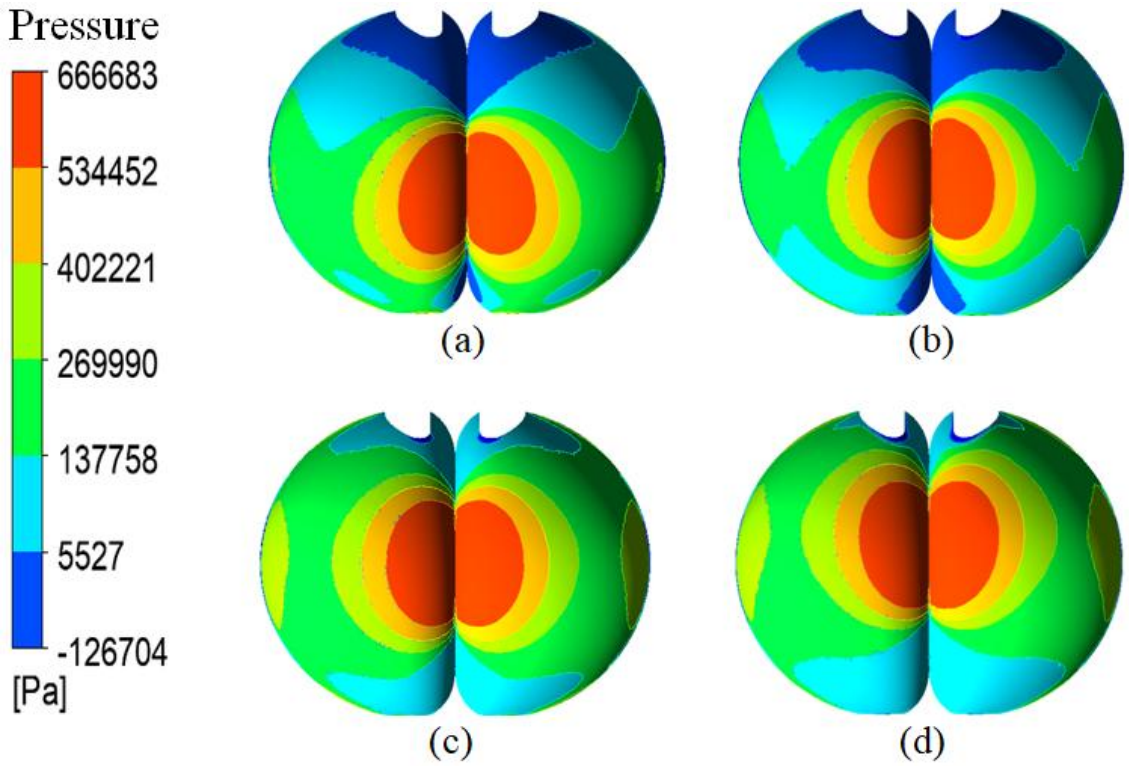

Figure 4.9. Demonstrates variation of pressure when velocity =35 m/s and diameter =40mm for model 1 at figure (a) splitter angle=55 degree, (b) splitter angle=75 degree, (c) splitter angle=90 degree and (d) splitter angle=115 degree.

The pressure distribution and calculation are displayed in these figures. In the splitter angle (55 degree), the pressure distribution in the bottom edge are varied according to the jet strike of the flow; and the generated pressure on the bucket in this splitter angle is low because the water force is divided into two components, one of these components does not affect the bucket (according to impulse- momentum principle). Additionally, another cause for the low pressure in the splitter angle of 55 degree is a flow leakage through the bottom edge. In addition, in the splitter angle (75 degree), the effect of pressure is located near the middle of the bucket and the pressure value was greater than 55 and 115 degrees, moreover the leakage of the flow is less in comparison to the splitter angle (55 and 115). Regarding the splitter angle 115 degree, the pressure value is lower than in the splitter angle of 115 and 90 degrees while it is higher than 55 degree splitter angle. Additionally, the location of the pressure is positioned at the top near the cut off. On the other hand, the pressure distribution in the splitter angle of 90 degree is located at the middle of the bucket and there is no leakage.

In addition, in comparison to the splitter angle of (55, 75 and 115 degree) the pressure value is the biggest. This is because the rate of the change of the momentum is equal to the applied force and happened in the direction of the force.

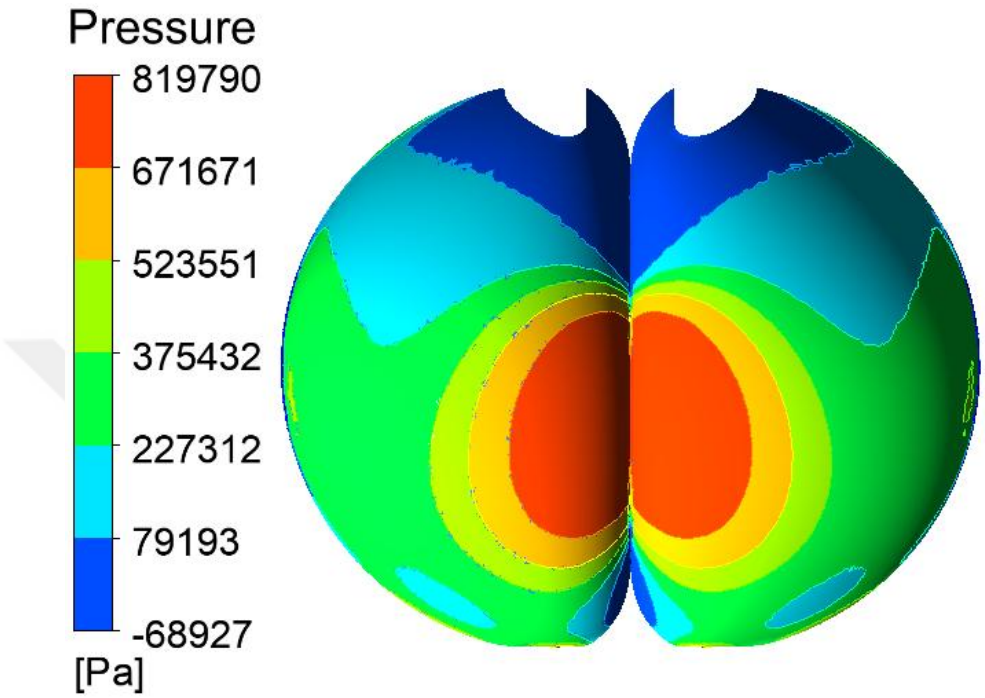

Figure 4.10 Demonstrates variation of pressure when velocity =40 m/s, diameter =40mm and splitter angle=55 degree for model 1.

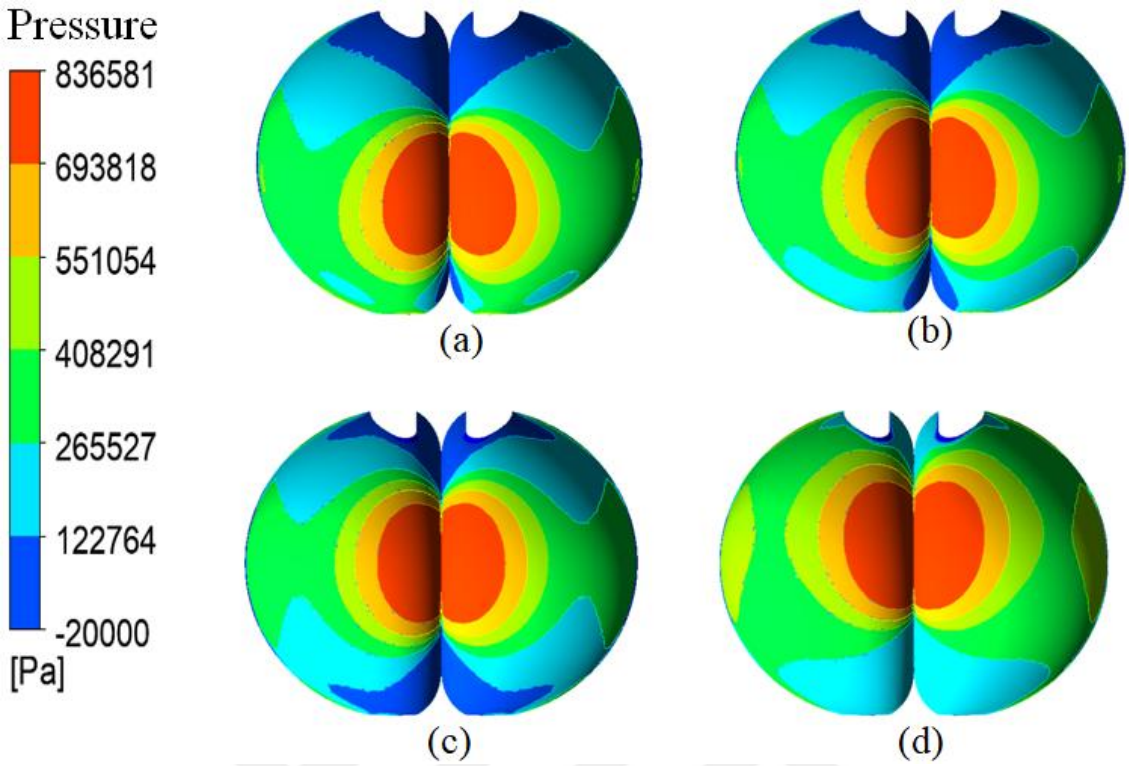

Figure 4.11. Demonstrates variation of pressure when velocity =40 m/s and diameter =40mm for model 1 at figure (a) splitter angle=55 degree, (b) splitter angle=75 degree, (c) splitter angle=90 degree and (d) splitter angle=115 degree.

In figures (4.12 and 4.13), the pressure distribution and calculation are illustrated. In regards to the jet strike of the flow, the distributions of the pressure in the bottom edge are varied, in the splitter angle (55 degree). As the water force is alienated into two parts, one of these part does not influence the bucket (according to impulse-momentum principle), the pressure generated on the bucket in this splitter angle is low. Moreover, a stream leakage during the bottom edge is another cause for the low pressure in the splitter angle of 55 degree. Additionally, the impact of pressure is sited close the middle of the bucket and the pressure value was greater in the splitter angle (75 degree), than 55 and 115 degrees, moreover the leakage of the flow is less in comparison to the splitter angle (55 and 115). Nevertheless, while pressure value is greater than 55 degree splitter angle. In addition, the site of the pressure is positioned at the top near the cut off, in the splitter angle 115 degree, the it is lower than the splitter angle of 115 and 90 degrees. In contrast, in the splitter angle of 90 degree, the distribution of pressure is located at the middle of the bucket and there is no leakage.

Furthermore, in comparison to the splitter angle of (55, 75 and 115 degree), the pressure value is the biggest in the splitter angle 90 degree. This variation might be owing to the alteration rate of the momentum is equal to the applied force and happened in the direction of force. These outcomes comply the results of both (Gupta and Prasad, 2012) and (Zoppe et al, 2006).

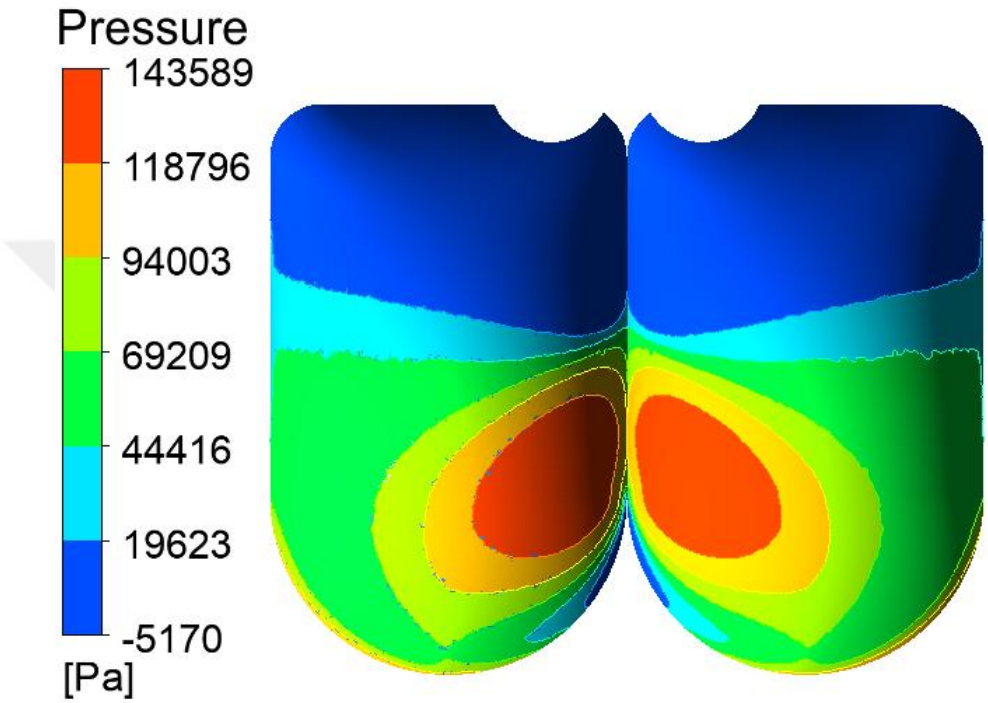

Figure 4.12. Demonstrates variation of pressure when velocity =20 m/s, diameter =40mm and splitter angle=55 degree for model 2.

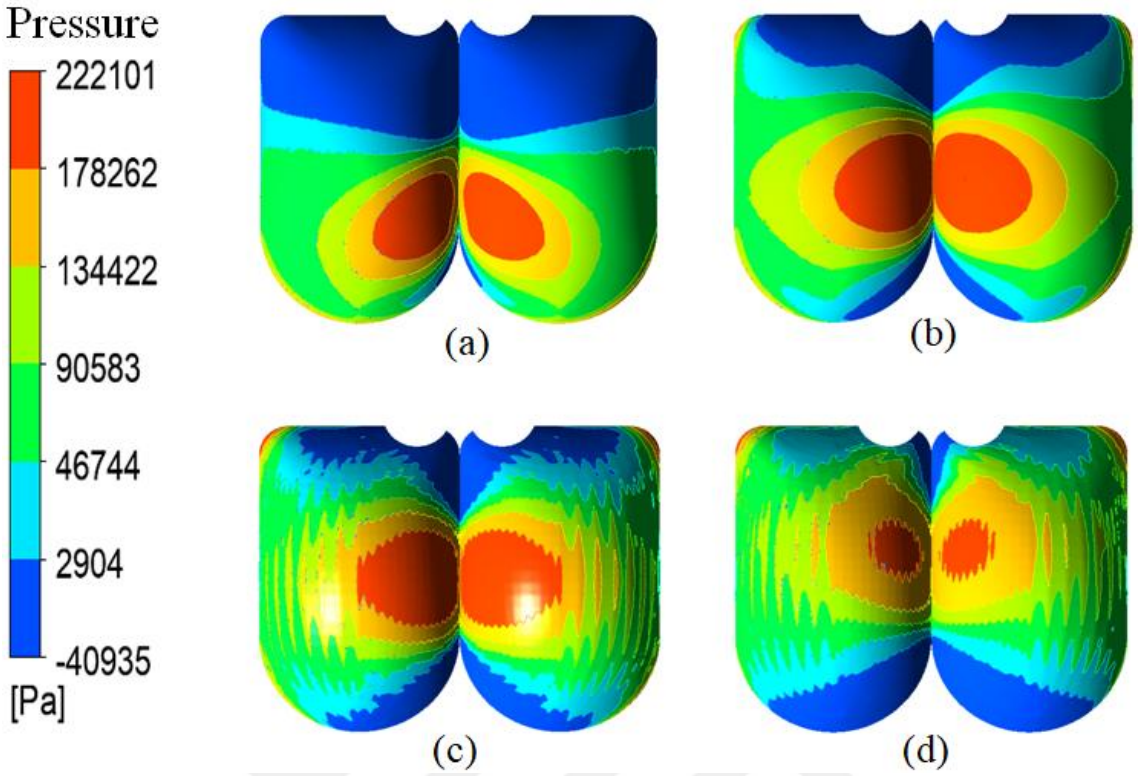

Figure 4.13. Demonstrates variation of pressure when velocity =20 m/s and diameter =40mm for model 2 at figure (a) splitter angle=55 degree, (b) splitter angle=75 degree, (c) splitter angle=90 degree and (d) splitter angle=115 degree.

In this figure, the pressure distribution and calculation are illustrated. In the splitter angle (55 degree), the pressure distribution in the bottom edge are differed consistent with the jet strike of the stream. The created pressure upon the bucket in this splitter angle is low as the force water is separated into two divisions, one of these parts does not influence the bucket (according to impulse- momentum principle). Furthermore, additional cause for the low pressure in the splitter angle of 55 degree is a stream leakage through the bottom edge. In addition, in the splitter angle (75 degree), the effect of pressure is located near the middle of the bucket and the pressure value was greater than 55 and 115 degrees, moreover the leakage of the flow is less in comparison to the splitter angle (55 and 115). In the splitter angle of 75 degree, the pressure value is lower than in the splitter angle of 115 and 90 degree while it is higher than 55 degree splitter angle. Additionally, the location of the pressure is positioned at the top near the cut off. In contrast, the distribution of pressure in the splitter angle of 90 degree is sited at the middle of the bucket and there is no leakage. Additionally, in comparison to the

splitter angle of (55, 75 and 115 degree), the pressure value is the greatest. This is due to the rate of the variation of the momentum is equal to the applied force and happen in the direction of the force.

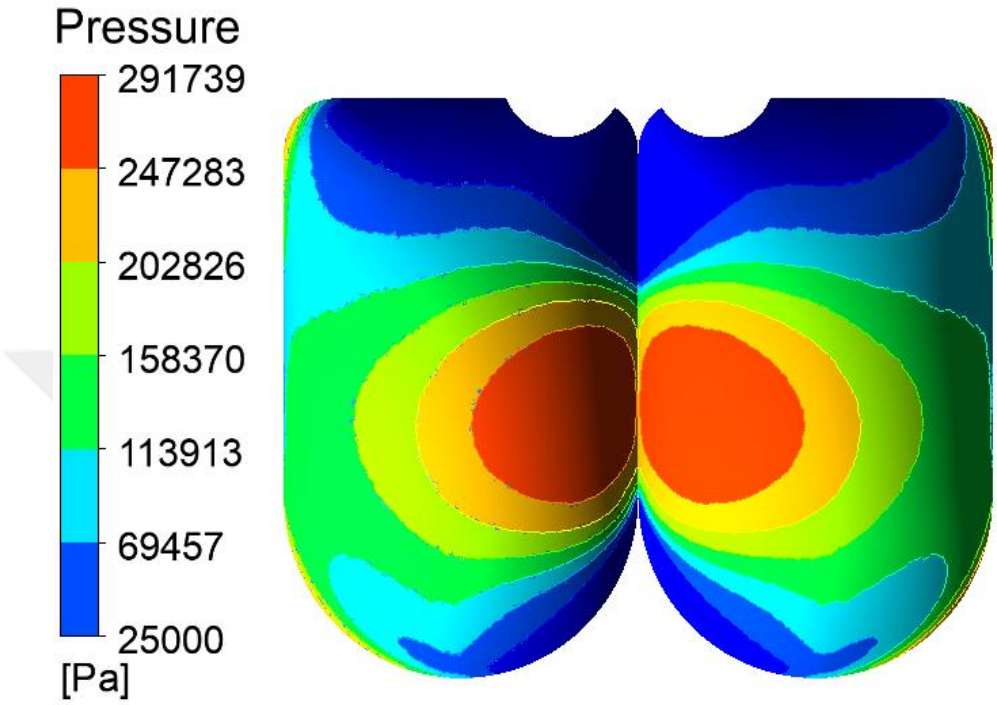

Figure 4.14. Demonstrates variation of pressure when velocity =25 m/s , diameter =40mm and splitter angle=75 degree for model 2.

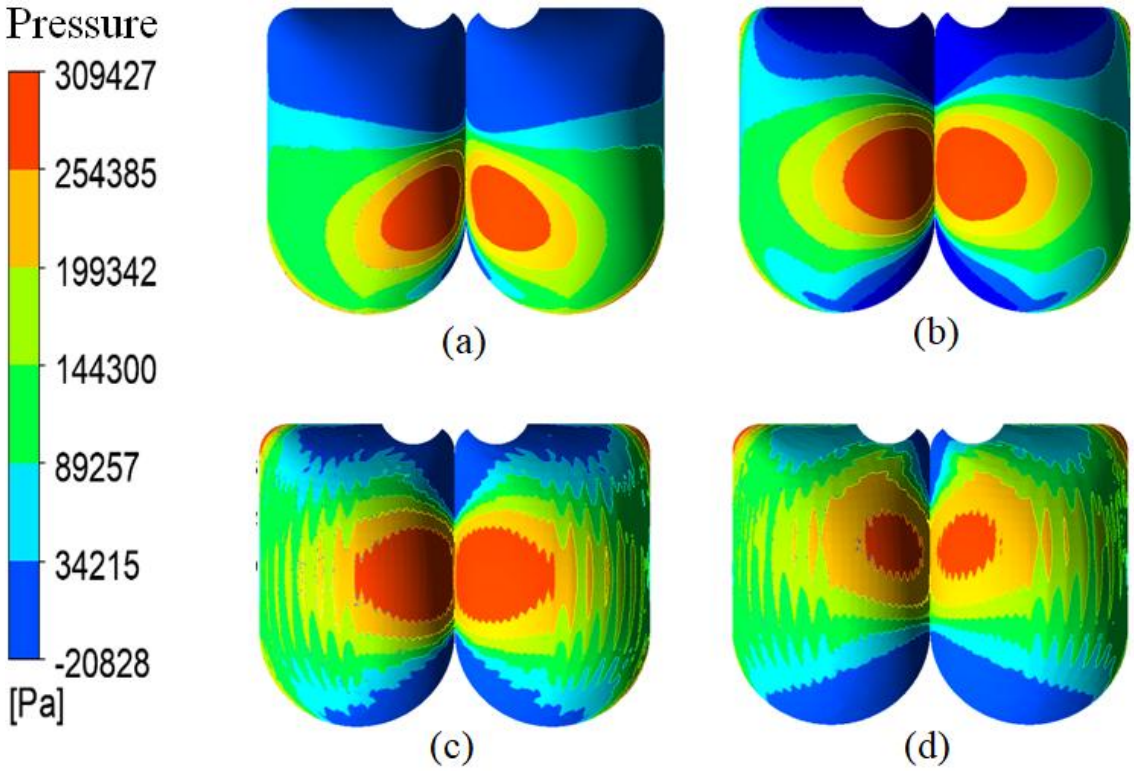

Figure 4.15. Demonstrates variation of pressure when velocity =25 m/s and diameter =40mm for model 2 at figure (a) splitter angle=55 degree, (b) splitter angle=75 degree, (c) splitter angle=90 degree and (d) splitter angle=115 degree.

Figure (4.16 and 4.17) illustrates the pressure distribution and calculation in four different splitter angles (55, 75, 90 and 115 degree). The pressure distribution in the bottom edge is differed consistent with the jet strike of the stream in the splitter angle (55 degree). The generated pressure upon the bucket in this splitter angle is low as the force water is separated into two divisions; one of these parts does not influence the bucket (according to impulse- momentum principle). Besides, the other cause for the low pressure in the splitter angle of 55 degree is a stream leakage through the bottom edge. In addition, the impact of pressure is positioned near the middle of the bucket in the splitter angle (75 degree) and the value of pressure was higher than 55 and 115 degrees. It has to be mentioned that the leakage of the flow the splitter angle of 75 is less in comparison to the splitter angle (55 and 115). While it is higher than 55 degree splitter angle, in the splitter angle of 75 degree, the pressure value is lower than in the splitter angle of 115 and 90 degree. Furthermore, the site of the pressure is positioned at the top close the cut off. In contrast, the distribution of pressure in the splitter angle of

90 degree is sited at the middle of the bucket and there is no leakage. Moreover, the pressure value is the greatest in the splitter angle of 90 degree in comparison to the splitter angle of (55, 75 and 115 degree). This is because of the rate of the variation of the momentum is equal to the applied force and happen in the direction of the force. The findings approved by (Gupta and Prasad, 2012) and (Zoppe et al, 2006).

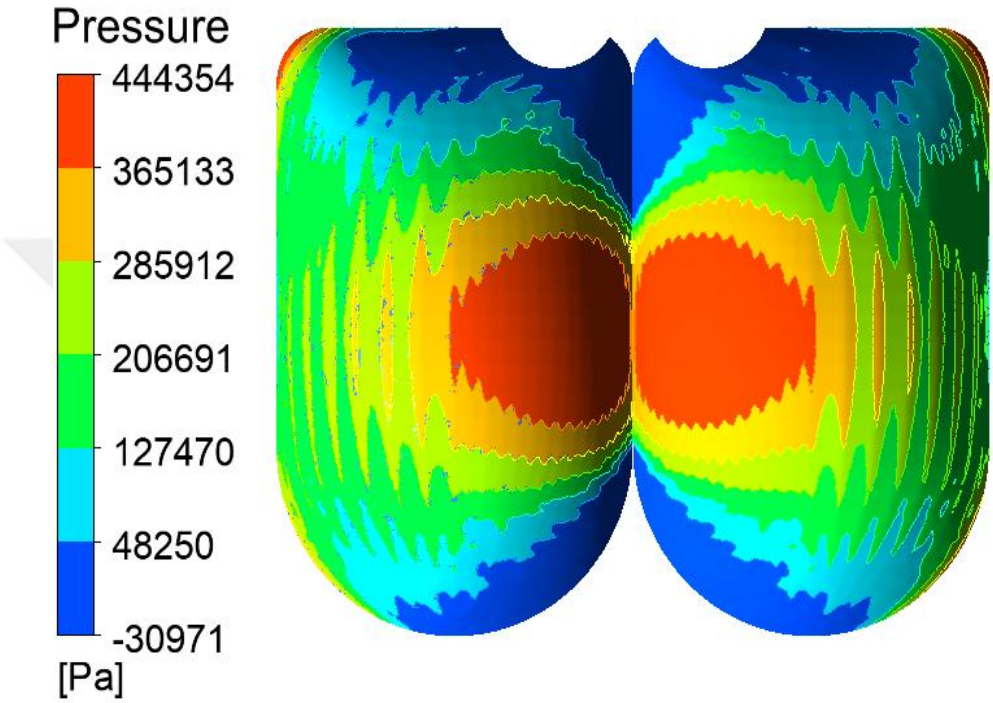

Figure 4.16. Demonstrates variation of pressure when velocity =30 m/s, diameter =40mm and splitter angle=90 degree for model 2.

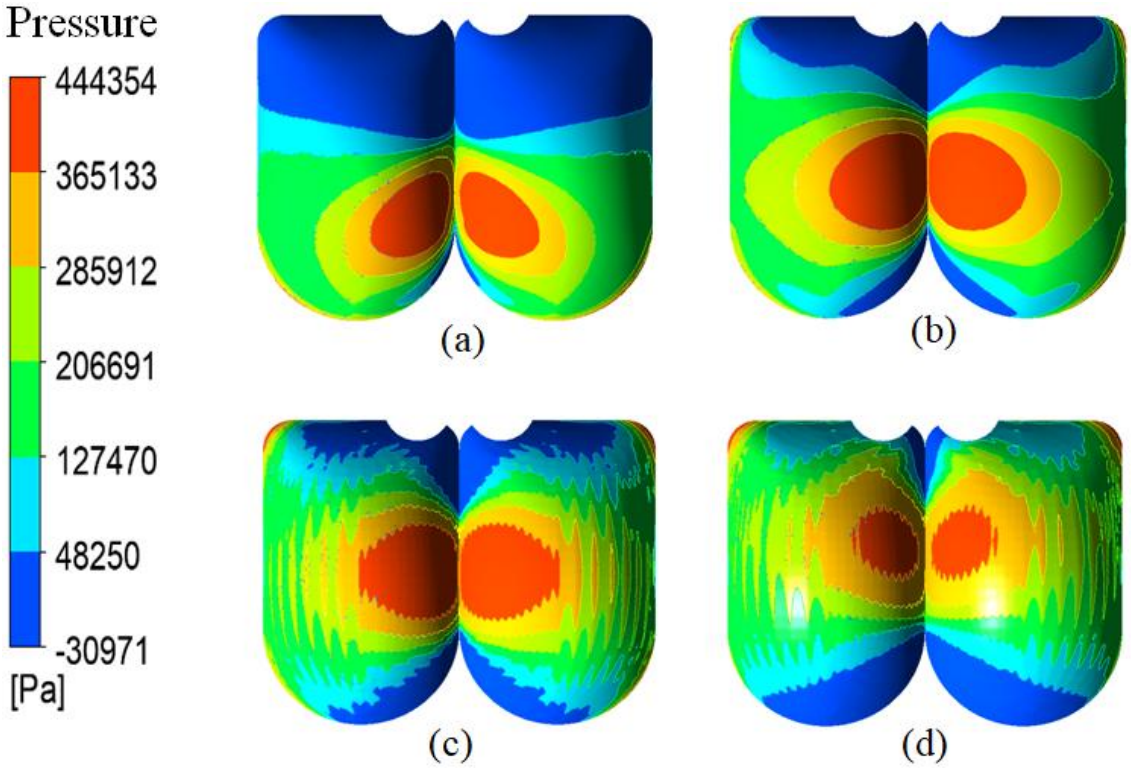

Figure 4.17.Demonstrates variation of pressure when velocity =30 m/s and diameter =40mm for model 2 at figure (a) splitter angle=55 degree, (b) splitter angle=75 degree, (c) splitter angle=90 degree and (d) splitter angle=115 degree.

The pressure distribution and calculation in four different splitter angles (55, 75, 90 and 115 degree) are illustrated in figures (4.18 and4.19). In consistent with the jet strike of the stream in the splitter angle (55 degree), the pressure distribution in the bottom edge is varied. The generated pressure upon the bucket in this splitter angle is low as the force water is separated into two divisions; one of these parts does not influence the bucket (according to impulse- momentum principle). Besides, a stream leakage through the bottom edge is another cause for the low pressure in the splitter angle of 55 degree. In addition, the pressure impact is located near the middle of the bucket in the splitter angle (75 degree) and the value of pressure was higher than 55 and 115 degrees. It has to be mentioned that the leakage of the flow the splitter angle of 75 is less in comparison to the splitter angle (55 and 115). While the pressure value is higher than 55 degree splitter angle, in the splitter angle of 75 degree, the pressure value is than in the splitter angle of 115 and 90 degree. Furthermore, the site of the pressure is located at the top close the cut off. In contrast, the pressure distribution in the splitter

angle of 90 degree is sited at the middle of the bucket and there is no leakage. Moreover, in comparison to the splitter angle of (55, 75 and 115 degree), the pressure value is the biggest in the splitter angle of 90 degree. This is as a consequent of the proportion of the variation of the momentum is equal to the applied force and it occurred in the direction of the force.

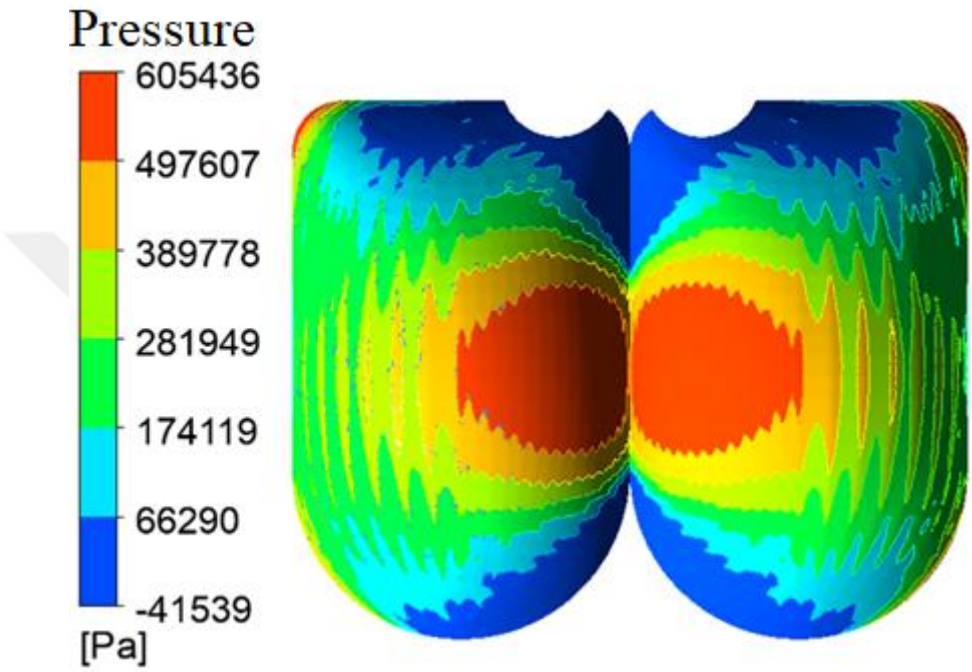

Figure 4.18. Demonstrates Variation of pressure when velocity =35 m/s, diameter =40mm and splitter angle=115 degree for model 2.

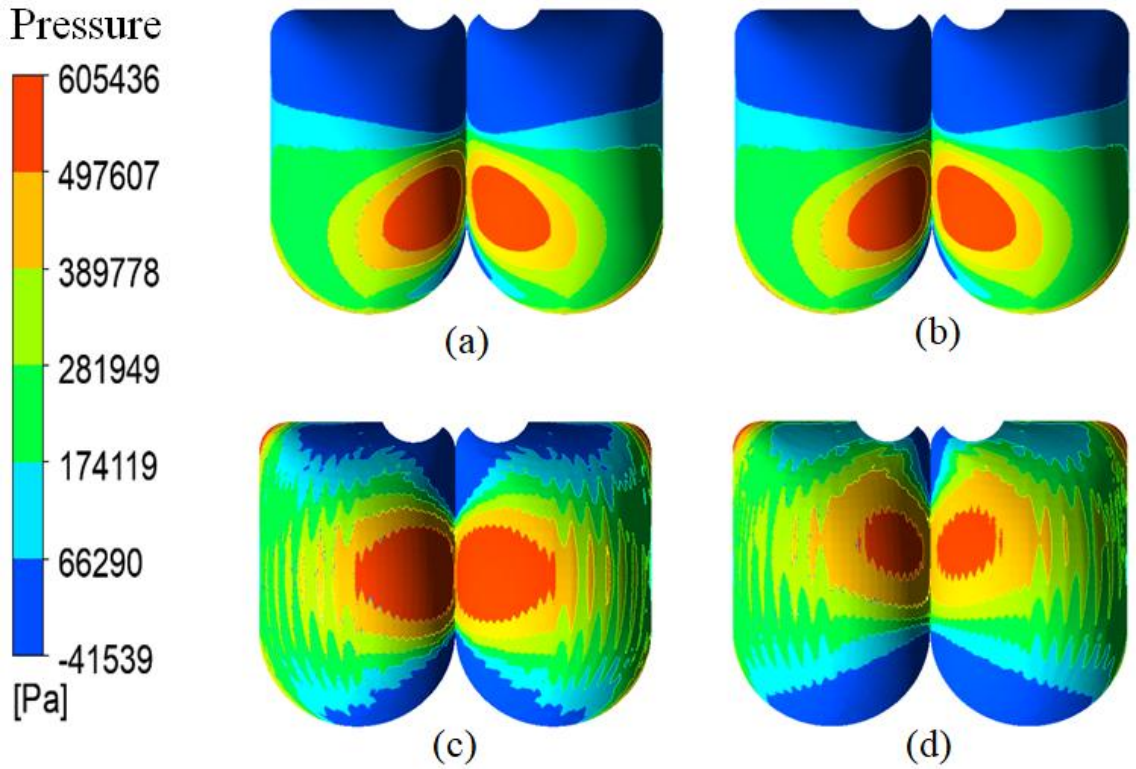

Figure 4. 19. Demonstrates variation of pressure when velocity =35 m/s and diameter =40mm for model 2 at figure (a) splitter angle=55 degree, (b) splitter angle=75 degree, (c) splitter angle=90 degree and (d) splitter angle=115 degree.

In four different splitter angles (55, 75, 90 and 115 degree), the pressure distribution and calculation are displayed in figures (4.20and4.21). The pressure distribution in the bottom edge are varied According to the jet strike of the stream in the splitter angle (55 degree). The generated pressure upon the bucket in this splitter angle is low as the force water is separated into two divisions; one of these parts does not influence the bucket (according to impulse- momentum principle). Besides, a stream leakage through the bottom edge is another cause for the low pressure in the splitter angle of 55 degree. In addition, in the splitter angle (75 degree), the pressure impact is sited near the middle of the bucket and the value of pressure was bigger than 55 and 115 degrees. It is obvious that the leakage of the flow the splitter angle of 75 is less comparing to the splitter angle (55 and 115). While the pressure value is higher than 55 degree splitter angle, in the splitter angle of 75 degree, the pressure value less is than in the splitter angle of 115 and 90 degree. Moreover, the pressure occurred at the top close the cut off. However, the pressure distribution in the splitter angle of 90 degree is sited

at the middle of the bucket and there is no leakage. Besides, the pressure value is the biggest in the splitter angle of 90 degree comparing to the splitter angle of (55, 75 and 115 degree). Thus, the proportion of the variation of the momentum is equal to the applied force and it occurred in the direction of the force.

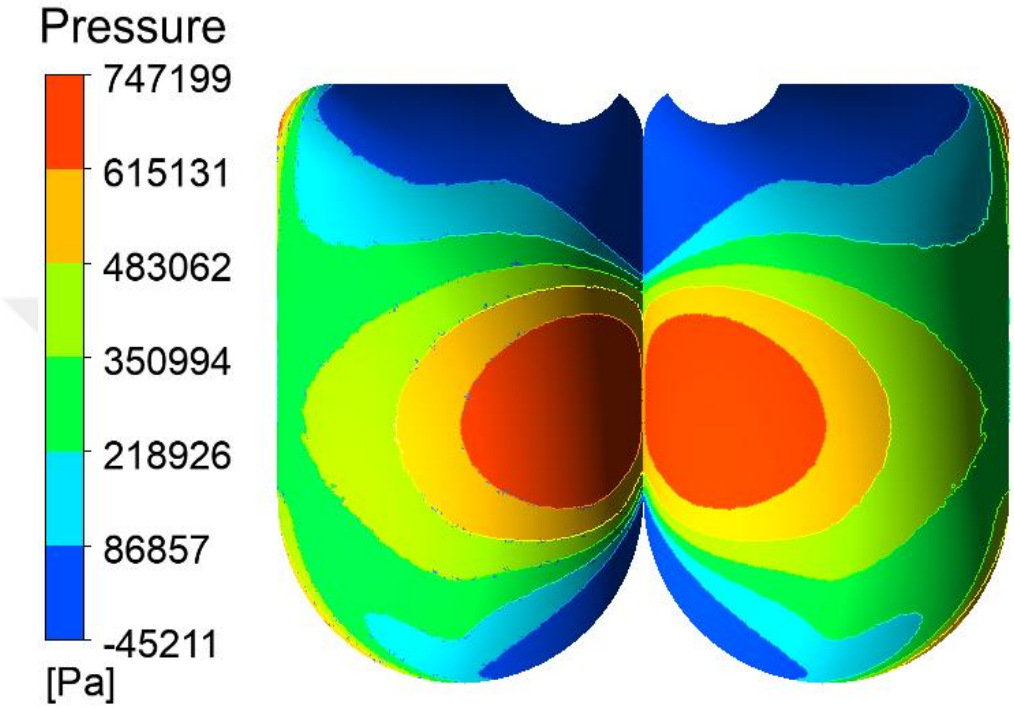

Figure 4.20. Demonstrates variation of pressure when velocity =40 m/s, diameter =40mm and splitter angle=75 degree for model 2.

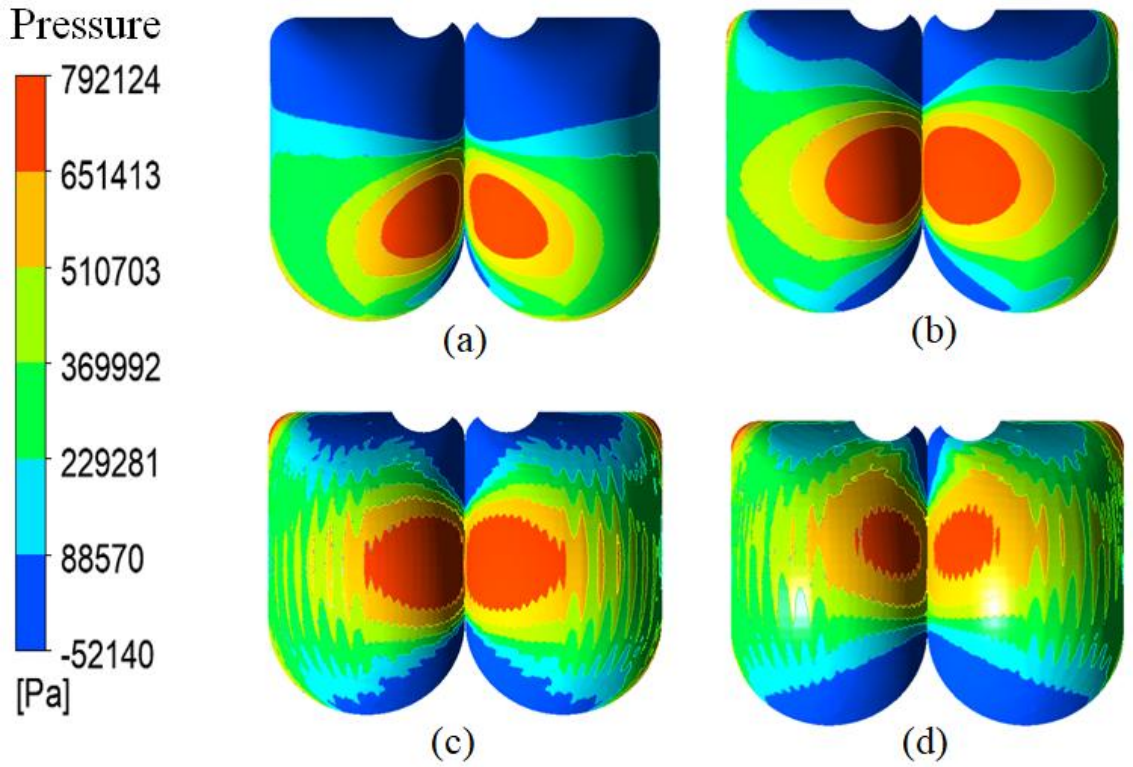

Figure 4.21. Demonstrates variation of pressure when velocity =40 m/s and diameter =40mm for model 2 at figure (a) splitter angle=55 degree, (b) splitter angle=75 degree, (c) splitter angle=90 degree and (d) splitter angle=115 degree.

4.2. Water Volume Fraction

The water distribution inside the bucket for four splitter angles and two models are demonstrated in Figures (4.22and4.23). Firstly, when the splitter angle is 55 degree, water distributed over the majority of the internal surface and at the bucket outlet, it concentrates on the back edge. In this angle, a portion of the jet does not infiltrate into the bucket, the equivalent amount of water does not affect the bucket. Secondly, in the splitter of 75 degree, the distribution of water is occurred slightly away from the bucket edge. In addition, higher amount of water penetrates into the bucket in comparison to the splitter of 55 degree. Moreover, when the splitter angle is 90 degree, the layer of water prolongs to the cut out edge, as well as it becomes thinner. In this case, the whole jet penetrates the bucket and the whole layer of water is confined in the bucket. Lastly, when utilizing a splitter of 115 degree, the layer of water is predominantly extensive a long side the edge of the bucket.

A tremendous amount of the jet exits the cut off, which infers for this case, a colossal force loss.

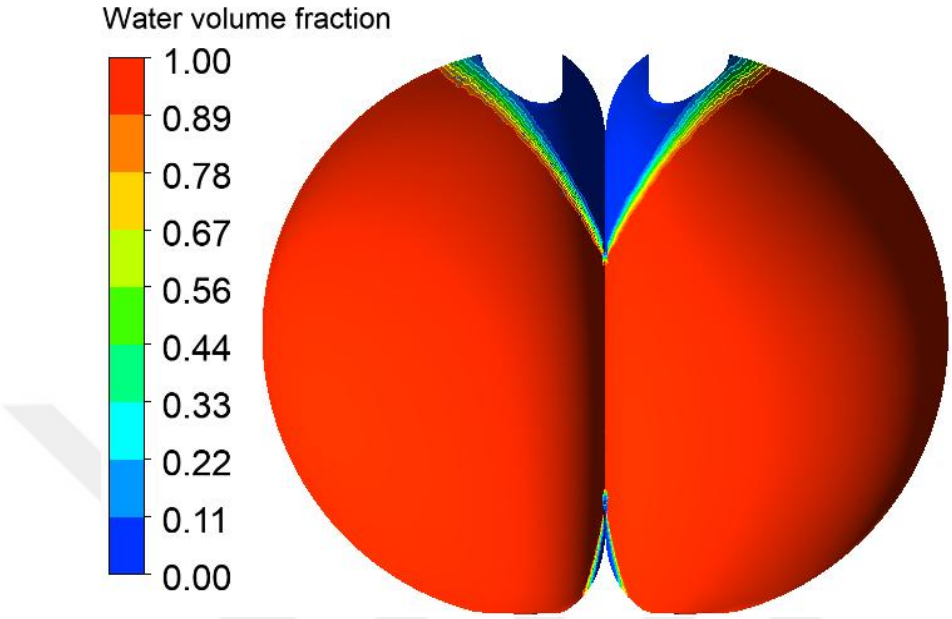

Figure 4.22. Shows variation of the water volume fraction when the velocity =20 m/s, d=40 mm and splitter angle =55 for model 1.

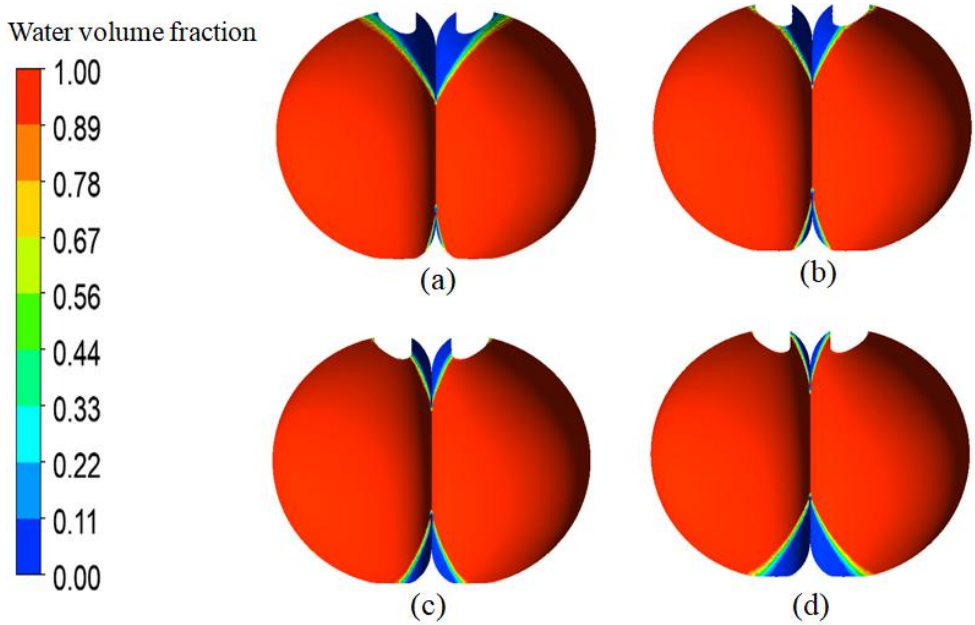

Figure 4.23. Shows variation of the water volume fraction when velocity =20 m/s and diameter =40mm for model 1 at figure (a) splitter angle=55 degree, (b) splitter angle=75 degree, (c) splitter angle=90 degree and (d) splitter angle=115 degree.

Figures (4.24 and 4.25) demonstrate the water distribution inside the bucket for four splitter angles and two models. Initially, water distributed over the majority of the internal surface and at the bucket outlet, it concentrates on the back edge when the splitter angle is 55 degree. In this angle, amount of the jet does not penetrate into the bucket; the same quantity of water does not impact the bucket. After that, the distribution of water is occurred slightly away from the bucket edge in the splitter of 75 degree. Furthermore, higher amount of water penetrates into the bucket in comparison to the splitter angle of 55 degree. Moreover, the layer of water prolongs to the cut out edge as well as it becomes thinner when the splitter angle is 90 degree. In this case, the whole jet penetrates the bucket and the whole layer of water is confined in the bucket. Lastly, when utilizing a splitter of 115 degree, the layer of water is predominantly extensive a long side the edge of the bucket. A huge quantity of the jet exits at the cut off, which means in this case, a colossal force loss.

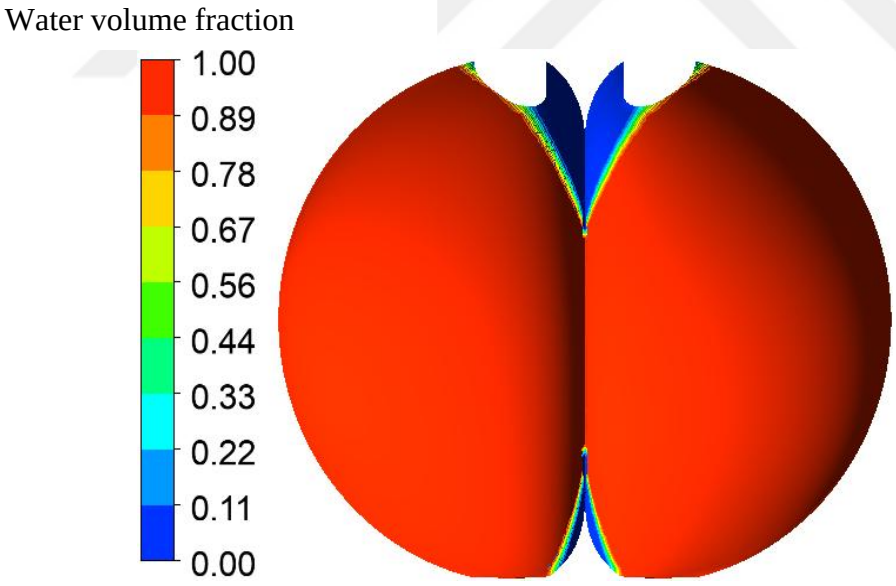

Figure 4.24. Shows variation of the water volume fraction when the velocity =25 m/s, d=40 mm and splitter angle =75 for model 1.

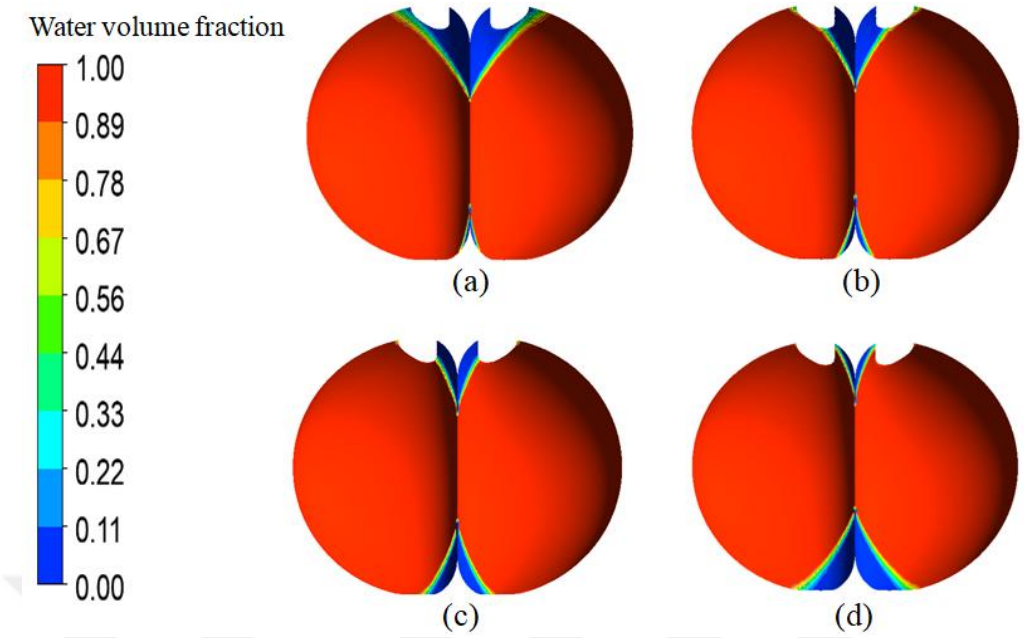

Figure 4.25. Shows variation of the water volume fraction when velocity =25 m/s and diameter =40mm for model 1 at figure (a) splitter angle=55 degree, (b) splitter angle=75 degree, (c) splitter angle=90 degree and (d) splitter angle=115 degree.

In Figures (4.26and4.27), the distribution water inside the bucket for four splitter angles and two models are displayed. At the beginning, water distributed most of the internal surface and at the bucket outlet. It focuses on the back edges the splitter angle is 55 degree. In this angle, an amount of the jet does not enter into the bucket. The same quantity of water does not impact the bucket. After that, the dispersal of water is happened slightly away from the bucket edge in the splitter of 75 degree. Moreover, bigger quantity of water penetrates into the bucket in comparison to the splitter angle of 55 degree. Furthermore, the layer of water extends to the edge of cut out and it becomes thinner as the splitter angle is 90 degree. The whole jet enters the bucket and the entire layer of water is limited in the bucket. Finally, the layer of water is mainly extensive a long side the edge of the bucket when utilizing a splitter of 115 degree. A great amount of the jet exits at the cut off, which in this case, a colossal force loss.

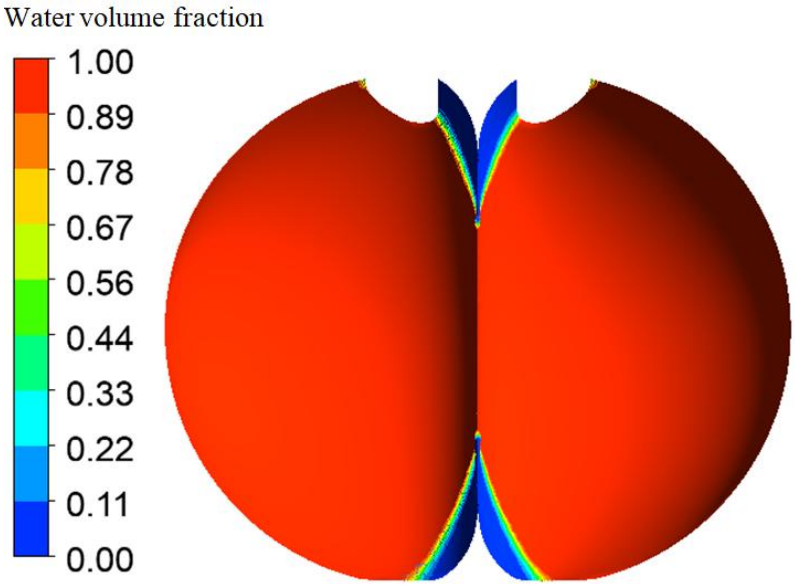

Figure 4.26. Shows variation of the water volume fraction when the velocity =30 m/s, d=40 mm and splitter angle =90 for model 1.

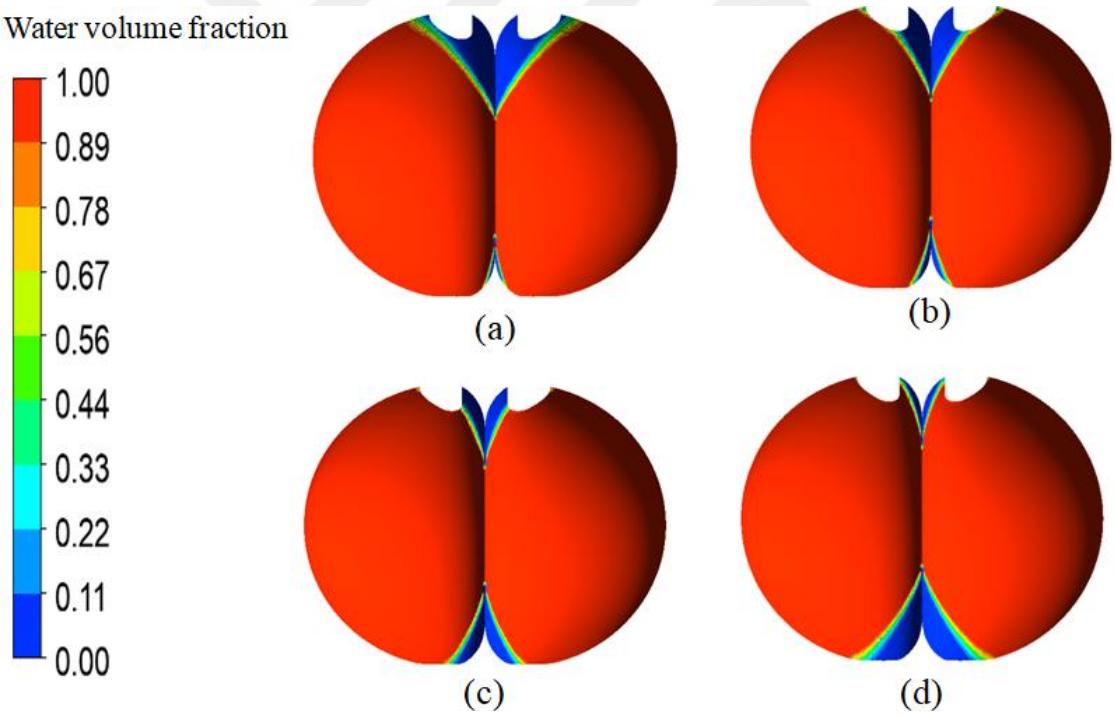

Figure 4.27. Shows variation of the water volume fraction when velocity =30 m/s and diameter =40mm for model 1 at figure (a) splitter angle=55 degree, (b) splitter angle=75 degree, (c) splitter angle=90 degree and (d) splitter angle=115 degree.

The distribution water inside the bucket for four splitter angles and two models are displayed in this figure. At the commencement, water distributes in most of the internal surface and at the bucket outlet. When the splitter angle is 55 degree, it concentrates on the back edge. Some quantity of the jet does not enter into the bucket. Similar quantity of water does not influence the bucket. Then, in the splitter of 75 degree, the dispersal of water is occurred slightly away from the bucket edge. Moreover, in comparison to the splitter angle of 55 degree, bigger quantity of water penetrates into the bucket. Besides, when the splitter angle is 90 degree, the layer of water extends to the edge of cut out and it becomes thinner. The whole jet enters the bucket and the entire layer of water is limited in the bucket. Lastly, when utilizing a splitter of 115 degree, the layer of water is mainly extensive a long side the edge of the bucket. A great amount of the jet exits at the cut off, which cause a colossal force loss when it showed in the figures (4.28 and 4.29).

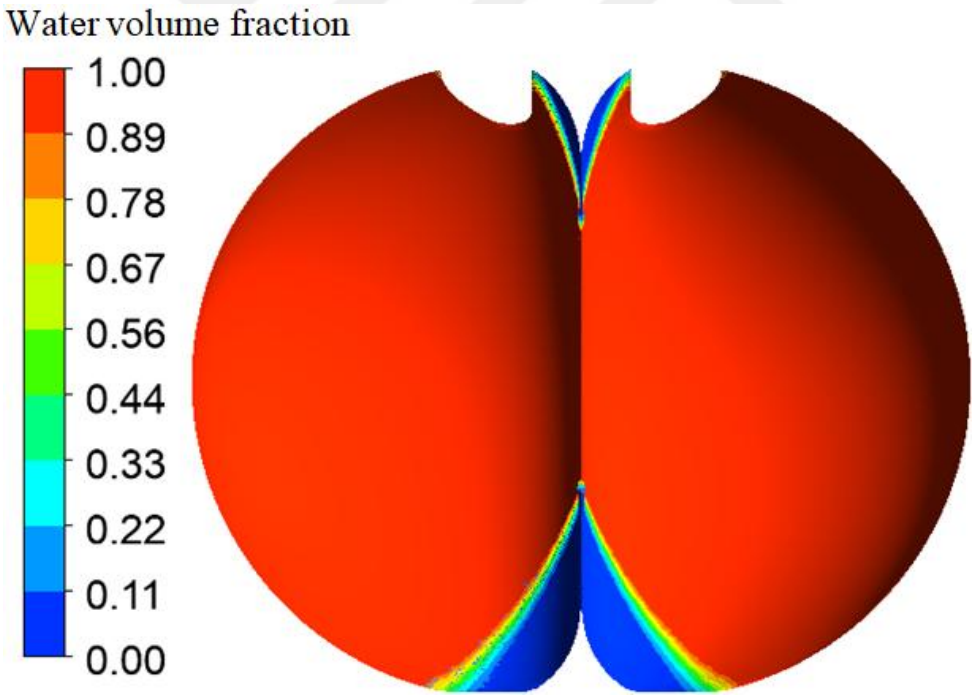

Figure 4.28. Shows variation of the water volume fraction when the velocity =35 m/s, d=40 mm and splitter angle =115 for model 1.

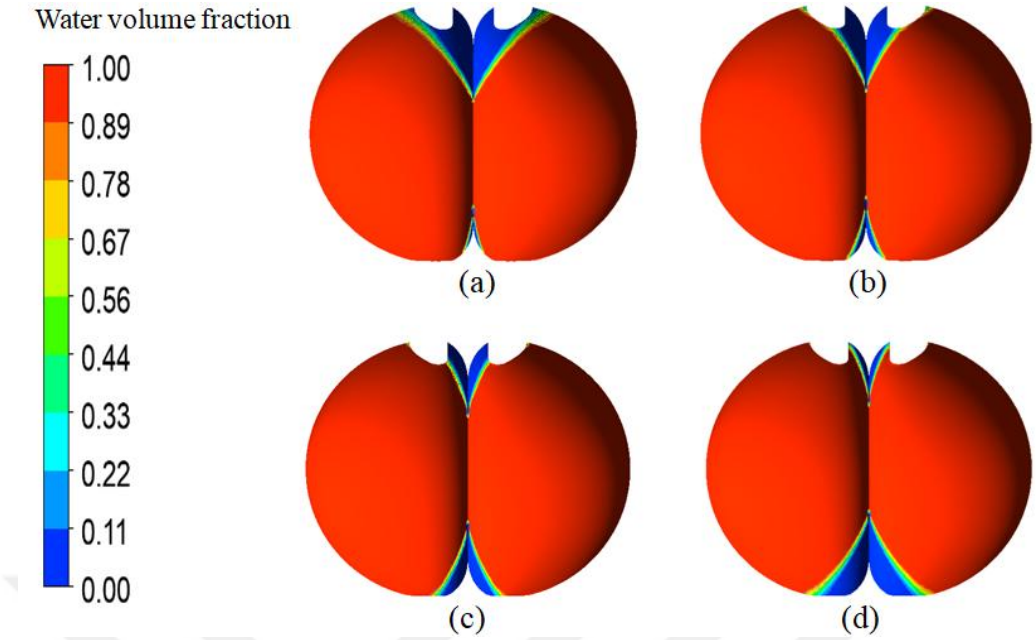

Figure 4.29. Shows variation of the water volume fraction when velocity =35 m/s and diameter =40mm for model 1 at figure (a) splitter angle=55 degree, (b) splitter angle=75 degree, (c) splitter angle=90 degree and (d) splitter angle=115 degree.

The water distribution inside the bucket for two models and four splitter angles are exhibited in these figures. At the beginning, in most of the internal surface and at the bucket outlet, the water is distributed. If the splitter angle is 55 degree, the water concentrates on the back edge. Some quantity of the jet does not enter into the bucket. Similar amount of water does not impact the bucket. Consequently, the diffusion of water is occurred slightly away from the bucket edge in the splitter of 75 degree. Additionally, comparing to the splitter angle of 55 degree, bigger amount of water infiltrates into the bucket. Also, the layer of water extends to the edge of cut out and it becomes thinner when the splitter angle is 90 degree. The entire jet enters the bucket and the entire layer of water is restricted in the bucket. Lastly, when utilizing a splitter of 115 degree, the layer of water is mainly extensive in conjunction with the edge of the bucket. A huge amount of the jet exits at the cut off, which resulted in a massive force loss.

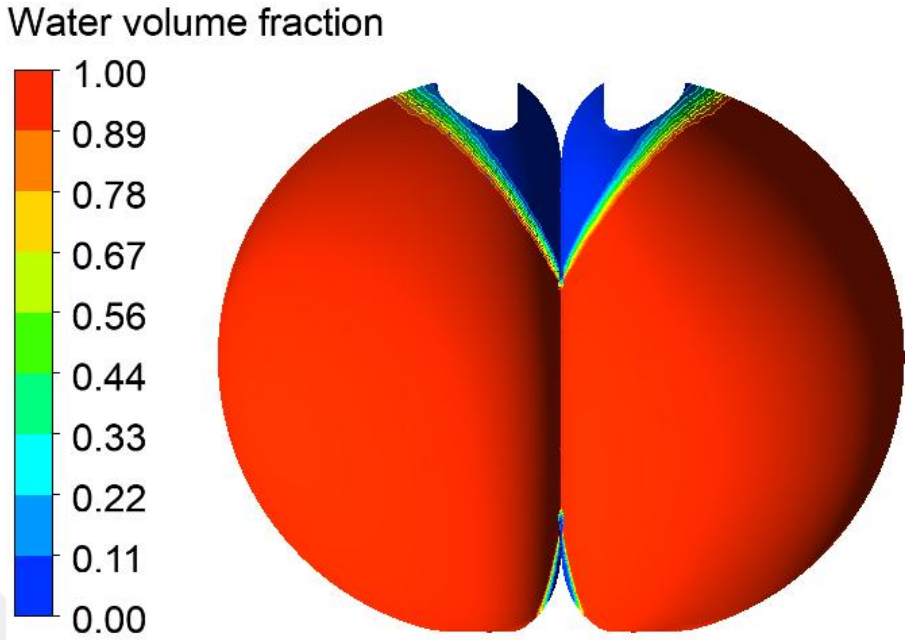

Figure 4.30. Shows variation of the water volume fraction when the velocity =35 m/s, d=40 mm and splitter angle =115 for model 1.

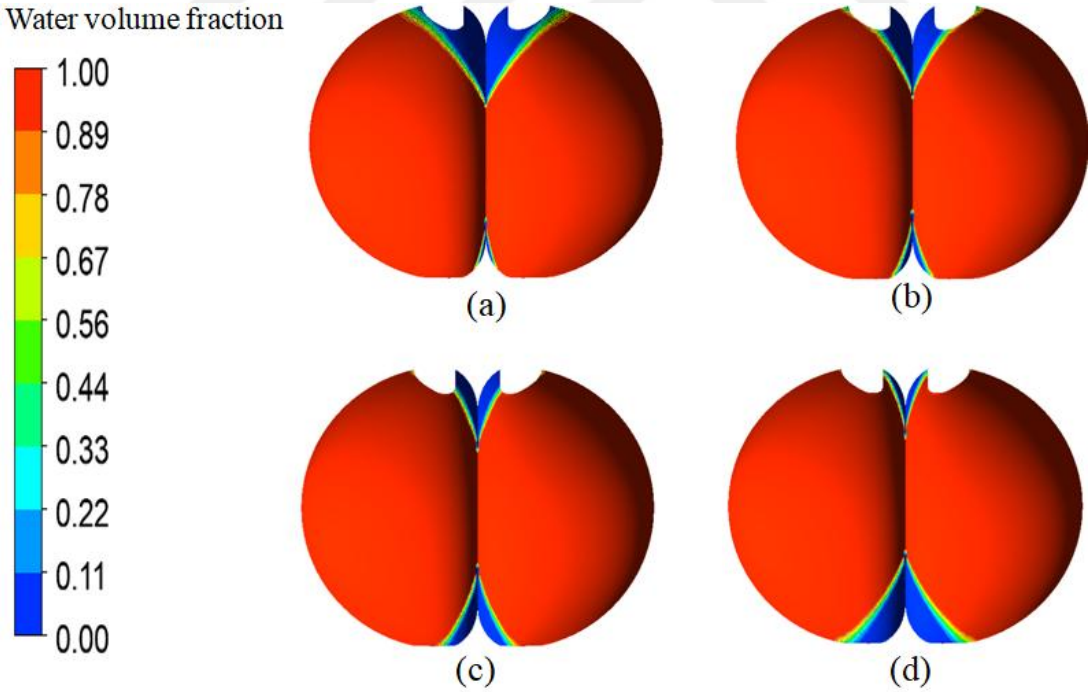

Figure 4.31. Shows variation of the water volume fraction when velocity =40 m/s and diameter =40mm for model 1 at figure (a) splitter angle=55 degree, (b) splitter angle=75 degree, (c) splitter angle=90 degree and (d) splitter angle=115 degree.

For four splitter angles and two models, the water distributions inside the bucket are demonstrated in figures (4.32 and 4.33). At the start, at the bucket outlet and in majority of the internal surface, the water is scattered. When the splitter angle is 55 degree, the water concentrates on the edge of the back. Similar amount of the jet does not enter into the bucket. Similar amount of water does not affect the bucket. Subsequently, in the splitter of 75 degree the water dissemination of is happened slightly away from the bucket edge. Additionally, in splitter angle of 55 degree, bigger amount of water infiltrates into the bucket in comparison to the other splitter angles. Moreover, as the splitter angle is 90 degree, the layer of water prolonged to the cut out edge and it becomes thinner. The entire jet enters the bucket and the whole layer of water is constrained in the bucket. Ultimately, the layer of water is chiefly extensive in conjunction with the edge of the bucket after applying a splitter of 115 degree. An enormous quantity of the jet exits at the cut off, which leads to a massive force loss.

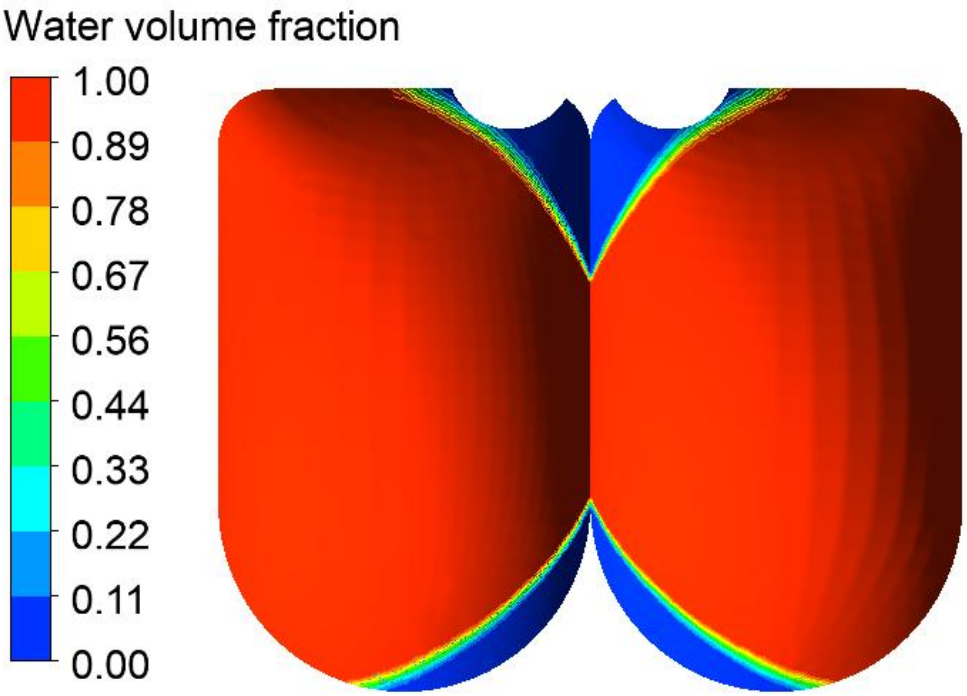

Figure 4.32. Shows variation of the water volume fraction when the velocity =25 m/s, d=40 mm and splitter angle =90 for model 2.

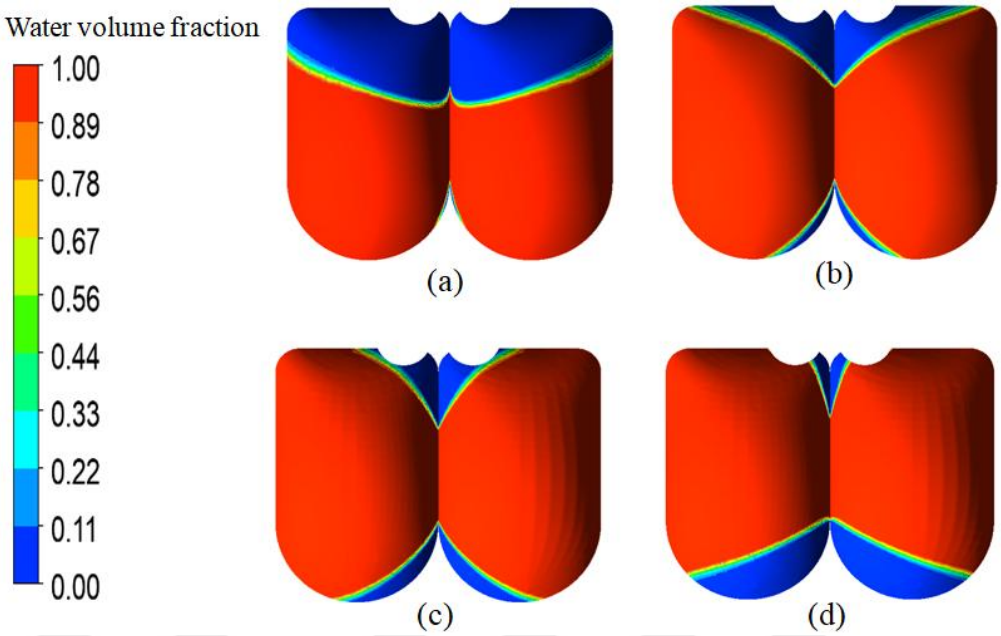

Figure 4.33. Shows variation of the water volume fraction when velocity =20 m/s and diameter =40mm for model 2 at figure (a) splitter angle=55 degree, (b) splitter angle=75 degree, (c) splitter angle=90 degree and (d) splitter angle=115 degree.

In this figure, in four splitter angles and two models, the water distributions inside the bucket are explained. At the outset, the water is scattered at the bucket outlet and in majority of the internal surface. When the splitter angle is 55 degree, the water concentrates on the edge of the back. Alike amount of the jet does not penetrate into the bucket. The bucket is not affected by similar amount of water. Later, slightly away from the bucket edge water distribution of is happened in the splitter of 75 degree the. Moreover, comparing to the bigger amount of water infiltrates into the bucket in comparison to the other splitter angles in splitter angle of 55 degree. Moreover, as the splitter angle is 90 degree, the layer of water prolonged to the cut out edge and it becomes thinner. The entire jet enters the bucket and the whole layer of water is constrained in the bucket. Ultimately, after applying a splitter of 115 degree, the layer of water is chiefly extensive in conjunction with the edge of the bucket. A giant quantity of the jet departs at the cut off, which initiate massive force loss

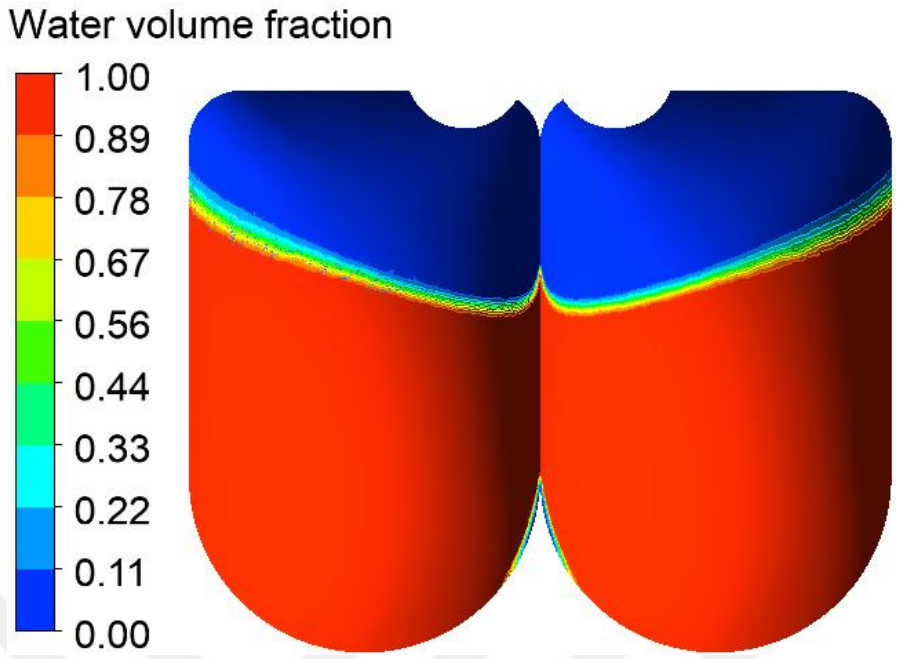

Figure 4.34. Shows variation of the water volume fraction when the velocity =25 m/s, d=40 mm and splitter angle =55 for model 2.

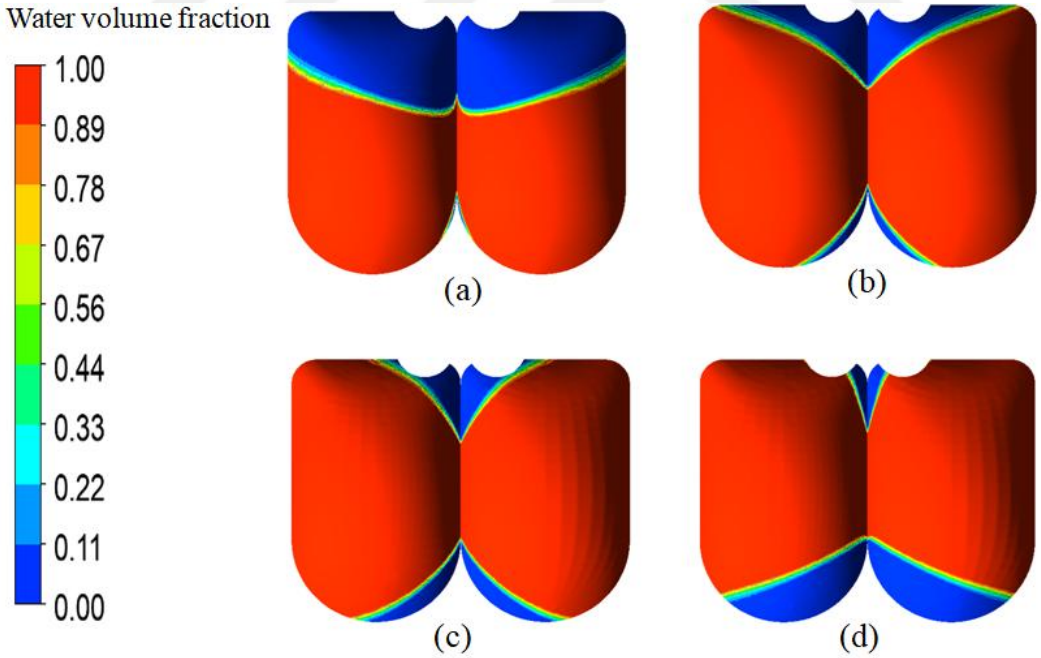

Figure 4.35. Shows variation of the water volume fraction when velocity =25 m/s and diameter =40mm for model 2 at figure (a) splitter angle=55 degree, (b) splitter angle=75 degree, (c) splitter angle=90 degree and (d) splitter angle=115 degree.

The distribution of water inside the bucket for two models and four splitter angles are indicated in these figures. First, when the splitter angle is 55 degree, water distributed over the majority of the internal surface and at the bucket outlet, it concentrates on the back edge. In this angle, a percentage of the jet does not infiltrate into the bucket, the equivalent amount of water does not impact the bucket. Then, the distribution of water is occurred slightly away from the bucket edge in the splitter of 75 degree. In addition, higher amount of water penetrates into the bucket in comparison to the splitter of 55 degree. Moreover, when the splitter angle is 90 degree, the layer of water prolongs to the cut out edge, as well as it becomes thinner. In this case, the whole jet penetrates the bucket and the whole layer of water is confined in the bucket. Lastly, when utilizing a splitter of 115 degree, the layer of water is predominantly extensive a long side the edge of the bucket. A great quantity of the jet exits the cut off, which means an immense force loss.

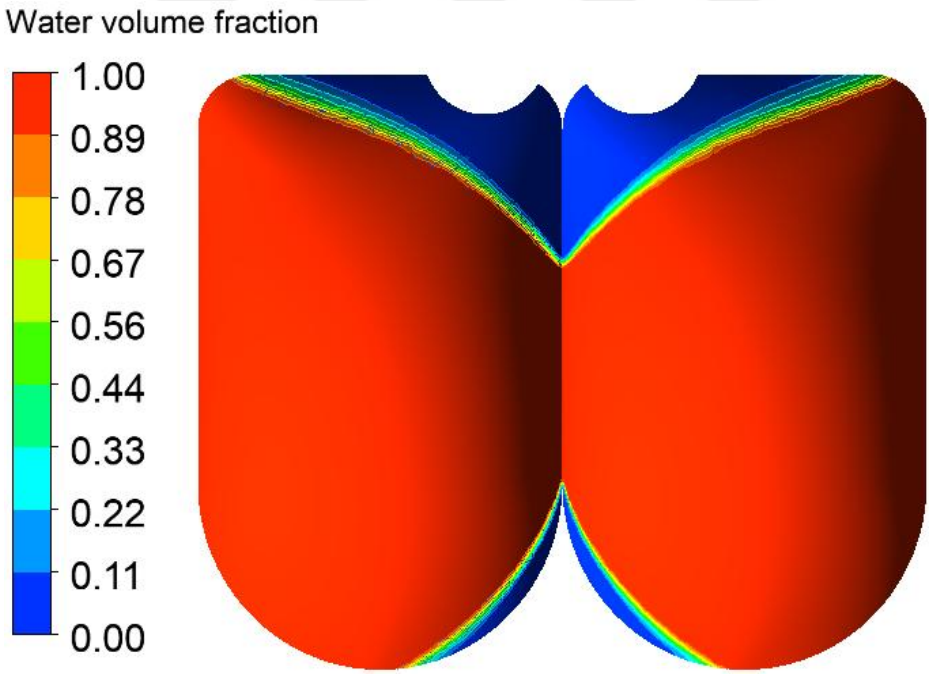

Figure 4.36. Shows variation of the water volume fraction when the velocity =30 m/s, d=40 mm and splitter angle =75 for model 2.

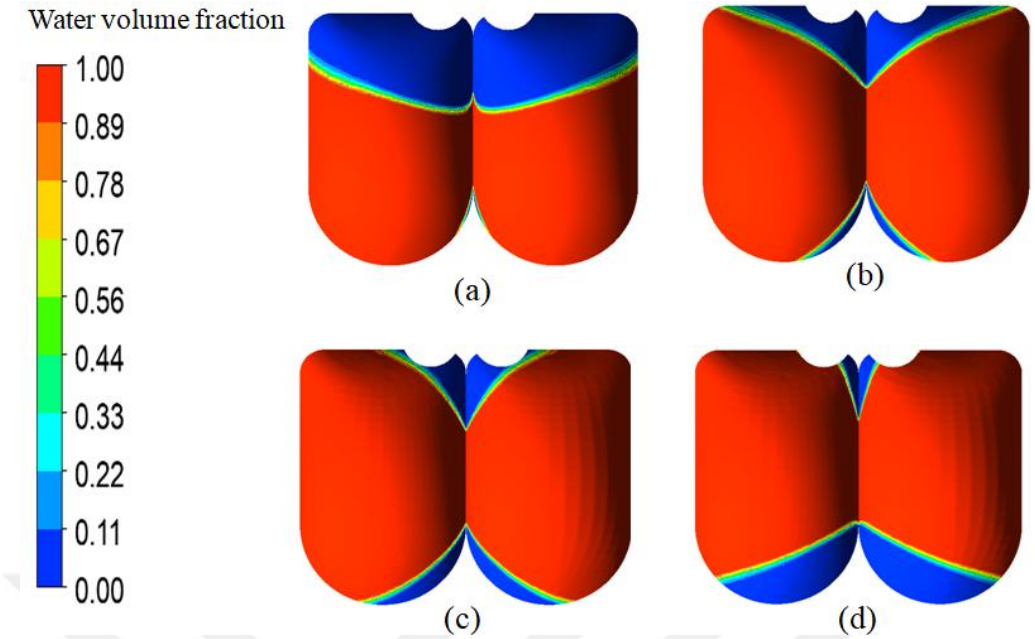

Figure 4.37. Shows variation of the water volume fraction when velocity =30 m/s and diameter =40mm for model 2 at figure (a) splitter angle=55 degree, (b) splitter angle=75 degree, (c) splitter angle=90 degree and (d) splitter angle=115 degree.

In figures (4.38 and 4.39), for two models and four splitter angles, the water distributions inside the bucket are described. At first, in majority of the internal surface the water is scattered at the bucket outlet. Once the splitter angle is 55 degree, the water concentrates on the edge of the back. Comparable quantity of the jet does not penetrate into the bucket. The bucket is not affected by similar amount of water. Next, in the splitter of 75 degree the distribution of water is occurred slightly away from the bucket edge. Furthermore, comparing to the bigger amount of water infiltrates into the bucket in comparison to the other splitter angles in splitter angle of 55 degree. Besides, the layer of water prolonged to the cut out edge and it becomes thinner as the splitter angle is 90 degree. The entire jet enters the bucket and the whole layer of water is constrained in the bucket. Eventually, when applying a splitter of 115 degree, the layer of water is chiefly extensive together with the edge of the bucket. A vast amount of the jet exits in the cut off, which initiates a massive force loss.

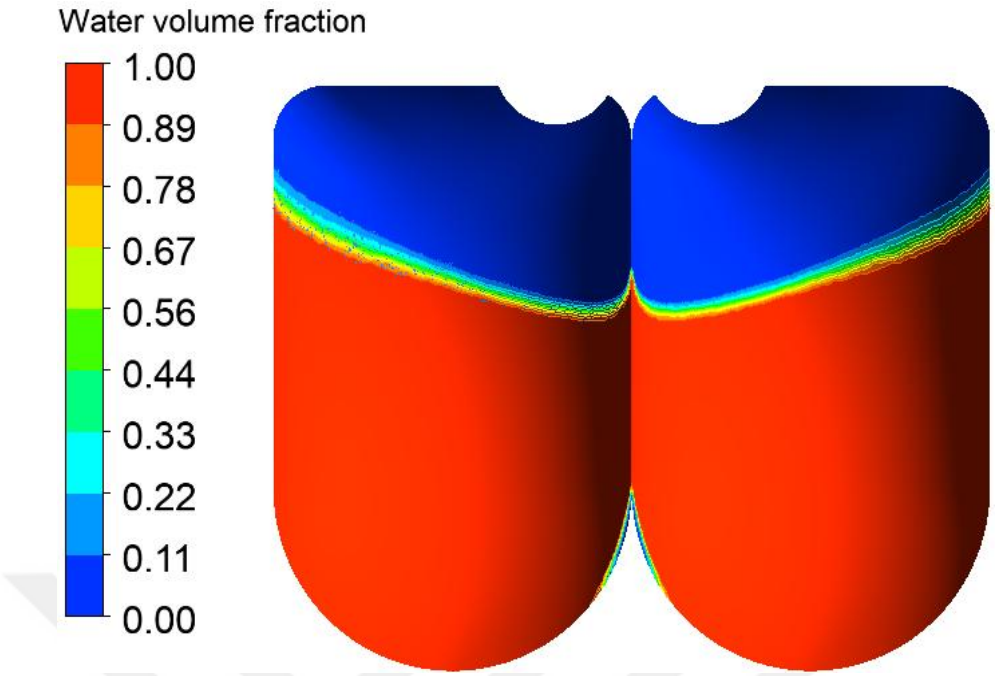

Figure 4.38. Shows variation of the water volume fraction when the velocity =35 m/s, d=40 mm and splitter angle =55 for model 2.

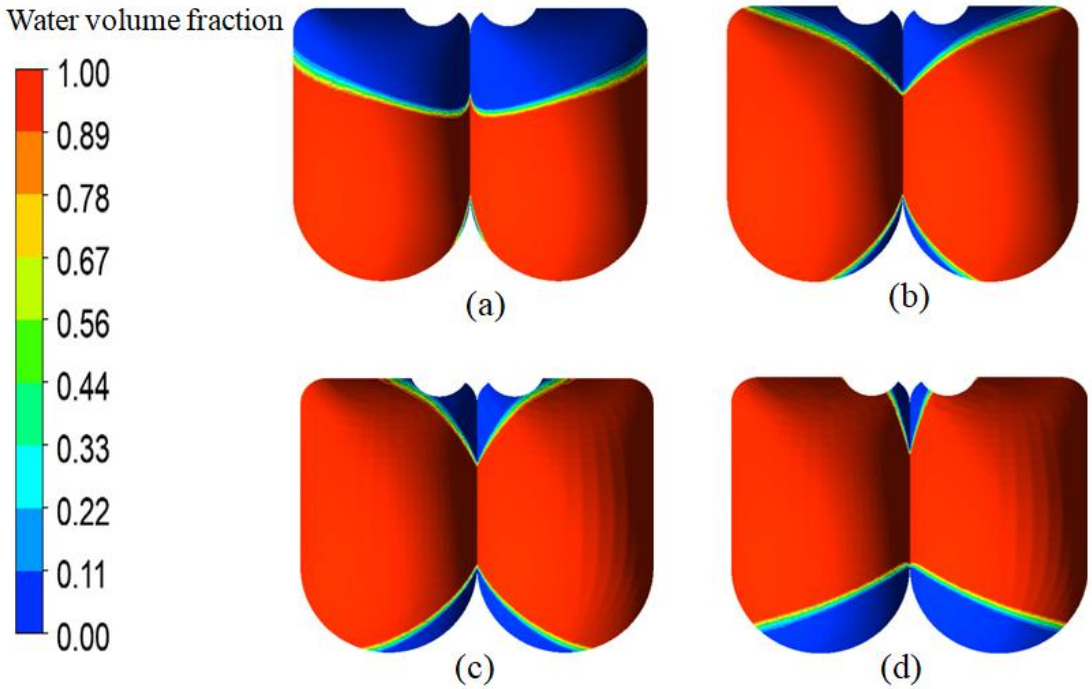

Figure 4.39. Shows variation of the water volume fraction when velocity =35 m/s and diameter =40mm for model 2 at figure (a) splitter angle=55 degree, (b) splitter angle=75 degree, (c) splitter angle=90 degree and (d) splitter angle=115 degree.

At the beginning, in most of the internal surface and at the bucket outlet, the water is distributed. If the splitter angle is 55 degree, the water concentrates on the back edge. Some quantity of the jet does not enter into the bucket. Similar amount of water does not impact the bucket. Consequently, the diffusion of water is occurred slightly away from the bucket edge in the splitter of 75 degree. Additionally, comparing to the splitter angle of 55 degree, bigger amount of water infiltrates into the bucket. Also, the layer of water extends to the edge of cut out and it becomes thinner when the splitter angle is 90 degree. The entire jet enters the bucket and the entire layer of water is restricted in the bucket. Lastly, when utilizing a splitter of 115 degree, the layer of water is mainly extensive in conjunction with the edge of the bucket. A huge amount of the jet exits at the cut off, which resulted in a massive force loss. The water distribution inside the bucket for two models and four splitter angles are exhibited in these figures.

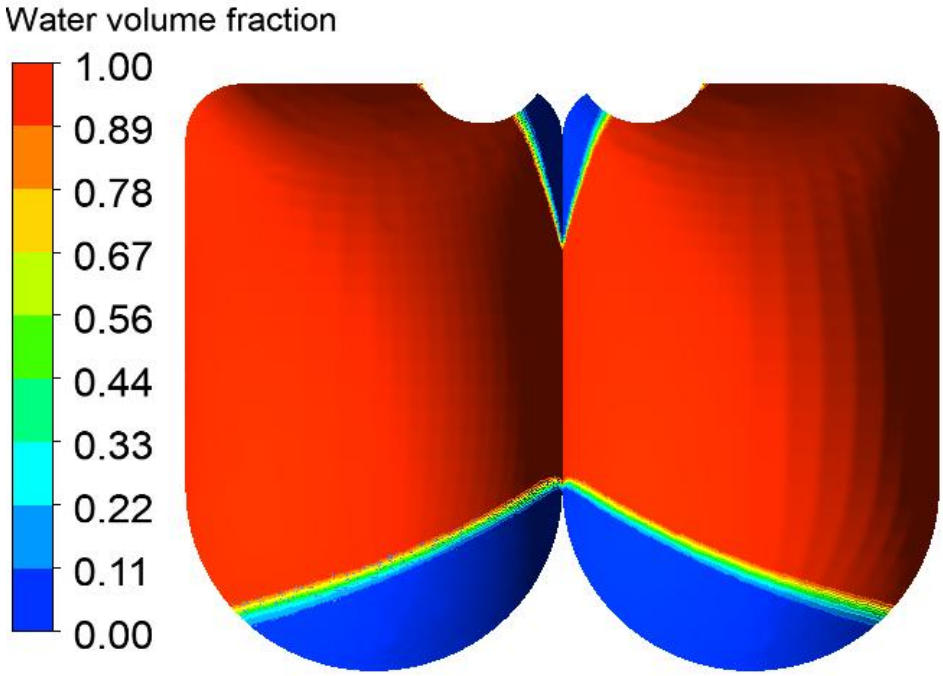

Figure 4.40. Shows variation of the water volume fraction when the velocity =40 m/s, d=40 mm and splitter angle =115 for model 2.

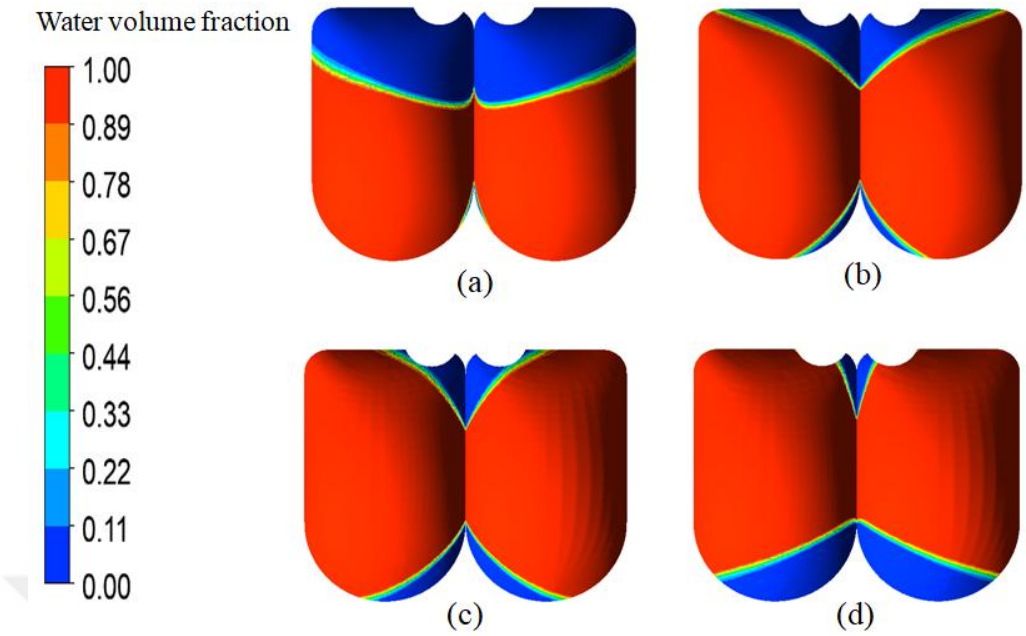

Figure 4.41. Shows variation of the water volume fraction when velocity =40 m/s and diameter =40mm for model 2 at figure (a) splitter angle=55 degree, (b) splitter angle=75 degree, (c) splitter angle=90 degree and (d) splitter angle=115 degree.

4.3. **Streamline**

Streamline is the direction of the velocity same as the velocity magnitude. It demonstrates the proportion of the change of the fluid position. In any flow system a single flow or a two-phase flow, velocity is a very important parameter that effects on design of the system. It affects the flow pattern transition and it is one of the parameters to specify the type of flow (laminar, transition and turbulent). There are two types of fluid flow, laminar flow stream lines and turbulent flow stream lines. Particles of a continuous phase of fluid can be advised to move along smooth continuous pathways which are given the term streamlines. These streamlines can be curved or straight, depending on the flow of the fluid. In the bucket of the pelton turbine, streamline is the maximum compared to the velocity in all position. It can be seen that the velocity at the inlet was high then decreased gradually for all cases. The jet has parallel streamlines prior crushing the bucket, as seen from vector pattern. Because of deflection of jet, the stream lines diverse near the bucket. After striking the bucket, the jet diffused. Therefore; vortex occurred at the near edge of bucket when it was changing with models

of the bucket and diameter which it clearly in the figures (4.42 and 4.43). It was monitored that higher amounts of water leave throughout the cut-out which result in wastage without contribution to impulse force. These results agree with (Gupta and Prasad, 2012).

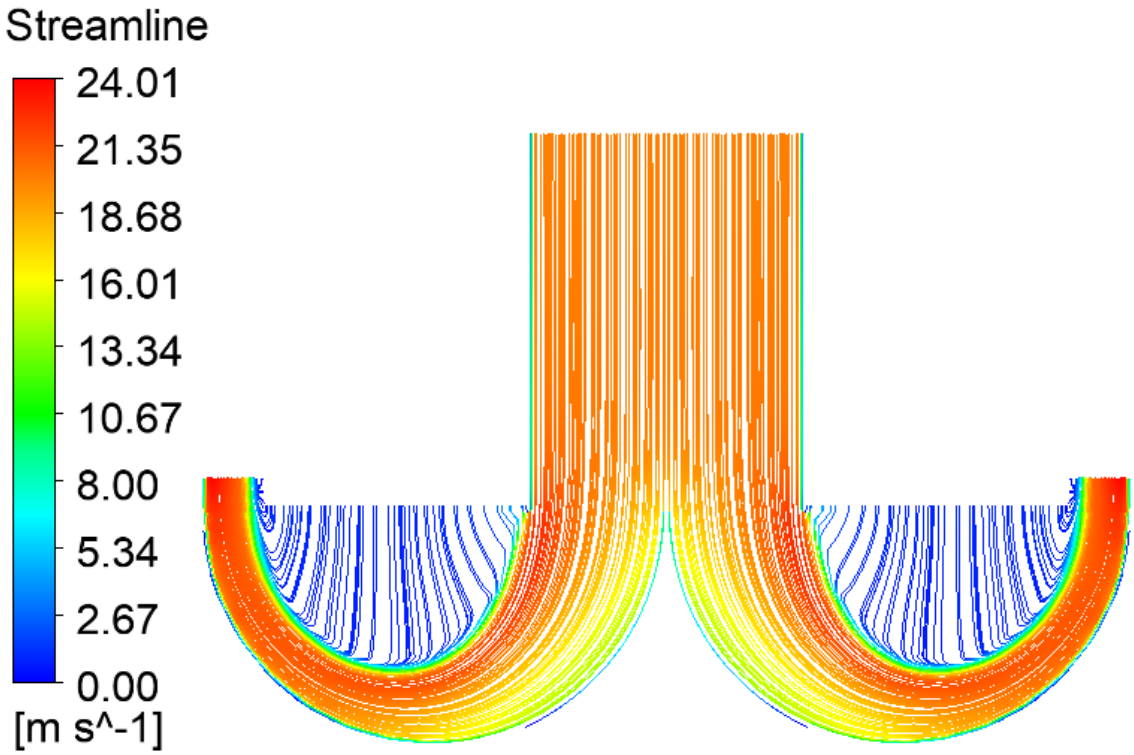

Figure 4.42. Shows that the XY plane streamline when splitter angle = 90degree and velocity = 20 m/s for model 2.

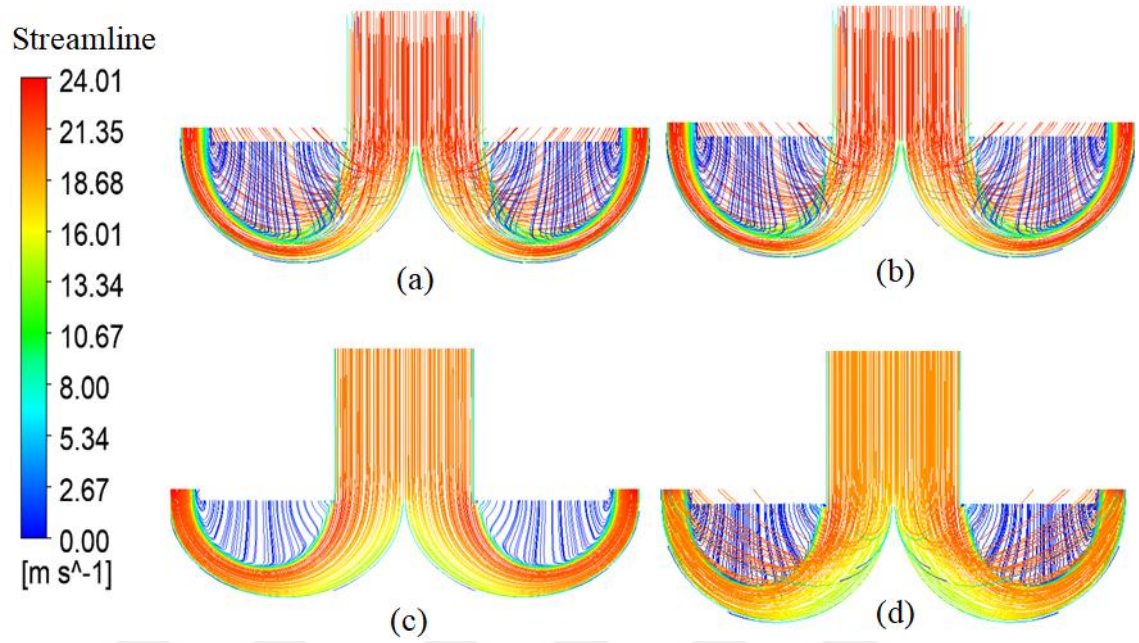

Figure 4.43. Shows that the XY plane streamline when velocity = 20 m/s and diameter =40mm for model 2 at figure (a) splitter angle=55 degree, (b) splitter angle=75 degree, (c) splitter angle=90 degree and (d) splitter angle=115 degree.

From figure 4.44 and 4.45, it is that the velocity at the inlet is high then declined progressively for all cases. As seen from vector pattern, the jet has parallel streamlines before crushing the bucket. Because of deflection of jet, the stream lines diverse near the bucket. The jet diffused, after striking the bucket. Thus, vortex happened at the close edge of bucket once it was altering with models of the bucket and diameter which it clearly in the figure. It was observed that bigger quantity of water leaves through the cut-out which leads to wastage without involvement to force impulse. These outcomes comply with

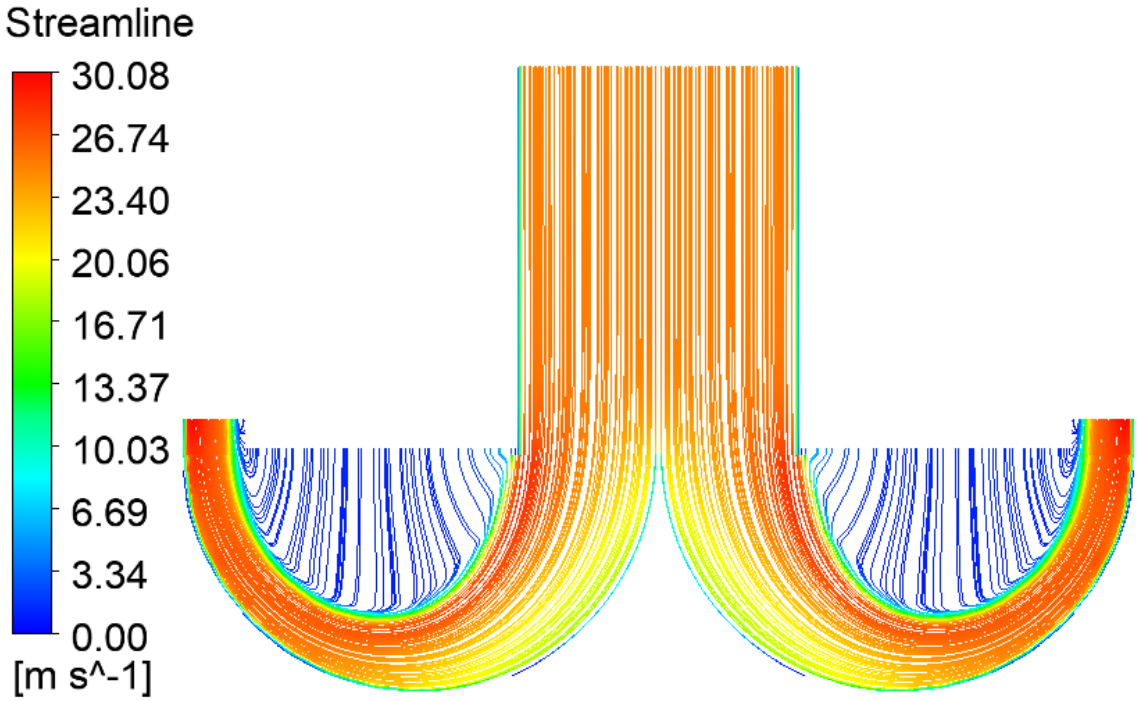

Figure 4.44. Shows that the XY plane streamline when splitter angle = 90 degree and velocity = 25m/s for model 2.

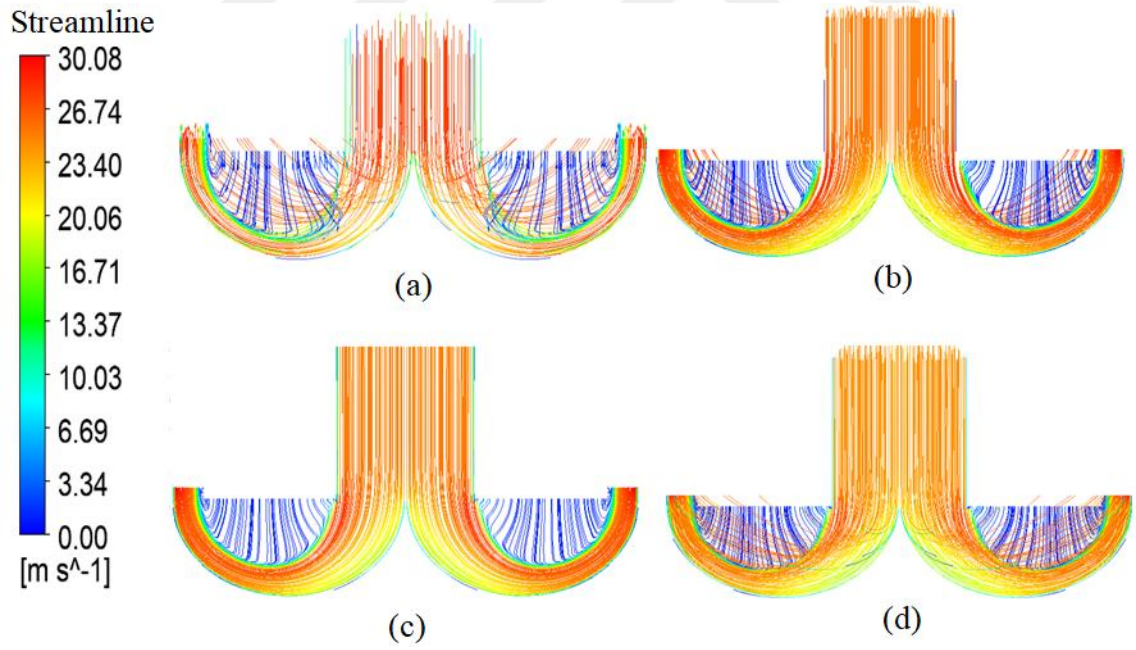

V=25m/s m2.

Figure 4.45. Shows that the XY plane streamline when velocity = 25 m/s and diameter =40mm for model 2 at figure (a) splitter angle=55 degree, (b) splitter angle=75 degree, (c) splitter angle=90 degree and (d) splitter angle=115 degree.

A figure (4.46 and 4.47) describes the velocity stream line for all cases. It is seen that the velocity is high at the inlet after that it progressively declined. As it is obvious from vector pattern, the jet has parallel streamlines before hitting the bucket. As a result of jet deflection, the stream lines varied close the bucket. Subsequent striking the bucket, the jet diffused. Hence, vortex happened at the near edge of bucket as it is altering with models of the bucket and diameter which is clearly seen in the figure. It is monitored that larger quantity of water leave via the cut-out which cause wastage without involvement to force impulse. These outcomes agree with (GuptaandPrasad, 2012).

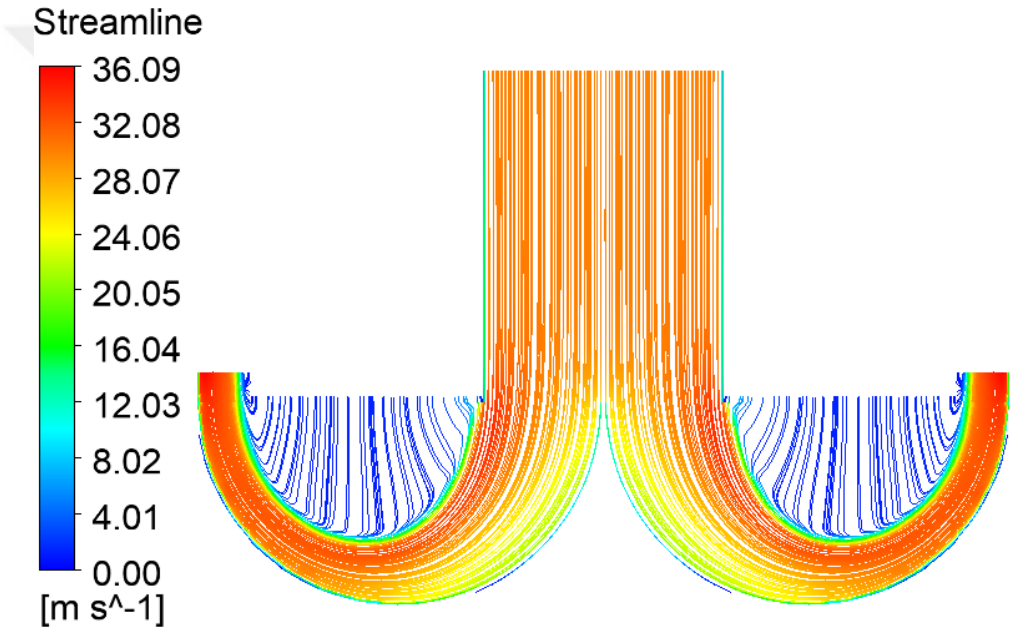

Figure 4.46. Shows that the XY plane streamline when splitter angle = 90 degree and velocity = 30 m/s for model 2.

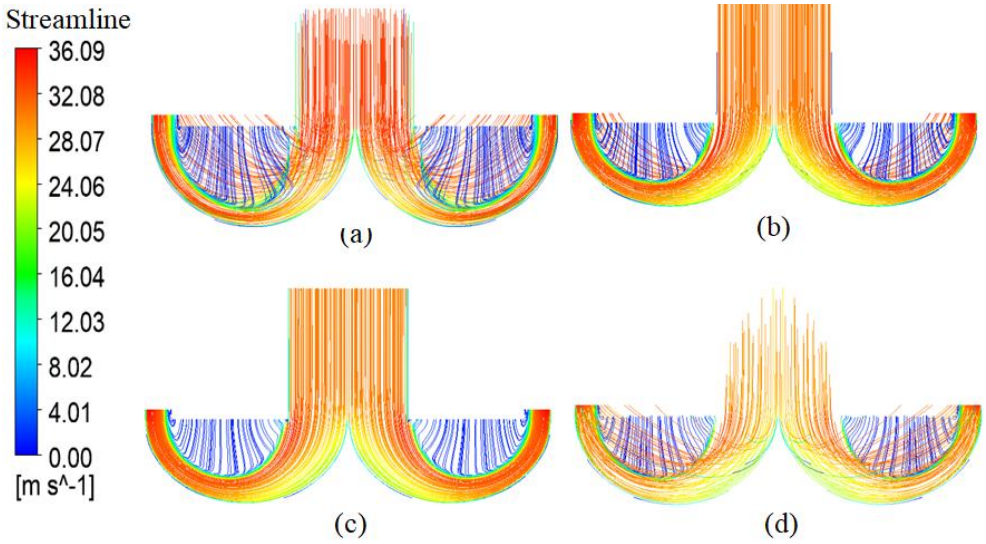

Figure 4.47. Shows that the XY plane streamline when velocity = 30 m/s and diameter =40mm for model 2 at figure (a) splitter angle=55 degree, (b) splitter angle=75 degree, (c) splitter angle=90 degree and (d) splitter angle=115 degree.

From figure 4.48 and 4.49, it is that the velocity at the inlet is high then declined progressively for all cases. As seen from vector pattern, the jet has parallel streamlines before crushing the bucket. Because of deflection of jet, the stream lines diverse near the bucket. The jet diffused, after striking the bucket. Thus, vortex happened at the close edge of bucket once it was altering with models of the bucket and diameter which it clearly in the figure. It was observed that bigger quantity of water leaves through the cut-out which leads to wastage without involvement to force impulse. These outcomes comply with

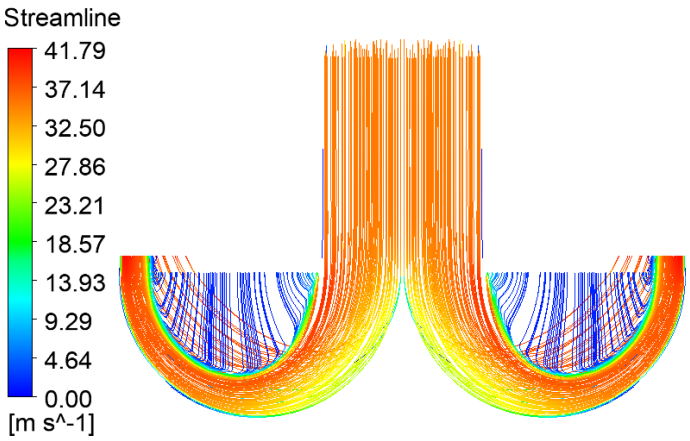

Figure 4.48. Shows that the XY plane streamline when splitter = 55 degree and velocity = 35 m/s for model 2.

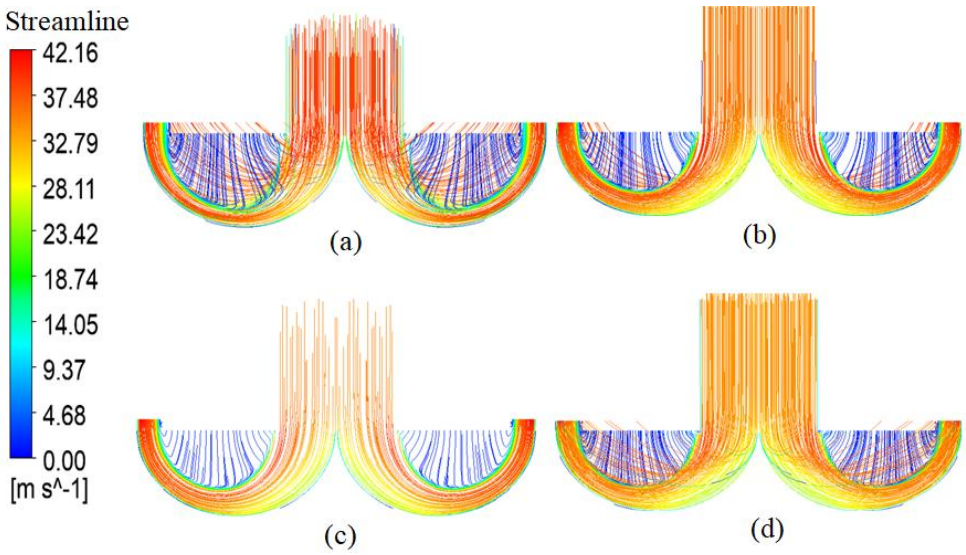

Figure 4.49. Shows that the XY plane streamline when velocity = 35 m/s and diameter =40mm for model 2 at figure (a) splitter angle=55 degree, (b) splitter angle=75 degree, (c) splitter angle=90 degree and (d) splitter angle=115 degree.

Table 4.1and 4.2 demonstrates the results when the splitter angle was 55. It can be seen that the five different velocities (20, 25, 30, 35, and 40) were utilized for both diameters. It is also visible that the highest Reynolds number and maximum force on the bucket were 1592023.9and 4197.6 N respectively for diameter is 40 mm so it is also visible that the highest Reynolds number and maximum force on the bucket were 1194975 and 2393.6 N respectively for diameter is 30 mm. However, the lowest Reynolds number maximum pressure and force on the bucket were 796011.96 and 1032N respectively for diameter is 40 mm so the lowest Reynolds number maximum pressure and force on the bucket were 597487.5, 172851.3 Pascaland 629.4N respectively for diameter is 30 mm. Therefore, it can be stated that the velocity is positively correlated with Reynolds number, maximum pressure and maximum force on bucket.

Table 4. 1. Shows the result when the angle 55 degree of the model 1

Item	Velocity (m/sec)	Diameter Of the nozzle (mm)	Reynolds number	Max force on the bucket	Max pressure on the bucket
1	20	40	796011.96	1032	204321.2
2	25	40	995014.95	1601	320141.5
3	30	40	1194017.9	2442	46070.7
4	35	40	1393020.9	3180	627627.5
5	40	40	1592023.9	4197.6	919789.5

Table 4.2. Shows the result when the angle 55 degree and D=30 mm of the model 1

Item	Velocity (m/sec)	Diameter Of the nozzle (mm)	Reynolds number	Max force on the bucket	Max pressure on the bucket
1	20	30	597487.5	629.4	172851.3
2	25	30	746859.4	979.9	272071.3
3	30	30	896231.3	1345.4	46070.7
4	35	30	1045603.1	1832	530567.2
5	40	30	1194975	2393.6	692890.3

Table 4.3 and 4.4 shows the outcomes when the splitter angle was 75 and velocities 20, 25, 30, 35, and 40 m/s for both diameters. It is also visible that the lowest Reynolds number maximum pressure and force on the bucket were 796011.96,206816.4 Pascaland 1082.2 N respectively for diameter equal 40mm therefore; the lowest Reynolds number maximum pressure and force on the bucket were 597487.5,124003.8 Pascaland 648.75 N respectively for diameter equal 30mm. Nevertheless, the highest Reynolds number, maximum pressure and maximum force on the bucket were 1592023.9.9, 830094.6 Pascal and 4337.4N respectively when diameter is 40 mm. however in the table 4.4 is also visible the highest Reynolds number, maximum pressure and maximum force on the bucket were 1194975, 468895.8 Pascal and 2453.12N respectively. Thus, it can be stated that the velocity is positively correlated with

Reynolds number, maximum pressure and maximum force on bucket once the diameter of the nozzle is stable.

Table 4. 3. Shows the result when the angle 75 degree of the model 1

Item	Velocity (m/sec)	Diameter Of the nozzle (mm)	Reynolds number	Max force on the bucket	Max pressure on the bucket
1	20	40	796011.96	1082.2	206816.4
2	25	40	995014.95	1693.4	324180.8
3	30	40	1194017.9	2513	466857.9
4	35	40	1393020.9	3319.6	633570.1
5	40	40	1592023.9	4337.4	830094.6

Table 4. 4.Shows the result when the angle 75 degree and D=30mm of the model 1

Item	Velocity (m/sec)	Diameter Of the nozzle (mm)	Reynolds number	Max force on the bucket	Max pressure on the bucket
1	20	30	597487.5	648.75	124003.8
2	25	30	746859.4	1025.4	195961.5
3	30	30	896231.3	1392.32	266082.6
4	35	30	1045603.1	1895.68	362345.3
5	40	30	1194975	2453.12	468895.8

From the table (4.5 and 4.6), it can be monitored that by increasing the velocity, Reynolds number, maximum pressure and maximum force on bucket are also escalated. The utilized splitter angle was 90 and velocities were 20, 25, 30, 35, and 40 m/s for both diameters. The lowest Reynolds number maximum pressure and force on the bucket were 796011.96, 209091.7 and 1159 N respectively for 40mm nozzle diameter when in the 4.6 display that the highest Reynolds number, maximum pressure and maximum force on the bucket were 1194975, 484737.7 and 2536 N respectively when the diameter is 30mm. Nevertheless, the highest Reynolds number, maximum pressure and

maximum force on the bucket were 1592023.9.9, 836581.3 and 4644.2 N respectively for 40 mm diameter. The lowest Reynolds number maximum pressure and force on the bucket were 597487.5, 131817.7and 689.63 N respectively for 30 mm nozzle diameter.

Table 4.5. The result when the angle 90 degree of the model 1

Item	Velocity (m/sec)	Diameter Of the nozzle (mm)	Reynolds number	Max force on the bucket(N)	Max pressure on the bucket(Pascal)
1	20	40	796011.96	1159	209091.7
2	25	40	995014.95	1823	326729.9
3	30	40	1194017.9	2615.4	470527.2
4	35	40	1393020.9	3554.6	640491.9
5	40	40	1592023.9	4644.2	836581.3

Table 4. 6.The result when the angle 90 degree and D=30 mm of the model 1

Item	Velocity (m/sec)	Diameter Of the nozzle (mm)	Reynolds number	Max force on the bucket(N)	Max pressure on the bucket(Pascal)
1	20	30	597487.5	689.63	131817.7
2	25	30	746859.4	1082	206816.3
3	30	30	896231.3	1435	274289.7
4	35	30	1045603.1	1968	376168.7
5	40	30	1194975	2536	484737.7

It is clear that the lowest Reynolds number maximum pressure and force on the bucket were 796011.96, 209091.7 and 1056 N correspondingly for model 1 and diameter is a 40mm. Nonetheless, the highest Reynolds number, maximum pressure and maximum force on the bucket were 1592023.9.9, 836581.3 and 4247.4 N respectively when it showed in table 4.7. The employed splitter angle was 115 and velocities were 20, 25, 30, 35, and 40 m/s for both diameters. Reynolds number, maximum pressure and

maximum force on bucket are positively correlated with the velocity. Table 4.8 displayed that the relation between velocity, Reynolds number, maximum force on the bucket pelton turbine and maximum pressure when the highest Reynolds number, maximum pressure and maximum force on the bucket were 1194975, 460653.7and 2410Nrespectively. The lowest Reynolds number, maximum pressure and force on the bucket were 597487.5, 122082.8 and 638.7 N correspondingly for nozzle diameter is 30mm.

Table 4. 7. Shows the result when the angle 115 degree of the model 1

Item	Velocity (m/sec)	Diameter Of the nozzle (mm)	Reynolds number	Max force on the bucket	Max pressure on the bucket
1	20	40	796011.96	1056	206564.9
2	25	40	995014.95	1635	323172.9
3	30	40	1194017.9	2483	461070.7
4	35	40	1393020.9	325.6	634089.6
5	40	40	1592023.9	4247.4	827670.9

Table 4. 8. Shows the result when the angle 115 degree and D= of the model 2

Item	Velocity (m/sec)	Diameter Of the nozzle (mm)	Reynolds number	Max force on the bucket	Max pressure on the bucket
1	20	30	597487.5	638.7	122082.8
2	25	30	746859.4	1012	193436.3
3	30	30	896231.3	1367	261291.9
4	35	30	1045603.1	1874	358201.2
5	40	30	1194975	2410	460653.7

As it is seen in the table 4.9and 4.10, any escalation in the velocity at the same splitter angle and nozzle diameter resulted in an increase in Reynolds number, maximum pressure and maximum force on bucket. Various velocities of 20, 25, 30, 35,

and 40m/s, and a splitter angle of 55 were utilized. In addition, the maximum Reynolds number, maximum pressure and maximum force on the bucket were 1592023.9, 836581.3Pascaland 3912.4 N correspondingly according to the 40 mm nozzle diameter. However, the minimum Reynolds number maximum pressure and force on the bucket were 796011.96, 143589and 979.4N correspondingly at the same diameter. The lowest Reynolds number, maximum pressure and force on the bucket were 597487.5, 99738.2 Pascaland 521.8 N correspondingly for nozzle diameter is 30mm. however in the table 4.10 is also visible the highest Reynolds number, maximum pressure and maximum force on the bucket were 1194975, 398838.2 Pascal and 2086.6 N respectively.

Table 4. 9. Shows the result when the angle 55 degree of the model 2

Item	Velocity (m/sec)	Diameter Of the nozzle (mm)	Reynolds number	Max force on the bucket	Max pressure on the bucket
1	20	40	796011.96	979.4	143589
2	25	40	995014.95	1544	226798.8
3	30	40	1194017.9	2199.4	326572.8
4	35	40	1393020.9	2994.8	444486.4
5	40	40	1592023.9	3912.4	580536.8

Table 4.10. Shows the result when the angle 55 degree and D =30 mm of the model 2

Item	Velocity (m/sec)	Diameter Of the nozzle (mm)	Reynolds number	Max force on the bucket	Max pressure on the bucket
1	20	30	597487.5	521.8	99738.2
2	25	30	746859.4	813	155398.9
3	30	30	896231.3	1169	223445.7
4	35	30	1045603.1	1592.2	304337.3
5	40	30	1194975	2086.6	398838.2

The variation in the Reynolds number, maximum pressure and maximum force on bucket by applying different velocity displays in the Table 4.11. The applied velocities were 20, 25, 30, 35, and 40m/s, and a splitter angle was of 75 degree for both tables. Additionally, the maximum Reynolds number, maximum pressure and maximum force on the bucket were 1592023.9, 747198.8 and 4082 N respectively as nozzle diameter is 40mm. Nonetheless, the minimum Reynolds number maximum pressure and force on the bucket were 796011.96, 186658.4 Pascal and 1021.8 N correspondingly in the table 4.11. Table 4.12 showed that the relation between Reynolds number, maximum force on the bucket pelton turbine, velocity, and maximum pressure when the highest Reynolds number, maximum pressure and maximum force on the bucket were 1194975, 416002.8 Pascal and 2176.4Nrespectively. The minimum Reynolds number, maximum pressure and force on the bucket were 597487.5, 103905.1 Pascal and 543.6 N correspondingly for nozzle diameter is 30mm.

Table 4. 11. Shows the result when the angle 75 degree of the model 2

Item	Velocity (m/sec)	Diameter Of the nozzle (mm)	Reynolds number	Max force on the bucket	Max pressure on the bucket
1	20	40	796011.96	1021.8	186658.4
2	25	40	995014.95	1593.6	291739.5
3	30	40	1194017.9	2295.2	420189.3
4	35	40	1393020.9	3132	572003.3
5	40	40	1592023.9	4082	747198.8

Table 4. 12. Shows the result when the angle 75 degree and D=30mm of the model 2

Item	Velocity (m/sec)	Diameter Of the nozzle (mm)	Reynolds number	Max force on the bucket	Max pressure on the bucket
1	20	30	597487.5	543.6	103905.1
2	25	30	746859.4	845	161515.5
3	30	30	896231.3	1220.2	233232.2
4	35	30	1045603.1	1666	318443.6
5	40	30	1194975	2176.4	416002.8

By applying different velocity, Table 4.13 and 4.14 shows the differences in the Reynolds number, maximum pressure and maximum force on bucket. The different velocities were 20, 25, 30, 35, and 40m/s, and a splitter angle was of 90 degree for model2. Additionally, the maximum Reynolds number, maximum pressure and maximum force on the bucket were 1592023.9, 790368.9 and 4153.8 N respectively. Nonetheless, the minimum Reynolds number maximum pressure and force on the bucket were 796011.96, 197305.6 and 1037.5N correspondingly according to nozzle diameter40mm. The lowest Reynolds number, maximum pressure and force on the bucket were 597487.5, 108569 Pascal and 568 N correspondingly for nozzle diameter is 30mm. the highest Reynolds number, maximum pressure and maximum force on the bucket were 1194975, 434543.6 Pascal and 2273.4 N Respectively at the same diameter.

Table 4.13. Shows the result when the angle 90 degree of the model 2

Item	Velocity (m/sec)	Diameter Of the nozzle (mm)	Reynolds number	Max force on the bucket	Max pressure on the bucket
1	20	40	796011.96	1037.5	197305.6
2	25	40	995014.95	1621.62	306216
3	30	40	1194017.9	2335.7	443357.5
4	35	40	1393020.9	3179.6	604983.9
5	40	40	1592023.9	4153.8	790368.9

Table 4.14. Shows the result when the angle 90 degree and D=30 mm of the model 2

Item	Velocity (m/sec)	Diameter Of the nozzle (mm)	Reynolds number	Max force on the bucket	Max pressure on the bucket
1	20	30	597487.5	568	108569
2	25	30	746859.4	886	169352.3
3	30	30	896231.3	1278.2	244318.5
4	35	30	1045603.1	1743.6	333276
5	40	30	1194975	2273.4	434543.6

The effect of the velocity and splitter angle is demonstrated in Table 4.15and4.16. The applied splitter angle was 90 and velocities were 20, 25, 30, 35, and 40m/s. It can be observed that Reynolds number, maximum pressure and maximum force on bucket are positively correlated with the velocity once the diameter of the nozzle is stable. The lowest Reynolds number maximum pressure and force on the bucket were 796011.96, 201283.8 and 992.8 N respectivelyso the lowest Reynolds number maximum pressure and force on the bucket were 597487.5, 186658.4Pascaland 568 N respectively for diameter is 30 mm. Nevertheless, the highest Reynolds number, maximum pressure and maximum force on the bucket were 1592023.9.9, 807671.3 Pascal and 3972 N respectively.

Table 4. 15. Shows the result when the angle 115 degree of the model 2

Item	Velocity (m/sec)	Diameter Of the nozzle (mm)	Reynolds number	Max force on the bucket	Max pressure on the bucket
1	20	40	796011.96	992.8	201283.8
2	25	40	995014.95	1550.6	311022.6
3	30	40	1194017.9	2230.7	449914.8
4	35	40	1393020.9	3038.6	615647.4
5	40	40	1592023.9	3972	807671.3

Table 4.16. Shows the result when the angle 115 degree and D=30mm of the model 2

Item	Velocity (m/sec)	Diameter Of the nozzle (mm)	Reynolds number	Max force on the bucket	Max pressure on the bucket
1	20	30	597487.5	568	186658.4
2	25	30	746859.4	886	291739.5
3	30	30	896231.3	1278.2	420189.3
4	35	30	1045603.1	1743.6	572003.3
5	40	30	1194975	2273.4	747198.8

The relationships between force on the bucket and Reynolds number in four various splitter angles is expressed In this figure for both models. It is clear that the Reynolds number progressively affected by mounting the splitter angle from 55 to 115 degree. Immediately, the quantity of force on the bucket is also augmented via escalating the splitter angle from 55 to 115 degree. Thus, it can be reported that the amount of force on the bucket and Reynolds number there is positively correlated by escalating the splitter angle. As it is described above in the alteration of the force, by escalating the velocity as it increased from the Momentum equation changed directlyForce on the bucket escalated. Hence, the velocity is positively correlated with the force as in the momentum equation. Moreover, the change of force value is impacted by the shape. in this figure, it is evident that, the rate of force increased at the

splitter angle 90 degree compared to other splitter angle. Thus, for both models, it causes the lowest flow leakage through the edge and cut-out of the bucket of pelton turbine.

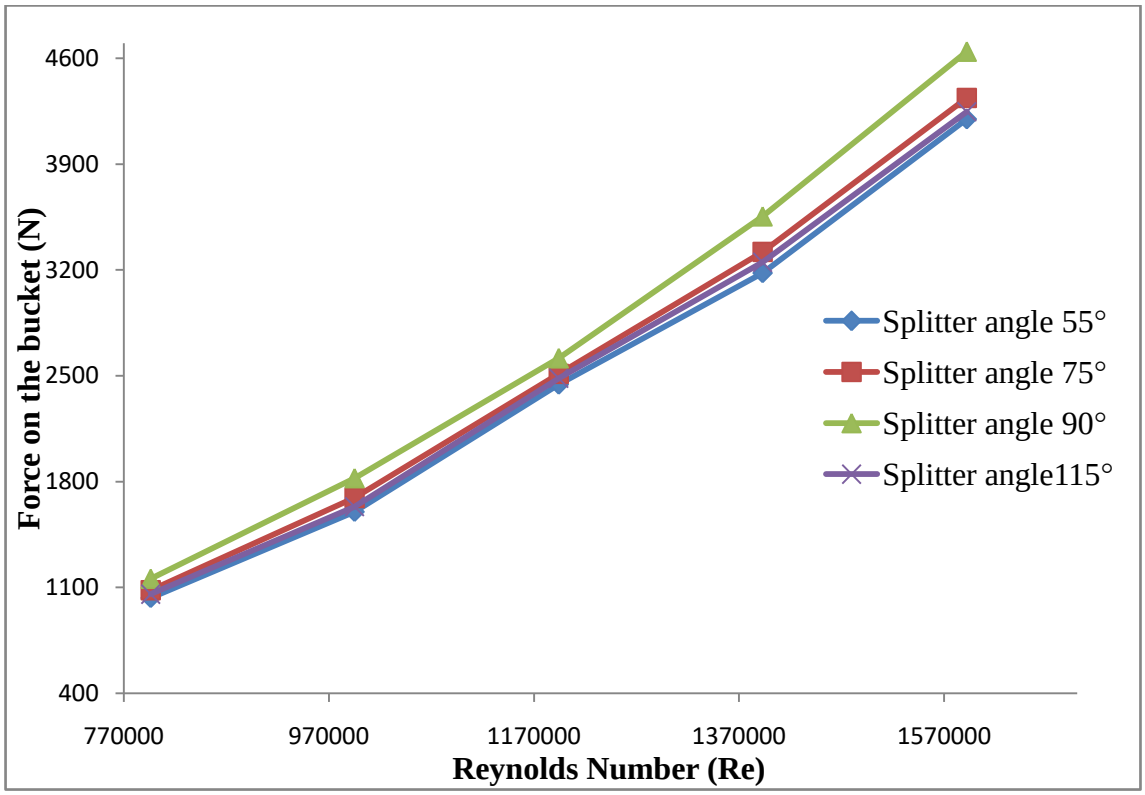

Figure 4.50. Effect of Reynolds number on force when the diameter was 40 mm and splitter angle was (55°, 75°, 90°, and115°) of model 1.

In this figure the relationships between Reynolds number and force on the bucket in four various splitter angles is expressed for both models. It is unveiled that by mounting the splitter angle from 55 to 115 degree, the Reynolds number affected progressively. Instantaneously, via escalating the splitter angle from 55 to 115 degree the quantity of force on the bucket is also augmented. Thus, it can be reported that the amount of force on the bucket and Reynolds number there is positively correlated by escalating the splitter angle. as it is described above in the alteration of the force, Force on the bucket escalated by escalating the velocity as it increased from the Momentum equation changed directly. Hence, the velocity is positively correlated with the force as in the momentum equation. Additionally, shape has an impact on the change of force value. It can be seen in this figure, the rate of force increased at the splitter angle 90

degree compared to other splitter angle. As explained in the figure (8), This might cause minimum leakage flow through the edge and cut-out of the bucket of pelton turbine for both models.

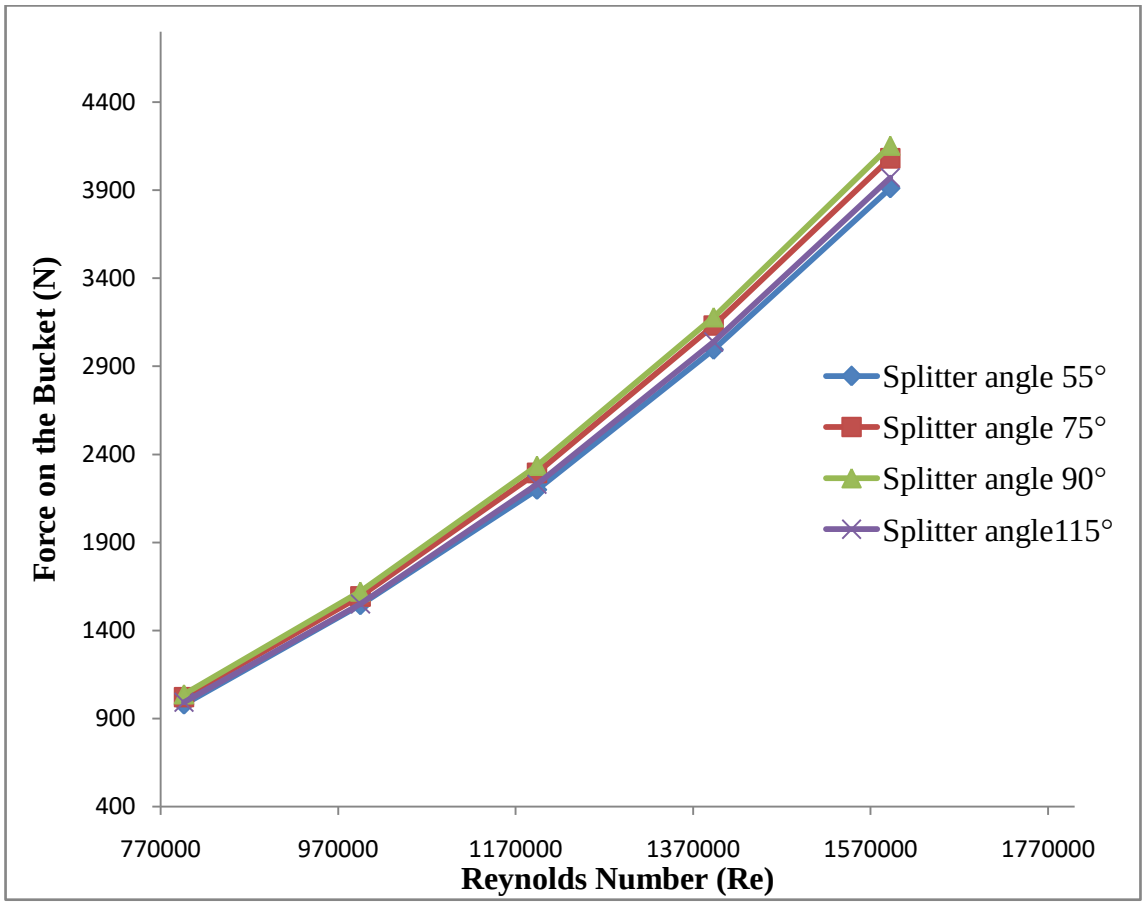

Figure 4.51. Effect of Reynolds number on force when the diameter was 40 mm and splitter angle was (55°, 75°, 90°, and115°) of model 2.

Figure (4.54) expresses the relationships between force on the bucket and Reynolds number in four different splitter angles is expressed for both models. It is demonstrated that by escalating the splitter angle from 55 to 115 degree, the Reynolds number impacted gradually. Simultaneously, by escalating the splitter angle from 55 to 115 degree the quantity of force on the bucket is also increased. Therefore, it can be stated that Reynolds number and the amount of force on the bucket there is positively correlated by escalating the splitter. Force on the bucket escalated by escalating the velocity as it increased from the Momentum equation changed directly as it is described above in the alteration of the force. Thus, the force is positively correlated with the

velocity as in the momentum equation. Moreover, shape has an impact on the change of force value. It can be seen in this figure, the rate of force increased at the splitter angle 90 degree compared to other splitter angle. This might result from minimum leakage flow through the edge and cut-out of the bucket of pelton turbine for both models.

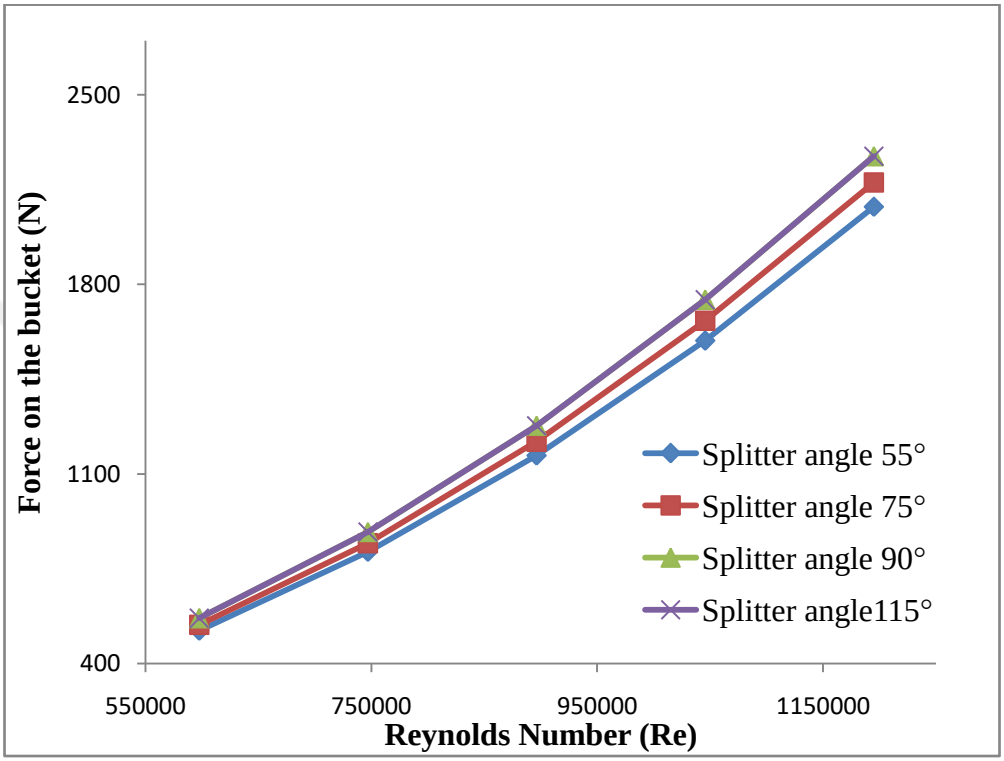

Figure 4.52. Effect of Reynolds number on force when the diameter was 30 mm and splitter angle was (55°, 75°, 90°, and115°) of model 1.

The relationships between force on the bucket and Reynolds number in four different splitter angles is expressed for both models is expressed in the figure (4.55). It is illustrated that Reynolds number progressively impacted by escalating the splitter angle from 55 to 115 degree. At the same time, the quantity of force on the bucket is also increased by escalating the splitter angle from 55 to 115 degree. Therefore, it can be stated that Reynolds number and the amount of force on the bucket there is positively correlated by escalating the splitter. Force on the bucket increased by increasing the velocity because it increased from the Momentum equation altered directly as it is described above in the alteration of the force. Thus, the force is positively correlated with the velocity as in the momentum equation. Furthermore, shape has an effect on the alteration of force value. It can be seen in this figure, the proportion of force increased

at the splitter angle 90 degree in comparison to other splitter angle this might result from minimum leakage flow through the cut-out and edge of the bucket of pelton turbine for both models.

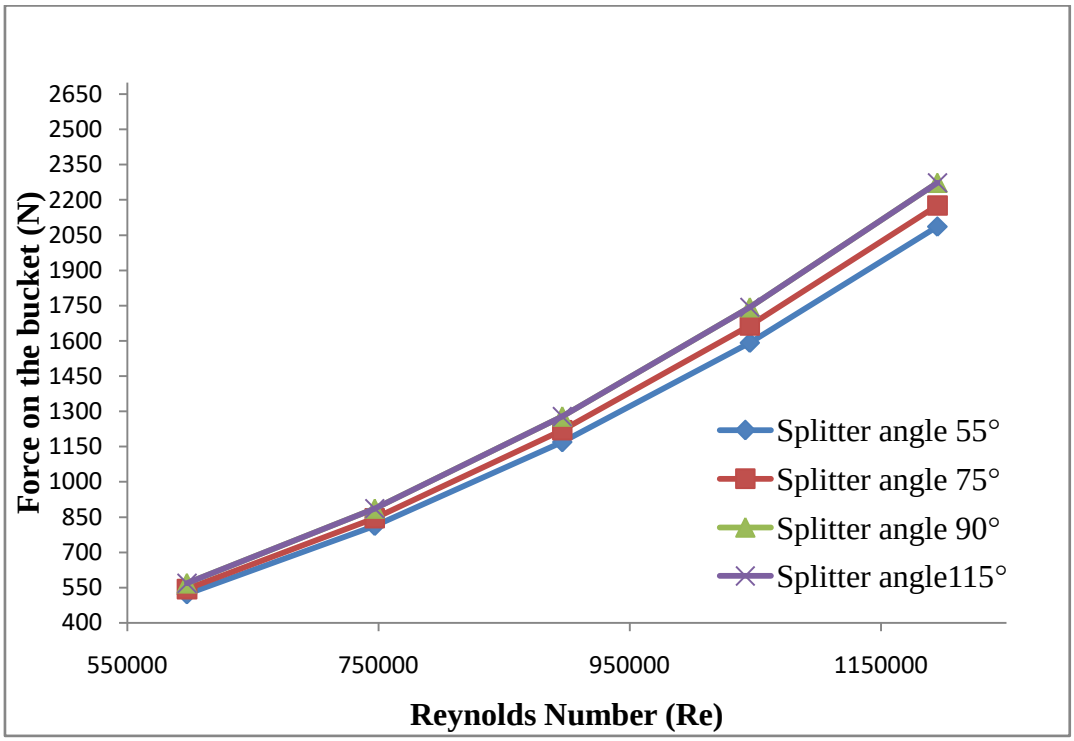

Figure 4.53. Effect of Reynolds number on force when the diameter was 30 mm and splitter angle was (55°, 75°, 90°, and115°) of model 2.

The relations between force on the bucket and splitter angle for four diverse velocities are displayed in Figure 4.56. In contrast to pressure, there is no leakage in force as it perpendicularly hits the bucket. It is clear that the increasing the splitter angle from 55 to 75resulted in the increase in the force on the bucket until reaches 90 degree, for all the cases. Then, the force on the bucket decreases for the whole cases after 90 degree. It is discovered that splitter angle has a noteworthy impact on the force of the bucket in the same velocity. However, increasing the splitter angle to 90 degree will influence the amount of force on the bucket. This is especially true in the higher velocities. The impulse force exerted by the contact fluid on the bucket pelton turbine. it is seen that the 90 impulse force reaches the maximum for all velocity and all cases because in this splitter angle water flow hit son the bucket perpendicularly as all The potential energy of water at height is changed into kinetic energy with minimum of the

losses. When it is out of 90 degree splitter angle, the force value declined, for both more than 90 degree an less than 90 degree, because the leakage of flow through the cut-out and edge of the bucket pelton turbine with changing of the splitter angle for all case which results in decreasing momentum force. It can be stated that there is a positive relation between the velocity and force.

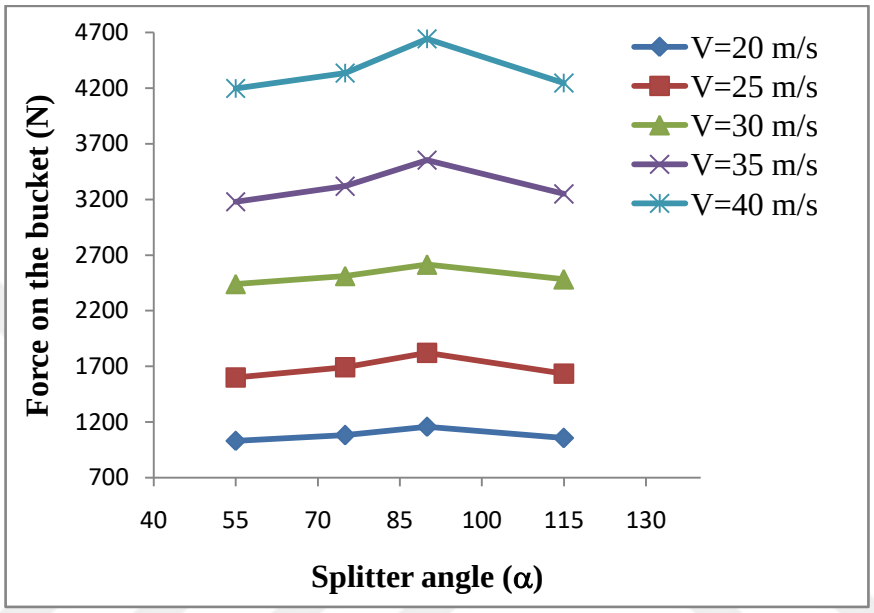

Figure 4.54. Show the relation between force and splitter angle when diameter = 40 mm for model 1.

Figure 4.57 displays the relations between force on the bucket and splitter angle for four diverse velocities. There is no leakage in force as it perpendicularly hits the bucket comparing to pressure. It is clear that the increase in the force on the bucket until reaches 90 degree, for all cases are resulted from the increase of the splitter angle from 55 to 75. After that, the force on the bucket declined for the whole cases after 90 degree. It is found that splitter angle has a remarkable effect on the force of the bucket in the same velocity. Nonetheless, the amount of force on the bucket is influenced by increasing the splitter angle to 90 degree. This is particularly true in the higher velocities. The impulse force exerted by the contact fluid on the bucket pelton turbine. it is seen in figure (4.57), that for all velocity and all cases the 90 impulse force reaches the maximum as in this splitter angle water flow hit on the bucket perpendicularly as all the potential energy of water at height is changed into kinetic energy with minimum of

the losses. the force value declined, for both more than 90 degree an less than 90 degree when it is out of 90 degree splitter angle because the leakage of flow through the cut-out and edge of the bucket pelton turbine with changing of the splitter angle for all case which results in decreasing momentum force. It can be reported that there is a positive correlation between the velocity and force.

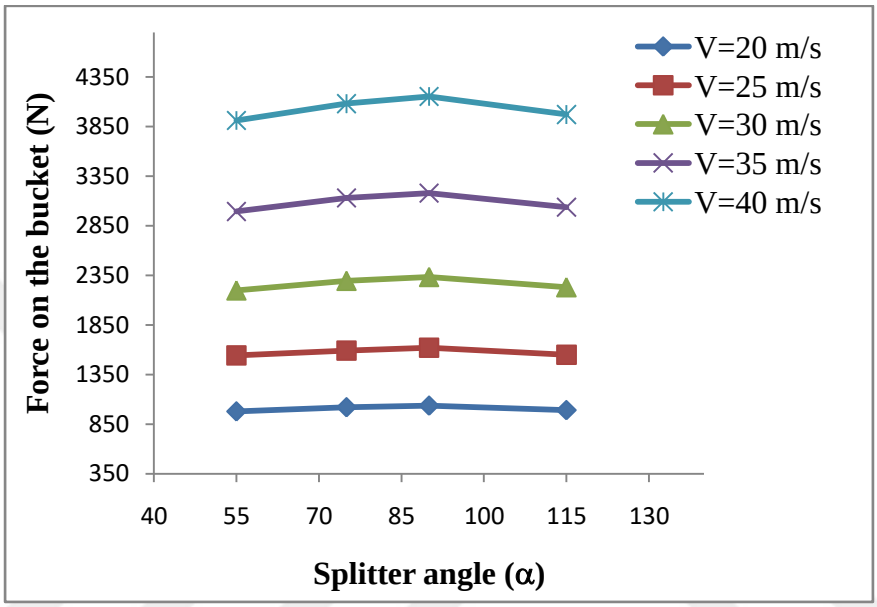

Figure 4.55. Show the relation between force and splitter angle when diameter = 40 mm for model 2.

This Figure illustrates the relations between force on the bucket and splitter angle for four different velocities. As it perpendicularly hits the bucket, there is no leakage in force comparing to pressure. It is clear that for all the cases, the escalation in the force on the bucket until reaches 90 degree, are resulted from the increase of the splitter angle from 55 to 75. Subsequently, the force on the bucket declined for the whole cases after 90 degree. It is revealed that in the same velocity, the splitter angle has a remarkable effect on the force of the bucket. Nevertheless, the amount of force on the bucket is influenced by escalating the splitter angle to 90 degree. In the higher velocities, this is particularly true. The impulse force exerted by the contact fluid on the bucket pelton turbine. figure (4.58) shows that for all velocity and all cases the 90 impulse force reaches the maximum as in this splitter angle water flow hit on the bucket perpendicularly as all the potential energy of water at height is changed into kinetic energy with minimum of the losses. for both more than 90 degree an less than 90 degree

the force value declined when it is out of 90 degree splitter angle because the leakage of flow through the cut-out and edge of the bucket pelton turbine with altering of the splitter angle for all case which results in declining momentum force. It can be stated that the velocity and force are correlated positively.

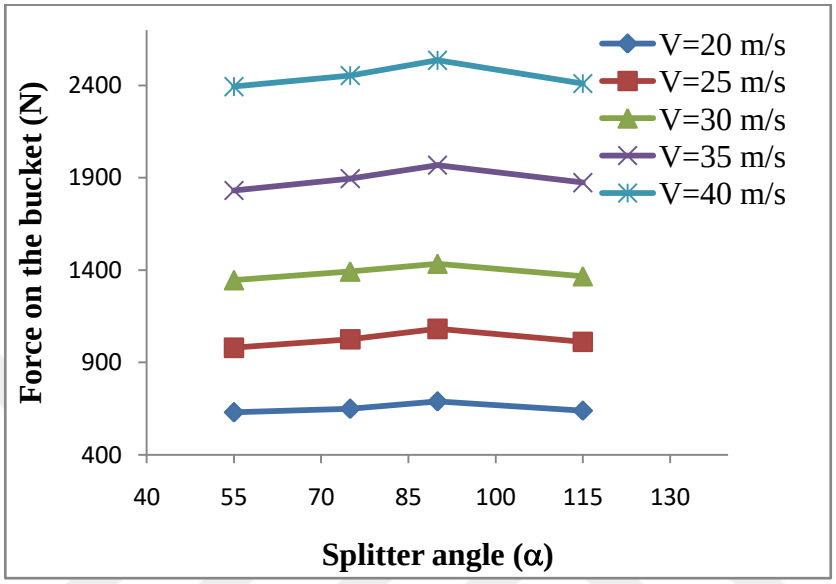

Figure 4.56. Show the relation between force and splitter angle when diameter = 30 mm for model 1.

The relations between splitter angle and force on the bucket for four dissimilar velocities are illustrated in this figure. There is no seepage in force comparing to pressure as it perpendicularly hits the bucket. For all the cases, it is evident that the acceleration in the force on the bucket until reaches 90 degree is caused by the increase of the splitter angle from 55 to 75 degree. Subsequently, the force on the bucket declined for the whole cases after 90 degree. It is revealed that the splitter angle has a remarkable effect on the force of the bucket in similar velocities. Nevertheless, the amount of force on the bucket is influenced by escalating the splitter angle to 90 degree. In the higher velocities, this is particularly true. The impulse force exerted by the contact fluid on the bucket pelton turbine. For all velocities and all cases, the 90 impulse force reaches the maximum as in this splitter angle water flow hit on the bucket perpendicularly as all the potential energy of water at height is changed into kinetic energy with minimum of the losses, as described in this figure. for both less than 90 degree and more than 90 degree, the force value dropped as it is out of 90 degree splitter

angle because the flow leakage via the cut-out and edge of the bucket pelton turbine with altering of the splitter angle for all case which results in deceasing momentum force. It is unveiled that that the velocity and force are positively correlated.

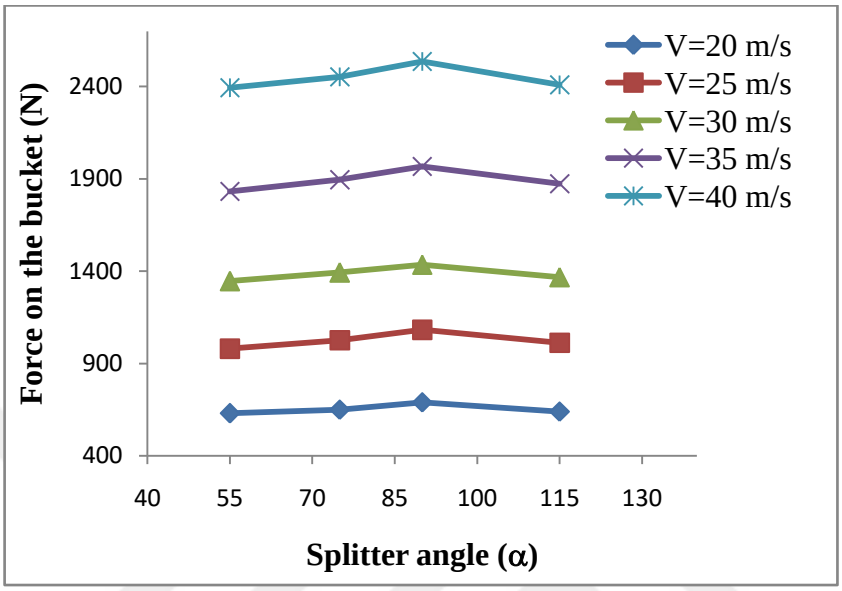

Figure 4.57. Show the relation between force and splitter angle when diameter = 30 mm for model 2.

5. CONCLUSION

In the current study, the research is carried out to have an understanding on the water –air two phase flow free surface phenomenon in bucket pelton turbine. The research supplies an outline with using ANSYS FLUENT commercially presented CFD simulation software so as to yield the benefit of using a CFD and selected volume of fluid (VOF) model.

The Pelton turbine is utilized in low water stream and high head in building micro-hydro-electric power plant. For obtaining a Pelton hydraulic turbine with highest efficiency throughout different working circumstances, the turbine parameters have to be encompassed in the designing process. The outcomes of pressure contour, stream line velocity, and force on the bucket, water volume of fraction and velocity vector were acquired from CFD simulations models. The simulation of visualized stream on the bucket and determined a force on the bucket in pelton turbine for four different inlet velocity (20, 25, 30, 35, and40m/s) for both models. Moreover, four dissimilar splitter angles 55, 75, 90 and 115degree, were applied for both models. This research utilized two jet diameters (30 and 40 mm) for both models. In the current examination, two different bucket models were employed at various inlet velocity such as 20, 25, 30,35and 40m/s, and four diverse splitter angle like 55, 75,90 and 115 for finding out the influences of every parameter on force on the bucket. It was discovered there is a linear relationship between inlet velocity and the force on the bucket. The examination revealed that until 90 degree, the relationship between splitter angle and force on the bucket is linear. However, subsequent the 90 degree. In addition, by increasing velocity, the amount of force on the bucket increased for both models.

1- The results of the research evidently indicated that the maximum force on the bucket is generated at 90 for both models and jet diameters. The generated force on the bucket in the (55, 75,115) degree of splitter angle is low according to 90 degree because the water force is divided into two components, one of these components does not affect the bucket (according to impulse- momentum principle).

2- Reynolds number and the amount of force on the bucket there is positively correlated by escalating the splitter. Force on the bucket increased by increasing the

velocity because it increased from the Momentum equation altered directly as it is described above in the alteration of the force. Thus, the force is positively correlated with the velocity as in the momentum equation. Furthermore, shape has an effect on the alteration of force value.

3- Distribution pressure was variation with changing model of the bucket pelton turbine, which it was very important for the pelton turbines design optimization process. In the splitter angle (55 degree) in both models, the pressure distribution in the bottom edge is varied according to the jet strike of the flow. In addition, in the splitter angle (75 degree) in both models, the effect of pressure is located near the middle of the bucket. When the splitter angle is 115 degree location of the pressure effect is positioned at the top near the cut off for both models.

The pressure distribution in the splitter angle of 90 degree is located at the middle of the bucket.

4- Displaying a leakage flow through the cut-out and edge of the bucket pelton turbine with changing of the splitter angle for all cases by water volume fraction figures in the ANSYS FLUENT program. When the splitter angle is 55 degree, water distributed over the majority of the internal surface and at the bucket outlet, it concentrates on the back edge. In this angle, a portion of the jet does not infiltrate into the bucket, the equivalent amount of water does not affect the bucket. Secondly, in the splitter of 75 degree, the distribution of water is occurred slightly away from the bucket edge. In addition, higher amount of water penetrates into the bucket in comparison to the splitter of 55 degree. Moreover, when the splitter angle is 90 degree, the layer of water prolongs to the cut out edge, as well as it becomes thinner. In this case, the whole jet penetrates the bucket and the whole layer of water is confined in the bucket. Lastly, when utilizing a splitter of 115 degree, the layer of water is predominantly extensive a long side the edge of the bucket. A tremendous amount of the jet exits the cut off, which infers for this case, a colossal force loss.

The most important thing is that generally flow visualization and determining force is altered by changing the shape of bucket of the pelton turbine. Furthermore, escalating the jet diameter is resulted in the decrease in the force on bucket.

REFERENCES

J. Ujam., S. O. Egbuna., N. E.Nwocha.,2014. Simulation of the Effect of Bucket Tip Angle on Bucket Splitter of a Pelton Turbine. ***American Journal of Engineering Research,*** 3: 85-92.

Abhishek,S.,Prashant,S.,Anil,K.,2012.Numerical Simulation of Pressure Distribution in Pelton Turbine Nozzle for the Different Shapes of Spear. International Journal of Innovations in Engineering and Technology,1:2319-1058.

Adriana,C., Mircea,B., Cristina,H.,2004. Numerical Simulation of A frees Jet inPelton Turbine. ***International Conference on Hydraulic Machinery and HydrodynamicsTimisoara, Romania,*** 6:79-84.

Alexander,P., François,A., Jean-Louis,K., Mohamed,F.,2005.**Flow in a Pelton Turbine Bucket Numerical and ExperimentalInvestigations.*Journal of Contributed by the Fluids Engineering Division of ASME for publication in the Fluid Engineering,***128:350-358.

Alnakhlani,M.M., Mukhtar, Himawanto,D.A., Alkurtehi,A.,2015. Effect of the Bucket and Nozzle Dimension on the Performance of a Pelton Water Turbine. ***Canadian Center of Science and Education,*** 9:1913-1844.

American Petroleum Institute (API), 1990. ***Design and Operation of Oil-Water Separators.*** Monographs on refinery environmental control management of water discharge publication 421, First Edition.

Amod,P., Hari,P.N., Bhola,T.,2014. CFD Analysis of Pelton Runner.***International Journal of Scientific and Research,*** 4: 2250-3153.

Ansys Cfx Inc.,2012. ***Modeling Theory*** and Version 14.

Ansys Inc.,2009.***AnsysFluent***.Theory and Guide 12.

Aung, K.M., Htay, H.W., Nyein, A.S., 2014. Design of 225kW Pelton Turbine.***International Journal of Scientific Engineering and Technology Research,*** 3: 4836-4842.

Awad, M.M., 2012. ***Two-Phase Flow, an Overview of Heat Transfer Phenomena.*** Dr M. Salim NewazKazi (Ed.), In Tech, DOI: 10.5772/54291.

Barstad, L. F., 2012. ***Cfd-Analysis of a pelton turbine***(Master thesis not published)**.** NorwegianUniversity of Science and Technology.

Bilal, A.N., 2013. Design of High Efficiency Pelton Turbine for Micro Hydropower Plant. ***International Journal of Electrical Engineering and Technology***, 4: 0976 – 6553.

Binaya ,K.C., Bhola ,T.,2009.Pressure Distribution Inner surface of Selected Pelton Bucket for Micro Hydro. ***Kathmandu University journal of Science***, 5: pp 42-50.

Çengel, Y.A., Turner, R., 2001.***Fundamentals of Thermal-Fluid Sciences***. McGraw Hill.

Chukwuneke, J. L., Achebe, C. H., Okolie ,P. C., Okwudibe, H. A.,2014.Modelling the Effect of Head and Bucket Splitter Angle on the Power Output of Pelton Turbine . ***International Journal of Engineering and Applied Sciences,*** 5:2305-8269.

Cousteix, J., 1986.Three-Dimensional and Unsteady Boundary Layer Computation," Annu. Rev. Fluid Mech., **18**, pp. 173–196.

D Jošt, P Mežnar, A Lipej,2010. Numerical prediction of Pelton turbine efficiency**.** ***IAHR Symposium on Hydraulic Machinery and Systems,*** 12:1088-1096.

Deepak,B., Shuneel,K.S., Sharma,2014.Review Paper on Nozzle in Hydro – Turbine.***International Journal of Advanced Technology in Engineering and S cience,*** 2:2348– 7550.

Emani, V.L., 2006. ***Computational Analysis for Multi-phase Flow in Helical Water Oil SeparatorUsing CFD*** (Master thesis not published). College of Graduate Studies Texas A&M University-Kingsville.

Gaurangkumar ,C., Chaudhari , Channiwala,S.A.,2010.Comparative Performance Evaluation of Designed Hooped Pelton Runner with Traditional Pelton Runner.***Journal of Applied Engineering Research,***5: 0973-4562.

Goldstein, D.E. (2004). Stochastic Coherent adaptive Large Eddy Simulation. ***Physics of Fluids,*** 16, 2497.

Gotfred,S.B.,2003.***Numerical analysis of the two-phase Pelton jet flow using a single-phase model and analytical discussions of the Pelton jet surface break-up phenomenon***(PhD thesis not published). Norwegian University of Science and Technology.

Grozev, G., Obretenov, V., Trifonov, T., 1988.Investigation of the Distribution of Pressure Over the Buckets of a Pelton Turbine. ***Proceedings of the Conference on Hydraulic Machinery and Flow Measurements***, pp. 119–125.

Hirt, C. W., and Nichols, B. D., 1981.Volume of Fluid Method for the Dynamics of Free Boundaries. ***J. Comput. Phys***, **39**1: pp. 201–225.

Ishii, M., 1975. ThermoFluid Dynamic—Theory of Two-Phase Flow.***Collection Direction Etudes Recherches Electrécité de France, Eyrolles.***

Janetzky, B., Göde, E., Ruprecht, A., Keck, H., andSchärer, C., 1998, "Numerical Simulation of the Flow in a Pelton Bucket," ***Proceedings of 19th Symposium, Singapore***, pp. 276–283.

John,S., Dimitris ,E.P., 2012. A fast lagrangian simulation method for flow analysis and runner design in pelton turbines. ***Journal of hydrodynamics,*** 24:930-941.

Klemetsen, L.E., 2010. ***An experimental and numerical study of the free surface pelton bucket flow*** (Master thesis not published)**.** Norwegian University of Science and Technology.

Kvicinsky, S., 2002, "Methoded Analysedes Ecoulements 3D a Surface Libre Application aux Turbines Pelton. ***Ecole Poly technique Fédérale de Lausanne***, 4: 457-464.

Leila,S., Mohammed,H.,2013. Numerical Simulation of the Flow Into a Rotating Pelton Bucket. ***International Journal of Emerging Technology and Advanced Engineering***, 3:2250-2459.

Lorentz, F.B., 2012.***CFD Analysis of a Pelton Turbine***(Master thesis not published)**.**Norwegian University of Science and Technology.

Mbiu, R. N., Nitrite, H., Maranga, S. M., 2003. ***Investigation of Stresses in Aluminium A356 Alloy Pelton Turbine Buckets*** (Master thesis not published)**.**Jomo Kenyatta University of Agriculture and Technology.

Mohr, K.S., 1993. ***A New Type of High Efficiency Oil-Water Separator for Better Water Quality Managemen***t, (Master thesis don't published). Faculty of the Graduate College of the Oklahoma University.

Nakanishi, Y., Fujii ,T., Morinaka, M., Wachi, K., 2006. Numerical Simulation of the flow in a Pelton bucket by a particle method. ***In Proceedings of the 23rd I.A.H.R. Symposium on Hydraulic machinery and systems.*** 17–21 October, Yokohama, Japan.

Nikhil ,J. G., S, S., Kevin, R. J. , Ashwin, C. A., 2014.Static Analysis on Pelton Wheel Bucket Structural Deformation and Material Property Study.***International Journal of Engineering Research & Technology***, 3:300-308.

Noor, A.I., 2012.Modelling ***of Micro Hydroelectric System Design***(Master thesis not published)**.** Faculty of Electrical and Electronic Engineering University Tun Hussein Onn Malaysia.

Pop, S. B. 2008. ***Turbulent Flow***. Chapter 10. Cambridge University.

Raj,K.K.,2009. An efficiency assessment analysis of a modified gravitational Pelton-wheel turbine. ***Journal of Energy in Southern Africa***,20.

Sam, A. 2010. ***Water Wheel CFD Simulation*** (Master thesis not published). Graduate School of Engineering of Lund University, Sweden.

Sanam,P., Hari,P.N., Amod,P., Anuj,P., Bhoj,B.C.,2014. Computational Fluid Dynamics (CFD) analysis of Pelton runner of Khimti Hydro-power Project of Nepal.***Rentech Symposium Compendium***, 4.

Sarvan, M.S., 2009. Analysis of a mini hydrokinetic turbine (Master thesis not published). Northern Illinois University.

Soran, S.I., 2016.CFD Simulation Coalescing Plate To Separating Water and Oil in Water Treatment Plant in Petroleum Project(Master thesis not published).*Yuzuncu Yil UniversityInstitute of Natural and Applied Sciences.*

Sourabh,K., Varun,K., Anoop,K.,2013. FEM Analysis of Turgo Impulse Turbine Blade. ***Walailak J Sci & Tech*** , 10(4): 363-368.

Suraj,Y.,2011. Some Aspects of Performance Improvement of Pelton Wheel Turbine with Reengineered Blade and Auxiliary Attachments.***International Journal of Scientific & Engineering Research,*** 2: 2229-5518.

Taylor, J. H. 2012. ***Numerical Simulation of a cross Flow Marine Hydrokinetic Turbine*** (Master thesis not published). Graduate School of Engineering of Washington University.

Traversaz, M., Leroy, P., Zoppé, B., andMaitre, T., 2002.Numerical Study of Pelton Bucket Flow: Comparison of Fluent and Cfx Results. ***Proceedings of 21th IAHR Symposium, Lausanne***, Sept. 9–12.

Varun,S., Sanjeev,K.D.,2014. Analysis of Stress on Pelton Turbine Blade Due to Jet Impingement.***International Journal of Current Engineering and Technology***, 4: 2347 – 5161.

Veronica, M., 2010. Dynamic modeling and environmental analysis of hydrokinetic energy (PhD thesis not published). University of Pittsburgh.

Versteeg ,H.K.,Malalasekra,W., 2007.***An Itroduction to Computational Fluid Dynamics the Finite Volume Method***.isbn 0-470-23515-2.

Vishal, G.,Ruchi,K.,Vishun,P.,2013. Performance Evaluation of PeltonTurbine. ***International Journal of Hydro Nepal,*** 13:1-35.

Vishal,G., Vishnu,P., Ruchi,K.,2014. Effect of Jet Shape on Flow and Torque Characteristics of Pelton Turbine Runner. ***Journal of Engineering Research and Applications,*** 4: 2248-9622.

Vishal,G., Vishnu,P.,2012. Numerical Investigations for Jet Flow Characteristics on PeltonTurbine Bucket. ***International Journal of Emerging Technology and Advanced Engineering***,2: 2250-2459.

Xia, Y., 2004. ***Numerical Simulation of Fine Particle Separation in Hindered – Settling BedSeparators by (CFD)***(PhD thesis not published).College of Engineering and Mineral Resources at West Virginia University.

Zoppe, B., C.pellone, T.maitre and P.leroy**.2006.Flow Analysis Inside a Pelton Turbine Bucket.*Journal of Turbo machinery,***128:500-511.

APPENDIX INDEX Eextended Turkish Summary (GENİŞLETİLMİŞ ÖZET)

GENİŞLETİLMİŞ ÖZET

1. ÖZET

PELTON TÜRBİNDE İKİ FARKLI KOVADAKİ AKIŞ ANALİZİ VE KUVVET BELİRLENMESİ

SABER, Azhin Abdullah
Yüksek Lisans Tezi, Makine Mühendisliği Anabilim Dalı
Tez Danışmanı: Doç. Dr. Sedat YAYLA
Ağustos 2017, 118 sayfa

Pelton türbini düşük su debisi ve yüksek rakımlarda mikro-hidroelektrik enerji santrali inşasında kullanılmaktadır. Değişik çalışma koşullarında en yüksek verimlilikle çalışabilen bir Pelton hidrolik türbini elde etmek için türbin parametrelerinin daha tasarım aşamasında ele alınması gerekmektedir. Bu çalışmada bu maksatla yapılan sıvı akışı simülasyonlarda ANSYS FLUENT yazılımı kullanılmıştır.

Bu çalışma kova ayraç açısının, besleme hızının ve iki farklı model için kova çaplarının etkilerini ve toplam gücü belirleyip pelton türbinindeki akış kalıbını tespit etmek amacıyla yapılmıştır. Çalışmada farklı besleme hızlarına sahip (20, 25, 30, 35 ve 40 m/sn.) iki farklı kova modeli, dört değişik ayraç açısı (55, 75, 90 ve 115) ve iki akış çapı (30 ve 40 mm), her bir parametrenin kova üzerindeki etkin güce olan etkileri açısından incelenmiştir. Elde edilen veriler, kova üzerindeki güç ile besleme hızı arasında lineer bir bağlantı ortaya çıkarmıştır. Sonuçlar aynı zamanda 90 derece açıya kadar ayraç açısı ile kova üzerine uygulanan güç arasındaki bağıntının da lineer olduğunu ortaya koymuştur. Sonuç olarak model 1 için türbin verimliliği 90 derecede azami seviyeye ulaşmıştır. Bu sonuçlar pelton türbini tasarımı optimizasyonu süreci için daimi akış hesapları kullanmanın beklenen faydaları üzerine bir öngörü kazandırmaktadır.

Anahtar kelimeler: CFD, iki-fazlı akış, serbest yüzey akışı, VOF, Kova Tasarımı

MATERYAL VE YÖNTEM

Bu çalışmadaki incelemelerde pelton türbini geometrisini oluşturmada ANSYS Workbench yazılımının modüler tasarım modülü kullanılmıştır (şekil 1 ve 2 de gösterildiği şekilde). Çalışmada iki model incelenmiştir ve her iki modelin de kova ebatları 67 mm'ye 40 mm iken ağız genişlikleri 30 mm'dir. Püskürtme uzunlukları ise 55 mm'dir. Bu şartlar altında çalışmada kovaya uygulanan güç pelton türbin şekilleri açısından değerlendirilmiş ve akış kalıbı incelenmiştir. 55, 75, 90 ve 115 derecelik ayraç açıları ile 20, 25,30,35 ve 40 m/sn'lik besleme hızları da değerlendirilmiştir. Örüntü (mesh) bağımsız incelemeler doğrultusunda, en ideal örüntü ebatları belirlenmiştir. Duvar yakınında asgari örüntü ebadı ilk tabakadan daha ince olacak şekilde ayarlanmış ve çözümleyicinin hatalı otomatik model oluşturmasının önüne geçmek için asgari örüntü boyutu olarak 0.000019 metre belirlenmiştir. Şekil 3 ve şekil 4 her iki model için tam boy örüntü elementlerini göstermektedir. Kova üzerindeki gücü belirlemek ve akışı hesaplayarak görselleştirmek için ANSYS FLUENT kullanılmıştır. Öncelikle her fazın sürekli olduğu varsayılmıştır. Ayrıca ilk fazın (su) kendisini ikinci (hava) faza aktardığı da varsayılmıştır. Bundan sonra ise serbest yüzey homojen iki fazlı model, çoklu sıvı modeli ya da sıvı VOF yöntemi ile modellenmiştir.

Serbest yüzey akış profilini elde etmek için ANSYS-FLUENT'in yeni bir tekniği olan tarama yöntemi kullanılmıştır. Ayrıca örüntü bağımsız testte varyasyonun, tablo 1'de gösterildiği şekilde problemin cinsine bağlı olarak, %4 ila %5 arasında olduğu tespit edilmiştir. Bu tekniğin amacı akış yönünde ilerledikçe ideal örüntü ebatlarını tespit edebilmektir.

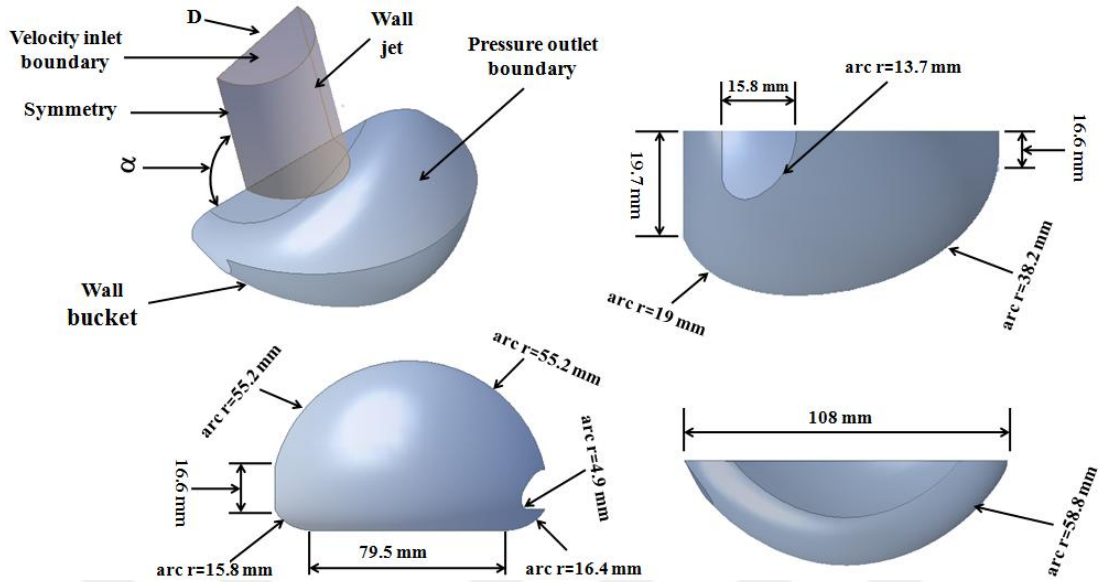

Şekil 1. Model 1'in çözüm alanını ve sınır koşulları.

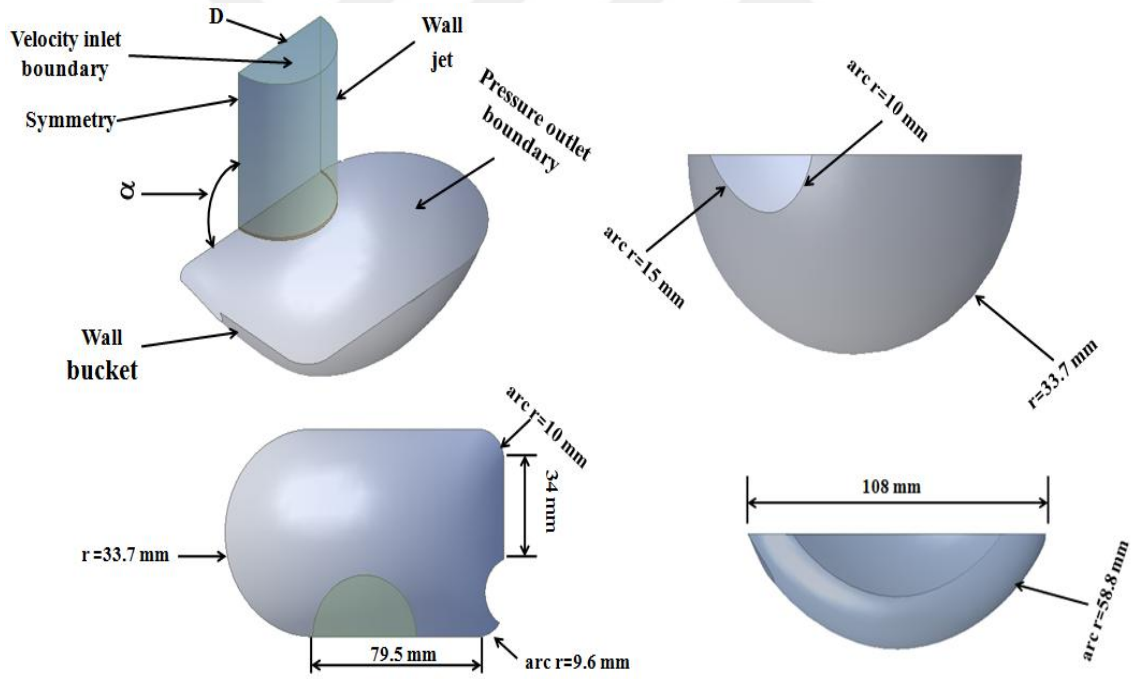

Şekil 2.Model 2'nin çözüm alanını ve sınır koşulları.

2. SONUÇ

Bu çalışma bir pelton türbini kovasında su-hava şeklinde iki fazlı bir akışın serbest yüzey olgusu konusunda bir fikir geliştirmek amacıyla yürütülmüştür. Bir sıvı hacmi (FOV) ölçeğinde CFD kullanmanın tüm avantajlarından istifade edebilmek için bu çalışmada ANSYS FLUENT ticari CFD programı kullanılmıştır.

Pelton türbini düşük su debisi ve yüksek rakımlarda mikro-hidro-elektrik enerji santrali inşasında kullanılır. Değişik çalışma koşullarında en yüksek verimlilikle çalışabilen bir Pelton hidrolik türbini elde etmek için türbin parametrelerinin daha tasarım aşamasında ele alınması gerekmektedir. Basınç konturu, akış hattı hızı ve kova üzerindeki güç, ayrışan suyun hacmi ve hız vektörleri CFD simülasyon modellerinden elde edilmiştir. Her iki pelton türbin modeli için değişik akış hızlarında (20,25,30,35 ve 40 m/sn) kovaya uygulanan güç miktarı simülasyon ile hesaplanmış ve aynı şekilde akışın bir görsel modeli de elde edilmiştir. Bunlarla beraber her iki türbin modeli için dört farklı ayraç açısı (55, 75, 90 ve 115 derece) da uygulanmıştır. Son olarak 30 ve 40 mm'lik iki farklı akış çapı da değerlendirilmeye alınmıştır. Bu çalışmadaki incelemelerde, her iki kova modeli için dört değişik hız, dört değişik ayraç açısı ve akış çapları tüm kombinasyonları ile simülasyonda denenmiş ve her parametrenin kovaya uygulanan güç üzerindeki etkileri incelenmiştir. Akış hızı ile kovaya uygulanan güç arasında lineer ilişki tespit edilmiştir. Ayrıca 90 dereceye kadar olan artışlarda ayraç açısının da kovaya uygulanan güç miktarı ile lineer ilişkide olduğu ortaya çıkmıştır. Her iki modelde de hızı artırmanın kovaya uygulanan gücü de arttırdığı tespit edilmiştir.

1- Çalışmanın sonuçları açıkça göstermiştir ki kovaya uygulanan azami güç her iki modelde ve akış çapında 90 derecelik ayraç açısında ortaya çıkmaktadır. 55, 75 ve 115 derecelik açılarda kovaya uygulanan basınç 90 derecedekine göre daha düşüktür çünkü su gücü iki farklı vektörsel bileşene ayrılmaktadır ve bu bileşenlerden bir tanesinin kova üzerinde etkisi olmamaktadır (darbe-momentum prensibi nedeniyle).

2- Reynolds sayısı ve kovaya uygulanan güç ile ayrımın hızlandırılması arasında da pozitif bağıntı mevcuttur. Kovaya uygulanan güç hızla birlikte artmaktadır

çünkü momentum eşitliği yukarıda açıklandığı üzere gücün değiştirilmesinden doğrudan etkilenmektedir. Bu nedenle güç ile hız arasında pozitif bağıntı ortaya çıkmaktadır. Ayrıca şeklin de güç değerinin değişime uğraması üzerinde etkisi vardır.

3- Basıncın dağılımı da pelton türbininkova modeli ile birlikte değişim göstermektedir ki bu durum pelton türbini tasarımı açısından büyük önem arz etmektedir. Her iki modelde de 55 derecelik ayraç açısında basınç dağılımının akışın darbesine göre alt kenar boyunca değiştiği görülmüştür. Açı 75 dereceye çıkarıldığında her iki model için de basınç etkisi kovanın orta noktasına kaymaktadır. Ayraç açısı 115 dereceye getirildiğinde ise basınç etkisi her iki modelde de kesim noktası olan üst tarafa kaydığı tespit edilmiştir.

   90 derecelik ayraç açısının basınç etkisi ise kovanın orta noktasında yer almaktadır.

4- ANSYS FLUENT programı ile pelton türbini kovası için ayraç açısı değiştirildiğinde akış ve sızdırma ile kesinti noktasının konumunda meydana gelen değişiklikler de akışın görüntülenmesi ile incelenmiştir. Ayraç açısı 55 derece olarak ayarlandığında, suyun iç yüzey ve kova tahliye noktası boyunca dağıldı görülmektedir, ancak kovanın arka kısmında yoğunlaşmaktadır. Bu açıda belli bir miktar akış kovanın içine girememektedir ve bu kısım kovaya güç uygulayamamaktadır. Ardından 75 derecelik açı incelendiğinde, su dağılımının kova kenarından biraz uzaklaştığı görülmektedir. Ayrıca 55 dereceye oranla daha çok su kovanın içine etki etmektedir. Ayraç açısı 90 dereceye çıkarıldığında su akışı kesinti noktasına kadar ilerleyebilmekte ve görece daha ince hale gelmektedir. Bu durumda da tüm akış kovaya etki edebilmekte ve suyun tamamı kova içinde yer bulmaktadır. Son olarak, 115 derecelik ayraç açısı kullanıldığında su yüzeyinin kovanın kenarı boyunca geniş bir yüzeye yayıldığı görülmektedir. Bu durum çok yüksek miktarda akışın çıkış noktasından kaçmasına neden olmakta ve büyük güç kaybına sebebiyet vermektedir.

   En önemli kısım, görselleştirilebilen akışın ve uygulanan gücün pelton türbini kova şeklinin değiştirilmesi ile değişmesi olmuştur. Ayrıca akış çapının artırılması kovaya uygulanan gücü azaltmaktadır.

CURRICULUM VITAE

She was born in Erbil in 1986. He completed his primary and secondary education in Erbil-Iraq. She educated from the Mechanical Engineering Department University of Salahaddin-Erbil in 2008. They have been employed ina Ministry of Municipality, Directorate Water Surrounding in Erbil.

UNIVERSITY OF YUZUNCU YIL
THE ISTITUTE OF NATURAL AND APPLIED SCIENCES
THESIS ORIGINALITY REPORT

Date: 20/06/2017...

Thesis Title: ''Flow Analyzing and Determining Force of Two Different Bucket in the Pelton Turbine''

The title of the mentioned thesis, above having total 117 pages with cover page, introduction, main parts and conclusion, has been checked for originality by Turnitin computer program on the date of 08/08/2017 and its detected similar rate was 0 % according to the following specified filtering originality report rules:

- Excluding the Cover page,
- Excluding the Thanks,
- Excluding the Contents,
- Excluding the Symbols and Abbreviations,
- Excluding the Materials and Methods
- Excluding the Bibliography,
- Excluding the Citations,
- Excluding the publications obtained from the thesis,
- Excluding the text parts less than 7 words (Limit match size to 7 words)

I read the Thesis Originality Report Guidelines of Yuzuncu Yil University for Obtaining and Using Similarity Rate for the thesis, and I declare the accuracy of the information I have given above and my thesis does not contain any plagiarism; otherwise I accept legal responsibility for any dispute arising in situations which are likely to be detected.

Sincerely yours,

AZhin Abdullah Saber
20/06/2017

Name and Surname: Azhin Abdullah SABER

Student ID#: 149101145

Science: Department of Mechanical Engineering

Program:

Statute: M. Sc. ☒ Ph.D. ☐

APPROVAL OF SUPERVISOR
SUITABLE

Assoc. Prof. Dr. Sedat YAYLA

APPROVAL OF THE INSTITUTE
SUITABLE

Yrd.Doç.Dr.Ayhan BAŞTÜRK
Fen Bilimleri Enstitüsü
Müdür Yardımcısı
(Title, Name-Surname, Signature)